Smectic-*A* and -*C* phases, and the transition between them, in uniaxial disordered environments

Leiming Chen
Institut für Theoretische Physik, Universität zu Köln, Zülpicher Strasse 77, D-50937 Köln, Germany

John Toner
Department of Physics and Institute of Theoretical Science, University of Oregon, Eugene, Oregon 97403, USA
(Received 16 September 2008; published 10 March 2009)

We present a theory of the elasticity and fluctuations of the smectic-*A* and -*C* phases in uniaxial, anisotropic disordered environments: e.g., stretched aerogel. We find that, bizarrely, the *low-temperature, lower-symmetry* smectic-*C* phase is *less* translationally ordered than the *high-temperature, higher-symmetry* smectic-*A* phase, with short-range "$m=1$ Bragg glass" and algebraic "*XY* Bragg glass" order, respectively. The smectic-*A*–smectic-*C* (*AC*) phase transition belongs to a new universality class, whose fixed points and exponents we find in a $d=5-\epsilon$ expansion. We give very detailed predictions for the very rich light-scattering behavior of both phases and the critical point.

DOI: 10.1103/PhysRevE.79.031703 PACS number(s): 61.30.Dk, 64.60.fh, 64.70.mf, 82.70.−y

I. INTRODUCTION

Randomly pinned elastic media occur in many contexts, including disordered superconductors [1], charge density waves [2], Josephson junction arrays [3], and helium in aerogel [4]. By far the most exotic phenomenon (at least in the—admittedly biased—opinion of the current authors) in such systems occurs in liquid crystals in aerogel: anomalous elasticity. That is, many liquid crystals in aerogel exhibit scalings of their elastic energies that differ radically (specifically, by nontrivial power laws) from those found in the absence of pinning.

However, despite the considerable amount of prior work done on these problems, there had, until recently [5], been no previous theoretical work on phase transitions in pinned liquid-crystal systems and little on equilibrium phase transitions in *any* pinned elastic system. In this paper we remedy this by treating the smectic-*A* to smectic-*C* (*AC*) transition in an *anisotropic*, *uniaxial* disordered environment. A brief summary of a few of our results has already appeared in [5]. Such an environment could be realized, e.g., by absorbing the liquid crystal in uniaxially stretched aerogel. For brevity, we will hereafter refer to the special uniaxial direction as the z axis of our coordinate system.

The *AC* phase transition in such a system separates the two novel, anomalously elastic glassy phases discovered (in a totally different context) and treated in Ref. [6]. The high-temperature phase ($T>T_{AC}$) is the glassy analog of the smectic-*A* phase of the pure problem, in that both the layer normal $\hat{N}$ and nematic director $\hat{n}$ lie, on average, along the z axis. This phase is in the universality class of the random field *XY* model [7]; hence, following [6], we call it the "random field *XY* smectic Bragg glass" (XYBG) for short.

The low-temperature phase is the glassy analog of the smectic-*C* phase, in that both the layer normal $\hat{N}$ and nematic director $\hat{n}$ tilt from the z axis. This tilting obeys the "geometrical constraint" that $\hat{N}$, $\hat{n}$, and $\hat{z}$ are in the same plane, with $\hat{z}$ between $\hat{N}$ and $\hat{n}$ and the angles between these three vectors non-fluctuating, albeit temperature dependent. Hence, as in the smectic-*C* phase in an *isotropic* environment, the only new "Goldstone mode" degree of freedom associated with the tilting is the overall azimuthal angle of rotation of the vectors $\hat{N}$ and $\hat{n}$ about $\hat{z}$.

The temperature dependences of the angles $\theta_L(T)$ between $\hat{N}$ and $\hat{z}$ and $\theta_n(T)$ between $\hat{n}$ and $\hat{z}$ are the same near T_c; that is, the ratio θ_L/θ_n is a (negative) constant near T_c. Hence, we are free to choose either the layer normal tilting angle $\theta_L(T)$ or the molecular tilting angle $\theta_n(T)$, both of which can be measured experimentally, as the magnitude of the order parameter for the *AC* transition.

The smectic-*C* phase is in the universality class of the "$m=1$ smectic Bragg glass" phase studied in [6].

We call both the *A* and *C* phases "glassy" because both lack long-range translational order due to the disordering effect of the random environment (i.e., the aerogel). The extent of this destruction, however, differs greatly between the two phases. Strikingly, it is the *low*-temperature, higher-symmetry, "smectic-*C* glass" that has *less* translational order.

Although surprising, it is not unprecedented in pinned elastic media for a low-temperature phase to have more symmetry than the high-temperature phase from which it developed. For example, in *XY* models with certain types of random fields [8], there are phase transitions from a phase with quasi-long-range (algebraic) spin order to lower-temperature phases with only short-range order. And on the surfaces of disordered crystals, a very similar "superroughening" transition occurs [9], in which mean-squared vertical fluctuations on the surface go from scaling logarithmically with surface area in the high-temperature "rough" phase to much larger fluctuations in the low-temperature "superrough" phase which scale like $[\ln(\text{area})]^2$.

In the glassy smectic-*A* or XYBG phase, translational correlations are quasi-long-ranged, by which we mean they decay as power laws with distance. In the glassy smectic-*C* or $m=1$ Bragg glass phase, these correlations are short ranged. These differences in the translational correlations lead to radically different x-ray-scattering signatures in the two phases which we will now describe.

In the glassy-*A* or XYBG phase, the x-ray-scattering intensity $I(\vec{q})$ diverges near the smectic Bragg peaks, which

occur at $\vec{q}=nq_0\hat{z}$ for all n integer, where $q_0=2\pi/a$, with a the smectic layer spacing. Because of the lack of true, long-range translational order, this divergence is *not* in the form of a δ function; rather, it is an integrable power-law divergence:

$$I(\vec{q}) \propto [(q_z - nq_0)^2 + \alpha q_\perp^2]^{(-3+.55n^2)/2}, \tag{1.1}$$

where α is a nonuniversal constant of order 1 and $q_\perp$ is the magnitude of the projection of $\vec{q}$ perpendicular to $\hat{z}$. Note that the power law $-3+0.55n^2$ characterizing the divergence of the nth peak depends on which peak we are considering. Indeed, only the first two peaks ($n=1$ and $n=2$) actually diverge.

In contrast, in the glassy-C or $m=1$ BG phase, the peaks in the x-ray-scattering intensity are broad, with $I(\vec{q})$ finite for all $\vec{q}$.

As $T \to T_{AC}$ from above (i.e., on the A side), the sharpness of the peak disappears in an unusual way. The peaks look broad and qualitatively Lorentzian for $\vec{q}$'s sufficiently far from the Bragg peak position $nq_0\hat{z}$, while for $\vec{q}$'s sufficiently close to the peak, it follows the power-law divergence (1.1). "Sufficiently close," in this context, means that *both* $|\vec{q}_\perp| \ll \delta q_\perp^c(n,T)$ *and* $|q_z - nq_0| \ll \delta q_z^c(T)$, where the crossover wave vectors $\delta q_\perp^c(n,T)$ and $\delta q_z^c(n,T)$ are given by

$$\delta q_\perp^c(n,T) \propto (\xi_\perp^c)^{-n^2/(3-0.55n^2)}, \tag{1.2}$$

$$\delta q_z^c(n,T) \propto (\xi_z^c)^{-n^2/(3-0.55n^2)}, \tag{1.3}$$

where n again is the index of the Bragg peak and $\xi_\perp^c$ and ξ_z^c are correlation lengths along and perpendicular to the smectic layers, respectively, that both diverge extremely strongly as $T \to T_{AC}$. Specifically,

$$\xi_{\perp,z}^c \propto \exp(A|T - T_{AC}|^{-\Omega}), \tag{1.4}$$

where Ω is a universal exponent, which we have calculated in the ϵ expansion discussed below, and A is a nonuniversal constant.

These x-ray-scattering predictions are illustrated in Figs. 1 and 2. The divergence of $\xi_{\perp,z}^c$ implies that, as $T \to T_{AC}^+$, the algebraic "spikes" on the top of the broad quasi-long-range peaks get narrower and less intense, vanishing completely at T_{AC}. Lowering temperature further leads only to the broad peaks of the smectic-C phase. This entire scenario of sharp peaks at high temperature and broad peaks at low temperature is completely counterintuitive and contrary to the behavior seen in almost every translationally ordered system without quenched disorder [10], although, as discussed earlier [8,9], there is some precedence for this phenomenon in the presence of quenched disorder.

We turn now to the smectic-C phase and in particular to the question of why this phase, though of lower symmetry than the smectic-A phase, is *less* translationally ordered. In fact, it is precisely the new broken symmetry of the smectic C phase—that is, the tilt of the layer normal and nematic director—that causes this. This is because, while the energetically preferred layer normal $\hat{N}$ and nematic director $\hat{n}$ in the smectic-A phase are *unique*—they must point *along* $\hat{z}$—there are *infinitely many* energetically preferred orientations of $\hat{N}$ and $\hat{n}$ in the C phase: $\hat{N}$ can lie anywhere on a cone making an angle $\theta_L(T)$ with $\hat{z}$, which, combined with the "geometrical constraint" (described in the third paragraph) on the directions of $\hat{N}$ and $\hat{n}$, also determines the similar cone of directions $\hat{n}$ can point. This *exact* symmetry of the elastic energy of the smectic-C phase means that the direction perpendicular to the $\hat{z}$-$\langle\hat{N}\rangle$ plane (where $\langle\hat{N}\rangle$ is the mean of $\hat{N}$—i.e., the direction of spontaneous tilt) becomes "soft": that is, an easy direction for layer displacements to vary in. Precisely such softness occurs (for different reasons) in the "$m=1$ smectic" studied in [6] and, indeed, expanding our elastic Hamiltonian around the new broken-symmetry, tilted smectic-C ground state, we obtain an elastic Hamiltonian describing small positional fluctuations about the tilted smectic-C ground state, which, after some manipulation, proves to be identical to that studied for $m=1$ smectic in [6]. Thus, we can simply transcribe the results of [6] to this problem.

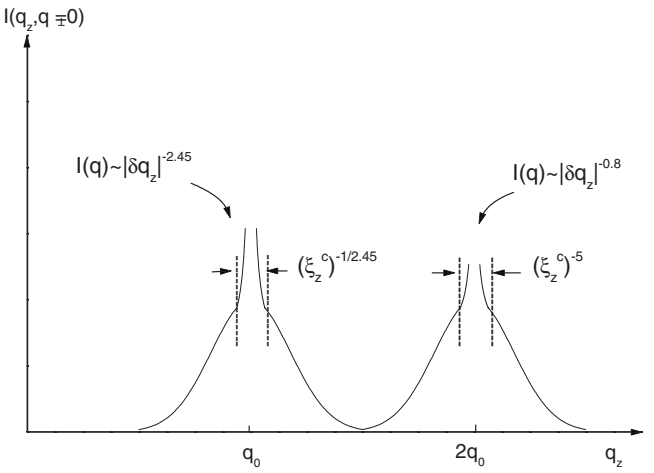

FIG. 1. The q_z dependence of the x-ray-scattering intensity for $q_\perp=0$ in the smectic-A phase. In the C phase, the sharp, power-law peaks disappear, leaving only the broad peak.

The most striking result of Ref. [6] is that this phase exhibits a bizarre phenomenon known as "anomalous elastic-

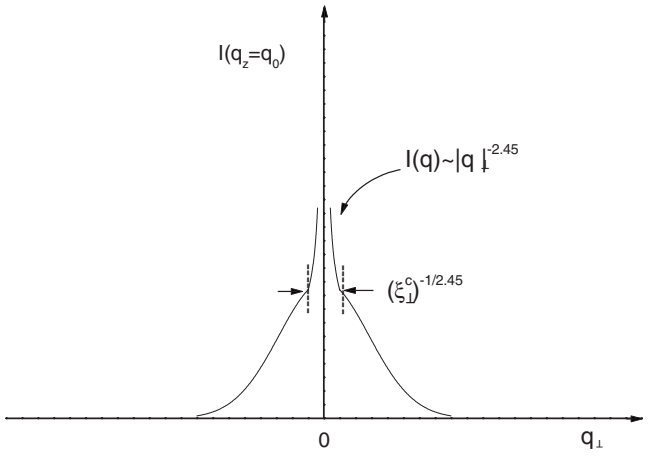

FIG. 2. The $q_\perp$ dependence of the x-ray-scattering intensity for $q_z=q_0$ in the smectic-A phase. Again, the sharp peak vanishes in the C phase.

ity." That is, the elastic moduli that characterize the elastic response of this phase can no longer be called "elastic constants," because they are *not* constants. Rather, they become *singular* functions of the length scale, or, equivalently, the wave vector, at which they are measured.

The elastic constants that characterize the smectic-*C* phase in uniaxial disordered media are defined in (6.14), which gives the "replicated" elastic Hamiltonian describing the disordered, glassy smectic-*C* phase. Of these, the bend modulus $\tilde{K}$ and the disorder variances or effective disorder strengths $\Delta_{s'}$ and $\Delta_{x'}$ diverge, while the in-plane tilt modulus γ [which gives the energy cost for changing the angle between $\hat{N}$ and $\hat{z}$ from $\theta_L(T)$] vanishes, as $|\vec{q}| \to 0$, according to

$$\tilde{K} \cong \begin{cases} \tilde{K}_c(T)(\xi_\perp q_{s'})^{-\tilde{\eta}_K}, & (\xi_\perp q_{s'})^{\tilde{\zeta}_{x'}} \gg \xi_\perp q_{x'}, \quad (\xi_\perp q_{s'})^{\tilde{\zeta}_{z'}} \gg \xi_z q_{z'}, \\ \tilde{K}_c(T)(\xi_\perp q_{x'})^{-\tilde{\eta}_K/\tilde{\zeta}_{x'}}, & \xi_\perp q_{x'} \gg (\xi_\perp q_{s'})^{\tilde{\zeta}_{x'}}, \quad \xi_\perp q_{x'} \gg (\xi_z q_{z'})^{\tilde{\zeta}_{x'}/\tilde{\zeta}_{z'}}, \\ \tilde{K}_c(T)(\xi_z q_{z'})^{-\tilde{\eta}_K/\tilde{\zeta}_{z'}}, & \xi_z q_{z'} \gg (\xi_\perp q_{s'})^{\tilde{\zeta}_{z'}}, \quad \xi_z q_{z'} \gg (\xi_\perp q_{x'})^{\tilde{\zeta}_{z'}/\tilde{\zeta}_{x'}}, \end{cases} \tag{1.5}$$

$$\Delta_{s',x'} \cong \begin{cases} \Delta^c_{s',x'}(T)(\xi_\perp q_{s'})^{-\tilde{\eta}_{s',x'}}, & (\xi_\perp q_{s'})^{\tilde{\zeta}_{x'}} \gg \xi_\perp q_{x'}, \quad (\xi_\perp q_{s'})^{\tilde{\zeta}_{z'}} \gg \xi_z q_{z'}, \\ \Delta^c_{s',x'}(T)(\xi_\perp q_{x'})^{-\tilde{\eta}_{s',x'}/\tilde{\zeta}_{x'}}, & \xi_\perp q_{x'} \gg (\xi_\perp q_{s'})^{\tilde{\zeta}_{x'}}, \quad \xi_\perp q_{x'} \gg (\xi_z q_{z'})^{\tilde{\zeta}_{x'}/\tilde{\zeta}_{z'}}, \\ \Delta^c_{s',x'}(T)(\xi_z q_{z'})^{-\tilde{\eta}_{s',x'}/\tilde{\zeta}_{z'}}, & \xi_z q_{z'} \gg (\xi_\perp q_{s'})^{\tilde{\zeta}_{z'}}, \quad \xi_z q_{z'} \gg (\xi_\perp q_{x'})^{\tilde{\zeta}_{z'}/\tilde{\zeta}_{x'}}, \end{cases} \tag{1.6}$$

$$\gamma \cong \begin{cases} \gamma_c(T)(\xi_\perp q_{s'})^{\tilde{\eta}_\gamma}, & (\xi_\perp q_{s'})^{\tilde{\zeta}_{x'}} \gg \xi_\perp q_{x'}, \quad (\xi_\perp q_{s'})^{\tilde{\zeta}_{z'}} \gg \xi_z q_{z'}, \\ \gamma_c(T)(\xi_\perp q_{x'})^{\tilde{\eta}_\gamma/\tilde{\zeta}_{x'}}, & \xi_\perp q_{x'} \gg (\xi_\perp q_{s'})^{\tilde{\zeta}_{x'}}, \quad \xi_\perp q_{x'} \gg (\xi_z q_{z'})^{\tilde{\zeta}_{x'}/\tilde{\zeta}_{z'}}, \\ \gamma_c(T)(\xi_z q_{z'})^{\tilde{\eta}_\gamma/\tilde{\zeta}_{z'}}, & \xi_z q_{z'} \gg (\xi_\perp q_{s'})^{\tilde{\zeta}_{z'}}, \quad \xi_z q_{z'} \gg (\xi_\perp q_{x'})^{\tilde{\zeta}_{z'}/\tilde{\zeta}_{x'}}, \end{cases} \tag{1.7}$$

where the wave-vector-independent quantities $\tilde{K}_c(T)$, $\Delta^c_{s',x'}(T)$, and $\gamma_c(T)$ are the "half-dressed" (i.e., renormalized by the critical fluctuations we will discuss in a moment, but unrenormalized by smectic-*C* fluctuations) values of the corresponding elastic moduli and disorder variances; we have defined a new, *nonorthogonal* set of wave-vector coordinates:

$$q_{x'} \equiv q_x - \Gamma q_z, \tag{1.8}$$

$$q_{s'} \equiv q_s, \tag{1.9}$$

$$q_{z'} \equiv q_z, \tag{1.10}$$

where q_s is the component of $\vec{q}$ perpendicular to the $\hat{z}$-$\langle\hat{N}\rangle$ plane and q_x is the component of $\vec{q}$ within the $\hat{z}$-$\langle\hat{N}\rangle$ plane, but orthogonal to $\hat{z}$, $\xi_\perp(T)$ and $\xi_z(T)$ are temperature-dependent lengths, and $\Gamma(T)$ is a dimensionless temperature-dependent constant. The temperature dependences of $\xi_\perp(T)$, $\xi_z(T)$, $\tilde{K}_c(T)$, $\Delta^c_{s',x'}(T)$, $\gamma_c(T)$, and $\Gamma(T)$ are all singular at the transition temperature T_{AC}, with $\xi_\perp(T)$, $\xi_z(T)$, $K_c(T)$, $\Delta^c_{s',x'}(T)$, and $\Gamma(T)$ diverging and $\gamma_c(T)$ vanishing, as $T \to T_{AC}$. These scaling laws governing their respective divergences and vanishings will be given later in this Introduction and in Sec. VIII.

Here and throughout the rest of this paper, a tilde ($\tilde{}$) over an exponent denotes an exponent describing anomalous elasticity of the *C* phase.

Since in this paper we have so many elastic constants, disorder invariances, power-law exponents, and characteristic lengths, it is necessary for us to summarize these parameters in Tables I–III.

The *universal* exponents $\tilde{\eta}_K, \tilde{\eta}_\gamma, \tilde{\eta}_{s'}, x', \tilde{\zeta}_{x'}$, and $\tilde{\zeta}_{z'}$ appearing in the above expressions were calculated in [6], using an approach that yielded numerical estimates and error bars for them. We will review the logic of their approach in Appendix A; here, we merely quote their results:

$$\tilde{\eta}_K = 0.50 \pm 0.03, \tag{1.11}$$

$$\tilde{\eta}_\gamma = 0.26 \pm 0.12, \tag{1.12}$$

$$\tilde{\eta}_{s'} = 0.132 \pm 0.002, \tag{1.13}$$

$$\tilde{\zeta}_{x'} = 1.62 \pm 0.08, \tag{1.14}$$

$$\tilde{\zeta}_{z'} = 1.75 \pm 0.02. \tag{1.15}$$

These exponents also obey the *exact* scaling relations (in $d=3$)

TABLE I. Overview of the elastic constants and disorder variances.

Symbols	Description	Values and/or scaling laws
B	Compression modulus in the Hamiltonian, Eq. (3.1)	$B=B_0$
K	Bend modulus in the Hamiltonian, Eq. (3.1)	(1.27)
Δ_t	Random tilt disorder variance in the Hamiltonian, Eq. (3.1)	(1.32)
Δ_c	Random compression disorder variance in the Hamiltonian, Eq. (3.1)	(1.32)
B_0	Bare value of B	
K_0	Bare value of K	
Δ_t^0	Bare value of Δ_t	
Δ_c^0	Bare value of Δ_c	
$\tilde{B}$	Compression modulus in the Hamiltonian, Eq. (6.14)	$\tilde{B}=B_0$
$\tilde{K}$	Bend modulus in the Hamiltonian, Eq. (6.14)	(1.5)
γ	Tilt modulus along $\hat{x}'$ in the Hamiltonian, Eq. (6.14)	(1.7)
$\Delta_{s'}$	Random tilt disorder variance along $\hat{s}'$ in the Hamiltonian, Eq. (6.14)	(1.6)
$\Delta_{x'}$	Random tilt disorder variance along $\hat{x}'$ in the Hamiltonian, Eq. (6.14)	(1.6)
$\Delta_{z'}$	Random compression disorder variance in the Hamiltonian, Eq. (6.14)	$\Delta_{z'}=\Delta_{z'}^c$
$\tilde{B}_c$	Half-dressed value of $\tilde{B}$	$\tilde{B}_c=B_0$
$\tilde{K}_c$	Half-dressed value of $\tilde{K}$	(8.6)
γ_c	Half-dressed value of γ	(8.7)
$\Delta_{s'}^c$	Half-dressed value of $\Delta_{s'}$	(8.8)
$\Delta_{x'}^c$	Half-dressed value of $\Delta_{x'}$	(8.8)
$\Delta_{z'}^c$	Half-dressed value of $\Delta_{z'}$	(8.9)

$$\tilde{\zeta}_{x'} = 2 - \left(\frac{\tilde{\eta}_\gamma + \tilde{\eta}_K}{2}\right), \tag{1.16}$$

$$\tilde{\zeta}_{z'} = 2 - \frac{\tilde{\eta}_K}{2}, \tag{1.17}$$

$$\tilde{\eta}_{s'} = \frac{\tilde{\eta}_\gamma}{2} + 2\tilde{\eta}_K - 1. \tag{1.18}$$

In addition to the above results derived in Ref. [6], we derive in Sec. III an additional *exact* scaling relation for $\tilde{\eta}_{x'}$:

$$\tilde{\eta}_{x'} = 2 + \tilde{\eta}_{s'} - \tilde{\eta}_K - \tilde{\eta}_\gamma, \tag{1.19}$$

from which it follows, upon inserting the numerical results, Eqs. (1.11)–(1.13), that

$$\tilde{\eta}_{x'} = 1.37 \pm 0.15. \tag{1.20}$$

Having described the A and C phases in this uniaxially disordered system, we now turn to the transition between them. We find that the upper critical dimension d_{uc} for this transition, below which it is no longer accurately described by a purely Gaussian theory, is $d_{uc}=5$. We have studied this phase transition in an $\epsilon=5-d$ expansion, where d is the dimension of the space filled by the liquid crystal (i.e., $d=3$ is the case of physical interest), and find that there *is* a stable renormalization-group fixed point, the existence of which implies a second-order phase transition with *universal* critical behavior. Of course, since $d_{uc}=5$, $\epsilon=2$ in the physically interesting case $d=3$, which is far too large an ϵ for the results for exponents that we quote to be quantitatively reliable in $d=3$. However, we expect the *qualitative* features of the transition that we find to be robust down to $d=3$ (although we will discuss some rather strong caveats to this statement later).

The second-order nature of the transition is, as usual, manifested in *universal* power-law dependence of many physical observables on reduced temperature $T-T_{AC}$. In particular, the layer normal and director tilt angle $\theta_{L,n}(T)$ obeys

$$\theta_{L,n}(T) = A_{L,n}(T_{AC} - T)^\beta, \tag{1.21}$$

where the order parameter exponent β *is universal* and given, to leading order in $\epsilon=5-d$, by

TABLE II. Overview of the exponents.

Symbols	Description	Values
η_B	Anomalous exponent of B	$\eta_B=0$
η_K	Anomalous exponent of K	(1.35)
η_t	Anomalous exponent of Δ_t	(1.36)
η_c	Anomalous exponent of Δ_c	(1.37)
ζ	Anisotropy exponent for the model (3.1)	(1.29)
$\tilde{\eta}_K$	Anomalous exponent of $\tilde{K}$	(1.11)
$\tilde{\eta}_\gamma$	Anomalous exponent of γ	(1.12)
$\tilde{\eta}_{s'}$	Anomalous exponent of $\Delta_{s'}$	(1.13)
$\tilde{\eta}_{x'}$	Anomalous exponent of $\Delta_{x'}$	(1.20)
$\tilde{\zeta}_{x'}$	Anisotropy exponent (between $q_{s'}$ and $q_{x'}$) for the model (6.14)	(1.16)
$\tilde{\zeta}_{z'}$	Anisotropy exponent (between $q_{s'}$ and $q_{z'}$) for the model (6.14)	(1.17)

$$\beta = \frac{1}{2} - \frac{\epsilon}{10} + O(\epsilon^2) \tag{1.22}$$

and the amplitudes $A_{L,n}$ are nonuniversal and depend on the system.

We have also calculated the specific heat exponent

$$\alpha = -\frac{\epsilon}{10} + O(\epsilon^2). \tag{1.23}$$

The order parameter $\vec{N}_\perp$ for this transition is the projection of the smectic layer normal $\hat{N}$ onto the xy plane (i.e., perpendicular to the direction along which the aerogel is stretched). Above T_{AC}, the two-point real-space correlations of $\vec{N}_\perp$ decay rapidly with distance, with correlation lengths ξ_z and $\xi_\perp$ parallel and perpendicular to the z axis, respectively, which behave quite differently as $T \to T_{AC}^+$. Specifically, both diverge as power laws in $(T-T_{AC})$,

$$\xi_{\perp,z} \propto |T - T_{AC}|^{-\nu_{\perp,z}}, \tag{1.24}$$

but with exponents $\nu_\perp$ and ν_z that differ from each other due to the strong anisotropy of the problem. From our ϵ expansion, we find

$$\nu_\perp = \frac{1}{2} + \frac{3\epsilon}{20} + O(\epsilon^2), \tag{1.25}$$

$$\nu_z = 1 + \frac{3\epsilon}{10} + O(\epsilon^2). \tag{1.26}$$

For $T < T_{AC}$—i.e., in the C phase, the correlation lengths ξ_z and $\xi_\perp$ can still be defined, now by looking at the *connected* correlations of $\hat{N}$. They continue to be given by the scaling law (1.24), with the same exponents (1.25) and (1.26).

In addition to their role as correlation lengths for $\hat{N}$, the lengths ξ_z and $\xi_\perp$ are also the ones that appear in the scaling laws, Eqs. (1.5)–(1.7) for the anomalous elasticity in the C phase.

We also find that, as in the C phase, the system exhibits anomalous elasticity right at T_{AC} as well. Specifically, right at T_{AC}, the smectic-layer bend modulus K becomes strongly wave vector dependent, vanishing as $\vec{q} \to 0$ according to the scaling laws

$$K(\vec{q}, T = T_{AC}) = K_0 (\xi_{NL}^\perp q_\perp)^{-\eta_K} f_K\left(\frac{\xi_{NL}^z q_z}{(\xi_{NL}^\perp q_\perp)^\zeta}\right) \approx \begin{cases} K_0 (\xi_{NL}^\perp q_\perp)^{-\eta_K}, & \xi_{NL}^z q_z \ll (\xi_{NL}^\perp q_\perp)^\zeta, \\ K_0 (\xi_{NL}^z q_z)^{-\eta_K/\zeta}, & \xi_{NL}^z q_z \gg (\xi_{NL}^\perp q_\perp)^\zeta, \end{cases} \tag{1.27}$$

where $\eta_K < 0$ and the anisotropy exponent

$$\zeta = 2 - \frac{\eta_K}{2}. \tag{1.28}$$

This anisotropy exponent also obeys

$$\zeta = \nu_z / \nu_\perp. \tag{1.29}$$

In Eq. (1.27), the constant K_0 is the "completely bare" (i.e., unrenormalized by *any* fluctuations) value of the bend modulus (i.e., the value it would have in the absence of the aerogel). While weakly temperature dependent, like all elastic moduli, K_0 has *no* critical singularity near T_{AC}.

Also, in Eq. (1.27), $\xi_{NL}^{\perp,z}$ are the length scales in the $\perp$ and z directions beyond which the elasticity becomes anomalous. These lengths depend on the disorder strength, and hence the aerogel density, and remain finite (and nonzero) as $T \to T_{AC}$, although both diverge as the aerogel density $\rho_A \to 0$. In three dimensions these length scales are given as

$$\xi_{NL}^\perp = \left(\frac{64\pi}{3}\right)^{1/2} \frac{K_0^{5/4}}{B_0^{1/4} \Delta_t^{01/2}}, \tag{1.30}$$

TABLE III. Overview of the characteristic lengths.

Symbols	Description	Values and/or scaling laws
λ	Smectic penetration length	$\lambda = \sqrt{K_0/B_0}$
$\xi_{NL}^{\perp,z}$	Nonlinear crossover lengths	(1.30) and (1.31)
$\xi_{\perp,z}$	Correlation lengths for the phase transition	(1.24)
$\xi_{\perp,z}^c$	Crossover lengths between the power-law and broad x-ray scattering patters	(1.4)
$\xi_{\perp,z}^x$	Linewidths of the broad x-ray scattering pattern	(8.23) and (8.24)

$$\xi_{NL}^{z} = \frac{64\pi}{3}\frac{K_0^2}{\Delta_t^0}, \tag{1.31}$$

where Δ_t^0 is the completely bare value of disorder variance Δ_t, which is discussed below.

The disordering effect of the random aerogel matrix can be quantified by disorder variances Δ_t and Δ_c describing tilt and compressive stresses, respectively. The former arise due to random torques exerted by the aerogel on the smectic layers, causing them to tilt, while the latter are caused by random compression (or stretching) of the smectic layer spacing induced by the aerogel, causing layers to move closer together (or further apart). These variances also become anomalous at $T=T_{AC}$, obeying

$$\Delta_{t,c}(\vec{q}, T = T_{AC}) = \Delta_{t,c}^0 (\xi_{NL}^{\perp} q_\perp)^{-\eta_{t,c}} f_{t,c}\left(\frac{(\xi_{NL}^{z} q_z)}{(\xi_{NL}^{\perp} q_\perp)^{\zeta}}\right) \approx \begin{cases} \Delta_{t,c}^0 (\xi_{NL}^{\perp} q_\perp)^{-\eta_{t,c}}, & \xi_{NL}^{z} q_z \ll (\xi_{NL}^{\perp} q_\perp)^{\zeta}, \\ \Delta_{t,c}^0 (\xi_{NL}^{z} q_z)^{-\eta_{t,c}/\zeta}, & \xi_{NL}^{z} q_z \gg (\xi_{NL}^{\perp} q_\perp)^{\zeta}, \end{cases} \tag{1.32}$$

where Δ_c^0 is the completely bare value of Δ_c.

Because our model at $T=T_{AC}$ proves remarkably similar (although not quite identical) to that for a smectic A in isotropic disordered media, we expected, when we began our study, to find anomalous behavior for the smectic-layer compression modulus B, with it *vanishing* as $\vec{q}\to 0$ according to

$$B(\vec{q}, T = T_{AC}) = B_0 (\xi_{NL}^{\perp} q_\perp)^{\eta_B} f_B\left(\frac{\xi_{NL}^{z} q_z}{(\xi_{NL}^{\perp} q_\perp)^{\zeta}}\right) \approx \begin{cases} B_0 (\xi_{NL}^{\perp} q_\perp)^{\eta_B}, & \xi_{NL}^{z} q_z \ll (\xi_{NL}^{\perp} q_\perp)^{\zeta}, \\ B_0 (\xi_{NL}^{z} q_z)^{\eta_B/\zeta}, & \xi_{NL}^{z} q_z \gg (\xi_{NL}^{\perp} q_\perp)^{\zeta}, \end{cases} \tag{1.33}$$

where B_0 is the completely bare value of B, as found [11] in the isotropic disordered smectic-A problem.

$f_{K,t,c,B}(x)$ are universal scaling functions, which have the property

$$f_{B,K,t,c}(x) = \begin{cases} 1, & x \ll 1, \\ x^{\eta_B, -\eta_{K,t,c}/\zeta}, & x \gg 1. \end{cases} \tag{1.34}$$

To our surprise, we found that, in this problem, B exhibits no such anomaly (i.e., $\eta_B=0$), remaining constant as $\vec{q}\to 0$. This result is *exact*, not an artifact of the $\epsilon=5-d$ expansion, and we expect it to hold in $d=3$.

The exponents η_K, η_t, and η_c *are* nonzero, however. Both η_K and η_t *are* zero to $O(\epsilon)$, but nonzero to $O(\epsilon^2)$, and given by

$$\eta_K = C_K \epsilon^2 + O(\epsilon^3), \tag{1.35}$$

$$\eta_t = C_\Delta \epsilon^2 + O(\epsilon^3), \tag{1.36}$$

with $C_K=[32\ln(4/3)-10]/225\cong -0.003\,53$ and $C_\Delta=[12\ln(4/3)-\frac{1}{3}]/225\cong 0.01386$. Note that $C_K<0$, which implies that K *vanishes* as $\vec{q}\to 0$. This is another unexpected result: K *diverges* as $\vec{q}\to 0$ in every other problem of this type [6,11,12] previously studied. Of course, whether η_K remains negative all the way down from $d=5$ to $d=3$ remains an open question.

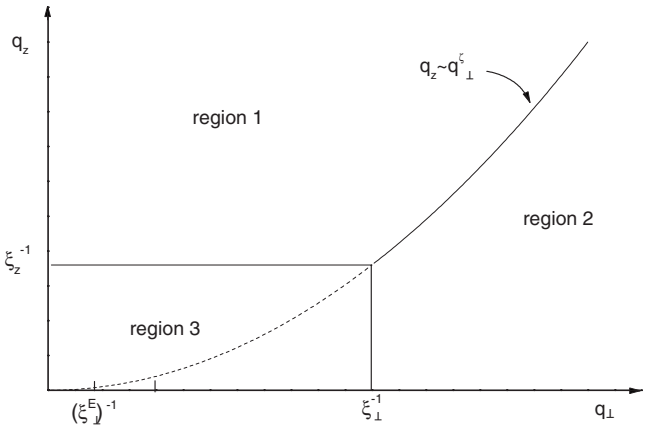

FIG. 3. Illustration of the three distinct regions in wave-vector space with different wave-vector dependences of $\Delta_{t,c}$ and K, which is given in Eq. (1.38).

The remaining exponent

$$\eta_c = 2 - \frac{\epsilon}{5} + O(\epsilon^2). \tag{1.37}$$

For T larger than T_{AC} the [wave-vector ($\vec{q}$-) and temperature-(T-) dependent] disorder variance $\Delta_{t,c}(\vec{q},T)$ and layer bend modulus $K(\vec{q},T)$ are given by their $T=T_{AC}$ forms, Eqs. (1.27) and (1.32), if *either* $q_\perp\xi_\perp \gg 1$ or $q_z\xi_z \gg 1$. Otherwise (i.e., if *both* $q_\perp\xi_\perp \ll 1$ and $q_z\xi_z \ll 1$), $\Delta_{t,c}\propto \xi_\perp^{\eta_{t,c}} \propto (T-T_{AC})^{-\nu_\perp \eta_{t,c}}$ and $K\propto \xi_\perp^{\eta_K}\propto (T-T_c)^{-\nu_\perp \eta_K}$, results which can be (and, in fact, were) straightforwardly obtained by matching the behavior for *either* $q_\perp\xi_\perp \gg 1$ or $q_z\xi_z \gg 1$ to the wave-vector-independent behavior expected in the A phase when *both* $q_\perp\xi_\perp \ll 1$ and $q_z\xi_z \ll 1$. This can be summarized as follows:

$$\Delta_{t,c}(\vec{q},T), \quad K(\vec{q},T) \propto \begin{cases} q_z^{-\eta_{t,c,K}/\zeta} & \text{region 1}, \\ q_\perp^{-\eta_{t,c,K}} & \text{region 2}, \\ \xi_\perp^{\eta_{t,c,K}} & \text{region 3}, \end{cases} \tag{1.38}$$

where $\xi_\perp \propto (T-T_{AC})^{-\nu_\perp}$, and the three regions in $\vec{q}$ space are illustrated in Fig. 3.

Having defined all of the critical exponents associated with this problem, we can now give several *exact* scaling relations between these exponents:

$$\alpha = 2 - \nu_\perp\left(d - 1 + \frac{\eta_K}{2} - \eta_t\right), \tag{1.39}$$

$$\beta = \nu_\perp(2d - 6 + 3\eta_K - 2\eta_t)/4, \tag{1.40}$$

$$\nu_z = \zeta\nu_\perp. \tag{1.41}$$

Note that α does *not* obey the usual anisotropic hyperscaling relation $\alpha=2-(d-1)\nu_\perp-\nu_z$; this is due to the strongly relevant disorder.

All of these exponents can be deduced experimentally from measurements either for $T>T_{AC}$ or $T<T_{AC}$. The spe-

cific heat can, of course, be measured by the usual thermodynamic measurements on either side of the transition.

The spontaneous tilt angle $\theta_L(T)$ is another matter. In pure systems, this is simply the angle between the sharp Bragg spot of the smectic C and $\hat{z}$ axis. However, as discussed earlier, in the smectic-C glass phase the x-ray-scattering peak is broad, with a width that remains *finite* as $T \to T_{AC}^-$. Hence, close to T_{AC}, the broad peak strongly overlaps the $\hat{z}$ axis, rendering measurement of $\theta_L(T)$ by this approach impossible. Unfortunately this is *precisely* the temperature range one needs to study to measure β.

Fortunately, an alternative measure of $\theta_L(T)$ is available in the disorder-averaged mean value of dielectric or diamagnetic susceptibility tensors χ_{ij} and ϵ_{ij}. In the A phase, one of the principal axes of both tensors is along the $\hat{z}$ axis. In the C phase, this axis spontaneously rotates away from the $\hat{z}$ axis due to the spontaneous tipping of the smectic layers and nematic directors. The rotation angle is proportional to $\theta_L(T)$.

The best experimental probe of the critical phenomena (in particular, the correlation lengths $\xi_\perp$ and ξ_z), as well as of the anomalous elasticity and disorder-induced fluctuations in both the A and C phases, is light scattering, which probes fluctuations in both the dielectric (ϵ_{ij}) and diamagnetic (χ_{ij}) susceptibility tensors.

Specifically, the large biaxial fluctuations on *both* sides of the transition lead to fluctuations in both ϵ_{ij} and χ_{ij} that are proportional to [13] $C_{ij}(\vec{q}) \equiv \overline{\langle N_i^\perp(\vec{q}) N_j^\perp(-\vec{q})\rangle}$, where $\vec{N}_\perp$ is the order parameter, which we remind the reader is the projection of the local layer normal perpendicular to the $\hat{z}$ axis.

The behavior of C_{ij} is radically different in the two phases and quite involved (as the intrepid reader is about to discover) in both. Here we will begin by summarizing the behavior in the (*relatively*) simpler A phase and then proceed to a description of the *even* more complicated behavior in the C phase.

In the A phase $(T > T_{AC})$, there are three important contributions to $C_{ij}(\vec{q})$: two arise from the previously discussed random tilt $[\Delta_t(\vec{q})]$ and compression $[\Delta_c(\vec{q})]$ disorders. The third is caused by random *positional* pinning Δ_p, which reflects the tendency of the aerogel to pin the smectic layers in particular *positions*. This type of disorder is *irrelevant* for $T \leqslant T_{AC}$, but becomes important at sufficiently long distance (or small $\vec{q}$) in the A phase (i.e., above T_{AC}). Indeed, as we will see in Sec. VIII, this random positional pinning Δ_p actually *dominates* the fluctuations at small $\vec{q}$ in the A phase; furthermore, it is precisely this pinning that leads to the destruction of long-range translational order and the replacement of sharp, δ-function Bragg peaks with power-law peaks, in the A phase.

Combining the contributions from these three distinct types of disorder gives

$$C_{ij}(\vec{q}) = L_{ij}^\perp(\hat{q}) \Bigg(\frac{\Delta_t(\vec{q},T) q_\perp^4}{[B q_z^2 + D(T) q_\perp^2 + K(\vec{q},T) q_\perp^4]^2} + \frac{\Delta_c(\vec{q},T) q_z^2 q_\perp^2}{[B q_z^2 + D(T) q_\perp^2 + K(\vec{q},T) q_\perp^4]^2} + \frac{C B^{1/2} D q_\perp^2}{[B q_z^2 + D(T) q_\perp^2 + K(\vec{q},T) q_\perp^4]^{3/2} q_0^2} \Bigg), \quad (1.42)$$

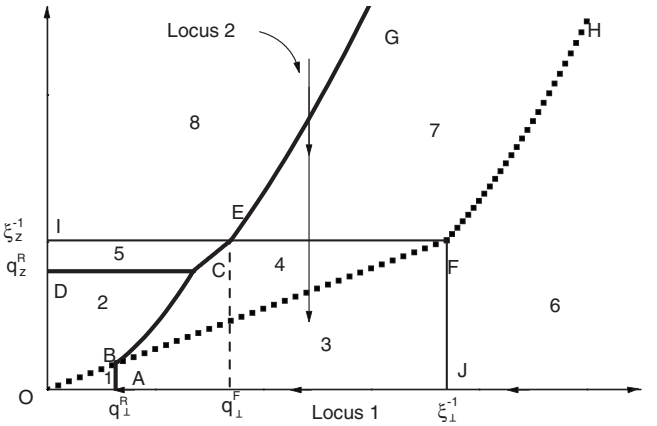

FIG. 4. Illustration of the eight regions listed in (1.44), each of which exhibits different scaling of the light-scattering intensity in the A phase as $T \to T_{AC}^+$. The light-scattering intensity is dominated by random field fluctuations in regions 1 and 2, by random tilt fluctuations in regions 3, 4, 6, and 7, and by random compression fluctuations in regions 5 and 8. Above locus OFH the common denominator in formula (1.42) is dominated by Bq_z^2, while below OFH it is dominated by $Kq_\perp^4$ in region 6 and by $Dq_\perp^2$ in regions 1 and 3, respectively.

where $L_{ij}^\perp(\hat{q}) \equiv q_i^\perp q_j^\perp / q_\perp^2$ is the projection operator along $\vec{q}_\perp$, the compression modulus B remains constant as $\vec{q} \to 0$, C is a universal, $O(1)$ constant $(C \approx 1.10\pi^2)$,

$$D(T) \propto \begin{cases} (T - T_{AC}) q_z^{-\eta_D/\zeta}, & \text{region 1}, \\ (T - T_{AC}) q_\perp^{-\eta_D}, & \text{region 2}, \\ \xi_\perp^{\eta_K - 2}, & \text{region 3}, \end{cases} \quad (1.43)$$

where $\eta_D = 2 - \eta_K - 1/\nu_\perp$ and the [wave-vector- $(\vec{q}$-) and temperature- (T)-dependent] disorder variances $\Delta_t(\vec{q},T)$ and $\Delta_c(\vec{q},T)$ and layer bend modulus $K(\vec{q},T)$ are given by Eq. (1.38). The C term comes from the periodic random pinning potential. The three regions in (1.43) are again illustrated in Fig. 3.

Clearly, expression (1.42) for C_{ij} is somewhat complicated due to the fact that *three* distinct types of disorder contribute to layer normal fluctuations. The situation is further exacerbated by the strong wave-vector and temperature dependence of the elastic constants D and K. Fortunately, there are well-defined regions of the wave vector $\vec{q}$, in each of which one of the three terms (i.e., Δ_t, Δ_c, or Δ_p embodied in the C term) dominate C_{ij}, thereby simplifying the expression for it. Each of these regions can be further subdivided according to which of the terms Bq_z^2, $D(T)q_\perp^2$, and $K(\vec{q},T)q_\perp^4$ dominates the common denominator $Bq_z^2 + D(T)q_\perp^2 + K(\vec{q},T)q_\perp^4$ of all three terms. In addition, $K(\vec{q},T)$, $\Delta_{c,t}(\vec{q},T)$, and $D(T)$ themselves have the crossovers embodied in Eqs. (1.38) and (1.43), which further subdivide some of the regions of $\vec{q}$ space into subregions of distinct behavior.

Painstakingly, but essentially straightforwardly, sorting out these different regions leads to the identification of *eight* distinct regions of qualitatively different wave-vector dependence for C_{ij}, which are illustrated in Fig. 4. The leading

wave-vector and temperature dependence of C_{ij} in each of these regions is

$$C_{ij}(\vec{q}) \sim \begin{cases} \frac{\xi_{NL}^{\perp}}{\lambda q_0^2}\left(\frac{\xi_{NL}^{\perp}}{\xi_{\perp}}\right)^{\eta_K/2-1}\frac{1}{q_{\perp}}, & \text{region 1,} \\ \frac{\lambda^2}{q_0^2(\xi_{NL}^{\perp})^2}\left(\frac{\xi_{NL}^{\perp}}{\xi_{\perp}}\right)^{2-\eta_K}\frac{q_{\perp}^2}{q_z^3}, & \text{region 2,} \\ \lambda(\xi_{NL}^{\perp})^2\left(\frac{\xi_{NL}^{\perp}}{\xi_{\perp}}\right)^{2\eta_K-\eta_t-4}, & \text{region 3,} \\ \frac{\lambda^5}{(\xi_{NL}^{\perp})^2}\left(\frac{\xi_{NL}^{\perp}}{\xi_{\perp}}\right)^{-\eta_t}\left(\frac{q_{\perp}}{q_z}\right)^4, & \text{region 4,} \\ \frac{\lambda^5\Delta_c^0}{(\xi_{NL}^{\perp})^2\Delta_t^0}\left(\frac{\xi_{NL}^{\perp}}{\xi_{\perp}}\right)^{-\eta_c}\left(\frac{q_{\perp}}{q_z}\right)^2, & \text{region 5,} \\ \frac{\lambda}{(\xi_{NL}^{\perp})^2}(\xi_{NL}^{\perp}q_{\perp})^{2\eta_K-\eta_t}\frac{1}{q_{\perp}^4}, & \text{region 6,} \\ \frac{\lambda^5}{(\xi_{NL}^{\perp})^2}(q_z\xi_{NL}^z)^{-\eta_t/\zeta}\left(\frac{q_{\perp}}{q_z}\right)^4, & \text{region 7,} \\ \frac{\lambda^5\Delta_c^0}{(\xi_{NL}^{\perp})^2\Delta_t^0}(q_z\xi_{NL}^z)^{-\eta_c/\zeta}\left(\frac{q_{\perp}}{q_z}\right)^2, & \text{region 8.} \end{cases} \tag{1.44}$$

In (1.44) we have used the standard "smectic penetration length" $\lambda \equiv \sqrt{K_0/B_0}$, where K_0 and B_0 are the "bare" smectic-layer bending modulus and compression modulus, respectively—i.e., the bending modulus and compression modulus for the smectic in the absence of disorder. The loci separating the regions in Fig. 4 are

$$FH: \quad q_z\xi_{NL}^z = (q_{\perp}\xi_{NL}^{\perp})^{2-\eta_K/2}, \tag{1.45}$$

$$EG: \quad q_z\xi_{NL}^z = (q_{\perp}\xi_{NL}^z\sqrt{\Delta_t^0/\Delta_c^0})^A, \tag{1.46}$$

$$CE: \quad q_z = \sqrt{\Delta_t^0/\Delta_c^0}\left(\frac{\xi_{NL}^{\perp}}{\xi_{\perp}}\right)^{1-(\eta_K+\eta_3)/2} q_{\perp}, \tag{1.47}$$

$$AB: \quad q_{\perp} = q_{\perp}^R = \frac{1}{q_0^2\lambda^2\xi_{NL}^{\perp}}\left(\frac{\xi_{\perp}}{\xi_{NL}^{\perp}}\right)^{3\eta_K/2-\eta_t-3}, \tag{1.48}$$

$$DC: \quad q_z = q_z^R = \frac{\Delta_t^0}{q_0^2\lambda^3\Delta_c^0}\left(\frac{\xi_{NL}^{\perp}}{\xi_{\perp}}\right)^{4+\eta_t-2\eta_K-\eta_3}, \tag{1.49}$$

$$OF: \quad q_z = \frac{\lambda}{\xi_{NL}^{\perp}}\left(\frac{\xi_{\perp}}{\xi_{NL}^{\perp}}\right)^{\eta_K/2-1} q_{\perp}, \tag{1.50}$$

$$BC: \quad q_z = q_0^2\lambda^3\left(\frac{\xi_{\perp}}{\xi_{NL}^{\perp}}\right)^{2+\eta_t-\eta_K} q_{\perp}^2, \tag{1.51}$$

where $q_0 \equiv 2\pi/a$, $\xi_{NL}^z \equiv (\xi_{NL}^{\perp})^2/\lambda$, $A \equiv \zeta/(1+\eta_3/2)$, and a is the smectic-layer spacing. Here the positive-definite universal exponent η_3 is defined in Eq. (B3). We have calculated it in the $\epsilon = 5-d$ expansion and found

$$\eta_3 = \frac{\epsilon}{5} + O(\epsilon^2). \tag{1.52}$$

Of course, none of these crossover lines is sharp, since none of the crossovers is abrupt. Rather, as is the nature of all crossovers, these are loci near which two terms start to become comparable. Hence, these crossover boundaries are only defined up to $O(1)$ factors.

The fairly complicated scaling behavior embodied in (1.42) simplifies considerably when we take $q_z=0$ and vary $q_{\perp}$ (i.e., move along locus 1 in Fig. 4). The second term in (1.42) then vanishes. For $q_{\perp} \gg \xi_{\perp}^{-1}$, $Kq_{\perp}^4$ dominates in the denominator of the first term in (1.42), which term itself dominates the third term, and using (1.44) we obtain $\langle N_i^{\perp}(\vec{q})N_j^{\perp}(-\vec{q})\rangle \propto q_{\perp}^{-4+2\eta_K-\eta_t}$. For $q_{\perp} \ll \xi_{\perp}^{-1}$, the first term dominates at short wavelengths and the third term dominates at long wavelengths. The crossover between these two is at

$$q_{\perp} = (\xi_{\perp}^R)^{-1} \propto \xi_{\perp}^{-3+(3/2)\eta_K-\eta_t}. \tag{1.53}$$

$\xi_{\perp}^R$ is much larger than $\xi_{\perp}$ as $T \to T_{AC}^+$, provided $3+\eta_t-\frac{3\eta_K}{2} > 1$, a condition we can show to be satisfied. Clearly, for $q \gg (\xi_{\perp}^R)^{-1}$, if there were *no* anomalous elasticity of K (i.e., *if* $\eta_K=0$), the light-scattering line shape would be a Lorentzian squared, with correlation length $\xi_{\perp}$. In reality, the line shape is *quantitatively* different (e.g., its tails scale like $q_{\perp}^{-4+2\eta_K-\eta_t}$), but still qualitatively like a Lorentzian squared, with linewidth $\xi_{\perp}^{-1}$. For $q \ll (\xi_{\perp}^R)^{-1}$ the light scattering diverges as a power law. More precisely,

$$\begin{aligned} C_{ij}(q_{\perp}, \vec{q_z}=0) &= L_{ij}^{\perp}(\hat{q})\left(\frac{\Delta_t(\vec{q}_{\perp}, q_z=0, T)}{[D(T)+K(\vec{q}_{\perp}, q_z=0, T)q_{\perp}^2]^2} + \frac{CB^{1/2}D}{[D(T)+K(\vec{q}_{\perp}, q_z=0, T)q_{\perp}^2]q_{\perp}q_0^2}\right) \\ &\sim \begin{cases} \frac{\lambda}{(\xi_{NL}^{\perp})^2}(\xi_{NL}^{\perp}q_{\perp})^{2\eta_K-\eta_t}\frac{1}{q_{\perp}^4}, & q_{\perp} \gg \xi_{\perp}^{-1}, \\ \lambda(\xi_{NL}^{\perp})^2\left(\frac{\xi_{NL}^{\perp}}{\xi_{\perp}}\right)^{2\eta_K-\eta_t-4}, & (\xi_{\perp}^R)^{-1} \ll q_{\perp} \ll \xi_{\perp}^{-1}, \\ \frac{\xi_{NL}^{\perp}}{\lambda q_0^2}\left(\frac{\xi_{NL}^{\perp}}{\xi_{\perp}}\right)^{\eta_K/2-1}\frac{1}{q_{\perp}}, & q_{\perp} \ll (\xi_{\perp}^R)^{-1}. \end{cases} \end{aligned} \tag{1.54}$$

Comparison of this expression with light-scattering data should allow easy determination of $\xi_{\perp}(T)$ and the combination of exponents $2\eta_K-\eta_t$. Fitting the T dependence of $\xi_{\perp}(T)$ to $(T-T_{AC})^{-\nu_{\perp}}$ then determines $\nu_{\perp}$.

Another simple locus is obtained by taking $q_{\perp}$ fixed in the range [14] $q_{\perp}^F \ll q_{\perp} \ll \xi_{\perp}^{-1}$ and varying q_z (i.e., moving along locus 2 in Fig. 4), which gives

$$C_{ij}(\vec{q}) \sim \begin{cases} \dfrac{\lambda^5 \Delta_c^0}{\Delta_t^0 (\xi_{NL}^{\perp})^2} (q_z \xi_{NL}^z)^{-\eta_c/\zeta} \left(\dfrac{q_\perp}{q_z}\right)^2, & q_z \gg (q_\perp \xi_{NL}^z)^A (\xi_{NL}^z)^{-1}, \\ \dfrac{\lambda^5}{(\xi_{NL}^{\perp})^2} (q_z \xi_{NL}^z)^{-\eta_t/\zeta} \left(\dfrac{q_\perp}{q_z}\right)^4, & (\xi_z)^{-1} \ll q_z \ll (q_\perp \xi_{NL}^z)^A (\xi_{NL}^z)^{-1}, \\ \dfrac{\lambda^5}{(\xi_{NL}^{\perp})^2} \left(\dfrac{\xi_{NL}^{\perp}}{\xi_\perp}\right)^{-\eta_t} \left(\dfrac{q_\perp}{q_z}\right)^4, & \dfrac{\lambda}{\xi_{NL}^{\perp}} \left(\dfrac{\xi_\perp}{\xi_{NL}^{\perp}}\right)^{\eta_K/2-1} q_\perp \ll q_z \ll (\xi_z)^{-1}, \\ \lambda (\xi_{NL}^{\perp})^2 \left(\dfrac{\xi_{NL}^{\perp}}{\xi_\perp}\right)^{2\eta_K - \eta_t - 4}, & 0 \ll q_z \ll \dfrac{\lambda}{\xi_{NL}^{\perp}} \left(\dfrac{\xi_\perp}{\xi_{NL}^{\perp}}\right)^{\eta_K/2-1} q_\perp, \end{cases} \tag{1.55}$$

where $q_\perp^F \sim \xi_z^{-1} (\xi_{NL}^{\perp}/\xi_\perp)^{(\eta_K+\eta_3)/2-1}$. From this locus ξ_z can be read from the point where a log-log plot of $I(\vec{q})$ vs q_z for fixed $\vec{q}_\perp$ changes slope from $-\frac{\eta_t}{\zeta}-4$ to -4. Again, once $\xi_z(T)$ is known, ν_z can be determined. Note that measurements of the exponents $\frac{\eta_t}{\zeta}+4$ and $\frac{\eta_c}{\zeta}+2$, taken in conjunction with knowledge of $\eta_t - 2\eta_K$ from locus 1, determine η_K, η_t, and η_c (recall that the anisotropy exponent $\zeta = 2 - \frac{\eta_K}{2}$).

To summarize our light-scattering predictions for the *A* side of the critical regime: measurements along locus 1 and 2 can be used to determine the exponents $\nu_\perp$, ν_z, η_K, and η_t, as well as testing that $\eta_B = 0$ (which was assumed in the above discussion). These exponents can then be quantitatively compared with our predictions and, furthermore, test the *exact* scaling relation (1.41), and, combined with specific heat measurements, test the *exact* scaling relation (1.39) for α and, with the aforedescribed dielectric measurement determination of β, test the equally *exact* scaling relation (1.40).

We now turn to the smectic *C* ($T < T_{AC}$). For $q_\perp \xi_\perp \gg 1$ or $q_z \xi_z \gg 1$, the light scattering is the same as in the high-temperature case, since this range of wave vectors corresponds to the critical regime, in which one cannot tell whether one is on the high-or low-temperature side of the transition. In the other limit—namely, when both $q_\perp \xi_\perp \ll 1$ and $q_z \xi_z \ll 1$—we are in the smectic-*C*-phase range of wave vectors and C_{ij} is given by

$$C_{ij}(\vec{q}) = L_{ij}^{\perp}(\hat{q}) \left(\frac{\Delta_{s'}(\vec{q}',T) q_{s'}^2 q_\perp^2}{[\gamma(\vec{q}',T) q_{x'}^2 + \tilde{B} q_{z'}^2 + \tilde{K}(\vec{q}',T) q_{s'}^4]^2} + \frac{\Delta_{z'}(T) q_{z'}^2 q_\perp^2}{[\gamma(\vec{q}',T) q_{x'}^2 + \tilde{B} q_{z'}^2 + \tilde{K}(\vec{q}',T) q_{s'}^4]^2} \right) + L_{ij}^{\perp}(\hat{q}) \frac{\Delta_{x'}(\vec{q}',T) q_{x'}^2 q_\perp^2}{[\gamma(\vec{q}',T) q_{x'}^2 + \tilde{B} q_{z'}^2 + \tilde{K}(\vec{q}',T) q_{s'}^4]^2}, \tag{1.56}$$

where $q_{x'}$, $q_{s'}$, and $q_{z'}$ are defined in Eqs. (1.8)–(1.10) respectively, $\tilde{K}$, γ, and $\Delta_{s',x'}$ are anomalous and given in Eqs. (1.5), (1.7), and (1.6), and $\Delta_{z'}$ is wave vector $\vec{q}$ independent. In addition, the temperature-dependent quantity $\Gamma(T)$ defined in the coordinate transformations, Eqs. (1.8)–(1.10) has the critical scaling

$$\Gamma(T) \propto \left(\frac{\xi_\perp}{\xi_{NL}^{\perp}}\right)^{1-(\eta_K+\eta_3)/2}. \tag{1.57}$$

Since the azimuthal symmetry about the $\hat{z}$ axis has been broken due to the tilting of the layers, the light scattering also loses azimuthal symmetry and becomes fully three dimensional. It is most conveniently described in the transformed, nonorthogonal wave-vector coordinates (i.e., $\vec{q}$ space), whose relation to the laboratory wave-vector coordinates (i.e., $\vec{q}$ space) are given in Eqs. (1.8)–(1.10).

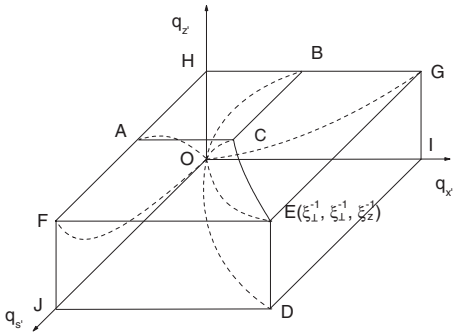

FIG. 5. Three-dimensional picture in the transformed reciprocal space ($\vec{q}$ space) illustrating the five distinct regions with different wave-vector dependences of $C_{ij}(\vec{q})$ in the *C* phase, which is given in (1.58).

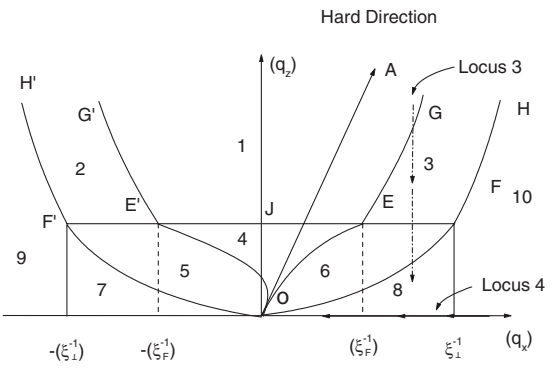

FIG. 6. Illustration of the ten distinct regions in the $q_z - q_x$ plane with different wave-vector dependences of $C_{xx}(\vec{q})$, which is given in (1.69) for the *C* phase. Line *OA* is define by $q_{x'} = 0$.

As in the A phase, in the C phase the light scattering displays many different regimes of very different scaling with wave vector and temperature, due, as there, to both the crossovers between domination by different types of disorder and by the crossovers between dependences on different components of $\vec{q}$. Here, the three-dimensional $\vec{q}'$ space is divided into the five regions illustrated in Fig. 5, in which the light-scattering intensity is given by

$$C_{ij}(\vec{q}) \approx L_{ij}^{\perp} q_{\perp}^2 \begin{cases} \dfrac{\Delta_n^0 \lambda^5}{\Delta_t^0 (\xi_{NL}^{\perp})^2} \left(\dfrac{\xi_{\perp}}{\xi_{NL}^{\perp}}\right)^{\eta_c} \left(\dfrac{1}{q_{z'}}\right)^2, & \text{region } O\text{-}ABCH, \\ \dfrac{\lambda^5}{(\xi_{NL}^{\perp})^2} \left(\dfrac{\xi_{\perp}}{\xi_{NL}^{\perp}}\right)^{\eta_t} (\xi_z q_{z'})^{-\tilde{\eta}_{s'}/\tilde{\zeta}_{z'}} \left(\dfrac{q_{s'}}{q_{z'}^2}\right)^2, & \text{region } O\text{-}AFEC, \\ \dfrac{\lambda^5}{(\xi_{NL}^{\perp})^2} \left(\dfrac{\xi_{\perp}}{\xi_{NL}^{\perp}}\right)^{\eta_t} (\xi_z q_{z'})^{-\tilde{\eta}_{x'}/\tilde{\zeta}_{z'}} \left(\dfrac{q_{x'}}{q_{z'}^2}\right)^2, & \text{region } O\text{-}CEGB, \\ \dfrac{\lambda}{(\xi_{NL}^{\perp})^2} \left(\dfrac{\xi_{\perp}}{\xi_{NL}^{\perp}}\right)^{\eta_t - 2\eta_K} (\xi_{\perp} q_{s'})^{2\tilde{\eta}_K - \tilde{\eta}_{s'}} \left(\dfrac{1}{q_{s'}}\right)^6, & \text{region } O\text{-}FJDE, \\ \lambda (\xi_{NL}^{\perp})^2 \left(\dfrac{\xi_{\perp}}{\xi_{NL}^{\perp}}\right)^{\eta_t - 2\eta_K + 4} (\xi_{\perp} q_{x'})^{(-2\tilde{\eta}_{\gamma} - \tilde{\eta}_{x'})/\tilde{\zeta}_{x'}} \left(\dfrac{1}{q_{x'}}\right)^2, & \text{region } O\text{-}EDIG. \end{cases} \tag{1.58}$$

The crossovers between these five regions obey

$$OAC: \quad q_{z'} \xi_z = \left[\sqrt{\frac{\Delta_t^0}{\Delta_n^0}} \left(\frac{\xi_{\perp}}{\xi_{NL}^{\perp}}\right)^{\eta_3/2} \left(\frac{\xi_{NL}^{\perp}}{\lambda}\right) \times (q_{s'} \xi_{\perp}) \right]^{\tilde{\phi}_{s'z'}}, \tag{1.59}$$

$$OFE: \quad q_{z'} \xi_z = (q_{s'} \xi_{\perp})^{\tilde{\zeta}_{z'}}, \tag{1.60}$$

$$OBC: \quad q_{z'} \xi_z = \left[\sqrt{\frac{\Delta_t^0}{\Delta_n^0}} \left(\frac{\xi_{\perp}}{\xi_{NL}^{\perp}}\right)^{\eta_3/2} \left(\frac{\xi_{NL}^{\perp}}{\lambda}\right) \times (q_{x'} \xi_{\perp}) \right]^{\tilde{\phi}_{x'z'}}, \tag{1.61}$$

$$OGE: \quad q_{z'} \xi_z = (q_{x'} \xi_{\perp})^{\tilde{\zeta}_{z'}/\tilde{\zeta}_{x'}}, \tag{1.62}$$

$$ODE: \quad q_{x'} \xi_{\perp} = (q_{s'} \xi_{\perp})^{\tilde{\zeta}_{x'}}, \tag{1.63}$$

$$OEC: \quad q_{x'} = (q_{z'} \xi_z)^{\tilde{\phi}_{s'x'}} q_{s'}, \tag{1.64}$$

where we have defined the C-phase crossover exponents

$$\tilde{\phi}_{s'z'} = 2\tilde{\zeta}_{z'}/(2\tilde{\zeta}_{z'} + \tilde{\eta}_{s'}), \tag{1.65}$$

$$\tilde{\phi}_{x'z'} = 2\tilde{\zeta}_{z'}/(2\tilde{\zeta}_{z'} + \tilde{\eta}_{x'}), \tag{1.66}$$

$$\tilde{\phi}_{s'x'} = (2 - \tilde{\eta}_K - \tilde{\eta}_{\gamma})/2\tilde{\zeta}_{z'}, \tag{1.67}$$

and the quantity $\Delta_n^0 = \Delta_c^0 + \Delta_t^0 g_0^2 (\xi_{NL}^{\perp})^2 / w_0 K_0$, where g_0 and w_0 are the completely bare values of of the coefficients of the anharmonic terms in the Hamiltonian (3.1).

Now let us narrow our discussion to wave vectors in the $q_z - q_x$ plane and measure $C_{ij}(\vec{q})$ given by

$$C_{xx}(\vec{q}) = \frac{[\Delta_{z'} q_{z'}^2 + \Delta_{x'}(\vec{q},T) q_{x'}^2] q_x^2}{[\gamma(\vec{q},T) q_{x'}^2 + \tilde{B} q_{z'}^2]^2}, \tag{1.68}$$

where we alert the reader to the fact that this expression contains *both* the *rotated* wave-vector component $q_{x'}$ and the *unrotated* wave-vector component q_x.

This two-dimensional $q_z - q_x$ plane can also be divided into different regions with different wave-vector dependences of $C_{xx}(\vec{q})$, including (for illustration) the critical regime (i.e., $q_z \gg \xi_z^{-1}$ or $q_{\perp} \gg \xi_{\perp}^{-1}$). (Note that we are now working with the *untransformed* $\vec{q}$'s). This leads to the ten regions which are illustrated in Fig. 6. In these regions, the light-scattering results are

$$C_{xx}(\vec{q}) \sim \begin{cases} \dfrac{\lambda^5 \Delta_c^0}{(\xi_{NL}^{\perp})^2 \Delta_t^0} (q_z \xi_{NL}^z)^{-\eta_c/\zeta} \left(\dfrac{q_x}{q_z}\right)^2, & \text{region 1,} \\ \dfrac{\lambda^5}{(\xi_{NL}^{\perp})^2} (q_z \xi_{NL}^z)^{-\eta_t/\zeta} \left(\dfrac{q_x}{q_z}\right)^4, & \text{region 2,3,} \\ \dfrac{\lambda^5 \Delta_c^0}{(\xi_{NL}^{\perp})^2 \Delta_t^0} \left(\dfrac{\xi_{\perp}}{\xi_{NL}^{\perp}}\right)^{\eta_c} \left(\dfrac{q_x}{q_z}\right)^2, & \text{region 4,} \\ \dfrac{\lambda^5}{(\xi_{NL}^{\perp})^2} (q_z \xi_z)^{-\tilde{\eta}_{x'}/\tilde{\zeta}_{z'}} \left(\dfrac{\xi_{\perp}}{\xi_N^{\perp}}\right)^{\eta_t} \left(\dfrac{q_x}{q_z}\right)^4, & \text{region 5,6,} \\ \dfrac{\lambda \xi_{\perp}^4}{(\xi_{NL}^{\perp})^2} (q_x \xi_{\perp})^{-(\tilde{\eta}_{x'}+2\tilde{\eta}_{\gamma})/\tilde{\zeta}_{x'}} \left(\dfrac{\xi_{\perp}}{\xi_{NL}^{\perp}}\right)^{-2\eta_K+\eta_t}, & \text{region 7,8,} \\ \dfrac{\lambda}{(\xi_{NL}^{\perp})^2} (q_x \xi_{NL}^{\perp})^{2\eta_K-\eta_t} q_x^{-4}, & \text{region 9,10.} \end{cases} \tag{1.69}$$

At short wavelengths (i.e., $q_x \gg \xi_{\perp}^{-1}$ or $q_z \gg \xi_z^{-1}$)—that is, in the critical regime—the crossovers between the different regions remain the same as those of the high-temperature phase, which were given in Eqs. (1.45) and (1.46). At long wavelengths (i.e., both $q_z \ll \xi_z^{-1}$ and $q_x \ll \xi_{\perp}^{-1}$) the crossovers are given by

$$OE, OE': q_z \xi_z = \left[\sqrt{\frac{\Delta_t^0}{\Delta_n^0}} \left(\frac{\xi_z}{\Gamma}\right) (q_x - \Gamma q_z) \right]^{\tilde{\phi}_{x'z'}},$$

$$OF, OF': (q_z \xi_z)^{\tilde{\zeta}_{x'}} = (q_x \xi_{\perp})^{\tilde{\zeta}_{z'}}.$$

Two possible experimental loci through the $q_x - q_z$ plane are shown in Fig. 6. By holding q_x fixed and varying q_z (locus 3), we can determine $-\tilde{\eta}_{x'}/\tilde{\zeta}_{z'} - 4$ from a log-log plot of $I(\vec{q})$ vs q_z and also deduce ξ_z from the location of the point at which the log-log plot changes slope from $-\tilde{\eta}_{x'}/\tilde{\zeta}_{z'} - 4$ to $-\eta_t/\zeta - 4$. Likewise $-(\tilde{\eta}_{x'} + 2\tilde{\eta}_{\gamma})/\tilde{\zeta}_{x'}$ and $\xi_{\perp}$ can be determined by moving along locus 4 (the q_x axis).

To completely determine the anomalous exponents for the low-temperature phase, one more experiment is necessary. One possibility is to measure the light scattering at both $q_z = 0$ and $q_x = 0$, varying q_s, for which (1.56) leads to

$$C_{ss}(\vec{q}) \sim \begin{cases} \dfrac{\lambda}{(\xi_{NL}^{\perp})^2} (\xi_{NL}^{\perp} q_s)^{2\eta_K - \eta_t} \left(\dfrac{1}{q_s}\right)^4, & q_s \gg \xi_{\perp}, \\ \dfrac{\lambda}{(\xi_{NL}^{\perp})^2} \left(\dfrac{\xi_{\perp}}{\xi_{NL}^{\perp}}\right)^{\eta_t - 2\eta_K} (\xi_{\perp} q_s)^{2\tilde{\eta}_K - \tilde{\eta}_{s'}} \left(\dfrac{1}{q_s}\right)^4, & q_s \ll \xi_{\perp}. \end{cases} \tag{1.70}$$

Such measurements along this experimental locus determine $2\tilde{\eta}_K - \tilde{\eta}_{s'} - 4$ and also measure $\xi_{\perp}$. Combining this result with the data for $-\tilde{\eta}_{x'}/\tilde{\zeta}_{z'} - 4$ and $-(\tilde{\eta}_{x'} + 2\tilde{\eta}_{\gamma})/\tilde{\zeta}_{x'}$ and the scaling relations (1.18), we can deduce the exponents $\tilde{\eta}_{\gamma}$, $\tilde{\eta}_K$, $\tilde{\eta}_{s'}$, and $\tilde{\eta}_{x'}$ and, furthermore, check the scaling relation (1.19).

Finally our prediction for the behavior of the thermodynamically sharp smectic-*A* to -*C* transition is valid only if the universal anomalous exponents η_K and η_t satisfy the bounds

$$\eta_t - \frac{3\eta_K}{2} < d - 3, \tag{1.71}$$

$$2\eta_t - \eta_K < 0, \tag{1.72}$$

which come from requiring the system to be orientationally ordered and dislocation bound right at the critical point. We test the two conditions using the values of η_K and η_t obtained by the ϵ expansion to $O(\epsilon^2)$. Unfortunately, the two conditions are not satisfied in the physical dimension $d=3$, which seems to imply that the second-order phase transition is not stable. However, since $\epsilon = 2$ in $d=3$, the ϵ expansion is not quantitatively reliable, and therefore whether the second-order phase transition is stable in $d=3$ remains an open question.

The remainder of this paper is organized as follows. In Sec. II, we derive our model for the smectic in stretched aerogel and perform the "replica trick" on it. In Sec. III, we derive the renormalization-group recursion relations for the model near the *AC* transition, identify their stable fixed point, and calculate the thermodynamic critical exponents in a $d = 5 - \epsilon$ expansion. In Sec. IV, we calculate the critical exponents. In Secs. V and VII, we calculate the wave-vector dependences of the elastic constants and disorder variances. In Sec. VI, we treat the smectic-*A* and -*C* phases of the model and show that the former is in the XYBG universality class, while the latter is in the $m=1$ smectic Bragg glass [6] universality class. In Sec. VIII, we calculate correlation functions near critical region. In Sec. IX, we discuss the validity of our predictions for the critical behavior against the unbinding of topological defects and the loss of orientational order.

II. MODEL

As in earlier treatments of smectic-*A* and -*C* phases [15] in *clean* environments, we expect, even in the presence of disorder, that the important fluctuating variables in our system the "layer displacement field" $u(\vec{r})$ and the molecular axis $\hat{n}(\vec{r})$. The layer displacement field $u(\vec{r})$ is defined, as usual, as the displacement along the mean layer normal of the layers relative to some ideal reference configuration of flat, uniformly spaced layers. We will choose the orientation of these reference layers to be perpendicular to the stretch axis.

We will derive our starting Hamiltonian by beginning with that for a smectic-*A* phase in a clean environment and then modifying it to reflect the effects of the aerogel and to allow the molecular axes $\hat{n}(\vec{r})$ to tilt away from the layer normal.

The Hamiltonian for the smectic-*A* phase in a clean environment is [15]

$$H_{cl} \equiv \int d^d r \left[\frac{K}{2}(\nabla_\perp^2 u)^2 + \frac{B}{2}\left(\partial_z u - \frac{1}{2}|\vec{\nabla}_\perp u|^2\right)^2 \right]$$
$$= \int d^d r \left[\frac{K}{2}(\nabla_\perp^2 u)^2 + \frac{B}{2}(\partial_z u)^2 - \frac{g}{2}(\partial_z u)|\vec{\nabla}_\perp u|^2 + \frac{w}{8}|\vec{\nabla}_\perp u|^4 \right], \tag{2.1}$$

where, in the second equality, $g=w=B$. This equality of g, w, and B, which is, of course, a consequence of simply expanding out the square of the B term in Eq. (2.1), is also a consequence of the global rotation invariance of a smectic in the clean system, since it is that invariance which forces the B term to be precisely the square of the rotation invariant quantity $E \equiv \partial_z u - \frac{1}{2}|\vec{\nabla}_\perp u|^2$ in the first place.

Once the smectic is placed in a non-rotation-invariant environment like stretched aerogel, we no longer have the constraint of rotation invariance. However, obviously, any term that was allowed by symmetry in the rotation-invariant case will certainly be allowed when the symmetry is lowered. Hence, the B, g, and w terms in the second equality of Eq. (2.1) are still *allowed* when the smectic is put in anisotropic aerogel. But since that system is no longer rotation invariant, there is no longer any symmetry requiring that $B=g=w$. Thus, for a smectic in anisotropic aerogel, part of the Hamiltonian will be just the expression after the second equality in (2.1) with *no* constraints relating B, g, and w; that is, all three will now be *independent* parameters of our model.

There are additional terms not present in (2.1) that are allowed in our Hamiltonian due to the absence of rotation invariance in our problem. In particular, there can and, hence, in general, *will* be terms picking out a preferred orientation for both the layer normal $\hat{N}$ and the molecular director $\hat{n}$. We will assume that both of these preferred directions are along the stretch axis $\hat{z}$. The simplest coupling that will accomplish this is

$$H_{stretch} \equiv -\int d^d r [M(\hat{N}\cdot\hat{z})^2 + Q(\hat{n}\cdot\hat{z})^2], \tag{2.2}$$

with M and N both >0. In addition, the molecular axis $\hat{n}$ and the layer normal $\hat{N}$ should couple. As noted by de Gennes [15], the simplest such coupling takes the form

$$H_{Nn} \equiv P \int d^d r |\hat{N} - \hat{n}|^2. \tag{2.3}$$

Using the well-known [15] geometrical relation

$$\hat{N} = \frac{\hat{z} - \vec{\nabla} u}{|\hat{z} - \vec{\nabla} u|} \tag{2.4}$$

between $\hat{N}$ and the layer displacement field u, defining $\vec{\delta n} \equiv \hat{n} - \hat{z}$, absorbing terms of $O(|\vec{\nabla}_\perp u|^4, |\vec{\delta n}|^4)$ in Eq. (2.2) into a shift of the quartic coupling w in Eq. (2.1), and adding terms reflecting the randomness of the aerogel, we obtain our starting Hamiltonian: $H=H_1+H_2$, with

$$H_1 \equiv \int d^d r \left[\frac{K}{2}(\nabla_\perp^2 u)^2 + \frac{B}{2}(\partial_z u)^2 - \frac{g}{2}(\partial_z u)|\vec{\nabla}_\perp u|^2 + \frac{w}{8}|\vec{\nabla}_\perp u|^4 + \vec{h}(\vec{r})\cdot\vec{\nabla} u + V_p(u - \phi(\vec{r})) \right] \tag{2.5}$$

and

$$H_2 \equiv \int d^d r [M|\vec{\nabla}_\perp u|^2 + P|\vec{\nabla}_\perp u + \vec{\delta n}_\perp|^2 + Q|\vec{\delta n}_\perp|^2]. \tag{2.6}$$

The $\vec{h}(\vec{r})$ in (2.5) is a quenched random field which we take to be Gaussian, zero mean, and characterized by short-range anisotropic correlations

$$\overline{h_i(\vec{r}) h_j(\vec{r}')} = [\Delta_t \delta_{ij}^\perp + \Delta_c \delta_{ij}^z]\delta^d(r - r'). \tag{2.7}$$

One might reasonably question this assumption of short-range correlations of the disorder, given the known fractal structure of aerogel. Indeed, while Ref. [12] argued that for liquid crystals in aerogel the components of $\vec{h}$ orthogonal to z do not have such long-range correlations, $h_z(\vec{r})$ *does*. Hence, our results are not directly applicable to these systems, although they could be applied to systems of higher aerogel density, which would have shorter-range correlations.

The field $\phi(\vec{r})$ in (2.5) is also a quenched random field with only short-range correlations and is uniformly distributed between 0 and a, the smectic-layer spacing. The function $V_p(u-\phi)$ is periodic with period a.

The physical interpretation of the quenched random fields $\vec{h}(\vec{r})$ and $V_p(u-\phi)$ is very simple. The random field $\vec{h}$ incorporates random torques and random compressions, coming from the $\perp$ and z components of $\vec{h}$, respectively. The function $V_p(u-\phi(\vec{r}))$ represents the tendency of the aerogel to pin the smectic layers in a set of random positions $\phi(\vec{r})$, modulo the smectic layer spacing a, which is why V_p is periodic in its argument. The Hamiltonian (2.5) is identical to the elastic

theory of a smectic *A* in isotropic aerogel developed in [12], with one crucial exception: in a smectic in isotropic aerogel, rotation invariance requires that $g=w=B$, while for our problem, even at $T=T_{AC}$, where softness is recovered, g and w are still free, because rotational invariance is still broken. The remaining effects of the anisotropy are incorporated in the M and Q terms in Eq. (2.6). It is the P term that actually drives the AC transition in this model. When P is positive, it is energetically favorable for $\hat{n}$ to be normal to the layers (which implies $\delta\vec{n}=-\vec{\nabla}_\perp u$), while, as we shall see in a moment, when P is sufficiently negative, it is energetically favorable for the molecules to tip relative to the layers, thereby putting the system in the *C* phase.

To see this, note that after a linear change of variable,

$$\delta\vec{n}'_\perp = \delta\vec{n}_\perp + R\vec{\nabla}_\perp u, \tag{2.8}$$

with $R\equiv P/(Q+P)$, Eq. (2.6) becomes

$$H_2 = \int d^d r\left[\frac{D(T)}{2}|\vec{\nabla}_\perp u|^2 + (P+Q)|\delta\vec{n}'_\perp|^2\right], \tag{2.9}$$

with $D(T)\equiv 2M+2QP/(Q+P)$. Assuming when temperature drops both M and Q remain positive and P decreases continuously from positive to negative, which drives the system from *A* phase into *C* phase, $D=M+QP/(Q+P)$ becomes negative first. Therefore just below T_{AC}, at the new ground state, $|\vec{\nabla}_\perp u|$ is nonzero, $\delta\vec{n}'_\perp=0$, which, combined with (2.8), gives $\delta\vec{n}_\perp=-R\vec{\nabla}_\perp u$. This implies that both the layers and the director tilt, but in opposite directions. Clearly, if $Q\gg M$, the layers tilt more than the molecules, while in the opposite limit ($M\gg Q$), the director tilts more, as observed in [17].

Since the fluctuations of $\delta\vec{n}'_\perp$ are massive, we can set $\delta\vec{n}'_\perp=0$ in (2.9) and use the sum of (2.5) and (2.9), which now only involves u, as our complete Hamiltonian:

$$H = \int d^d r\left[\frac{K}{2}(\nabla_\perp^2 u)^2 + \frac{B}{2}(\partial_z u)^2 + \frac{D}{2}|\vec{\nabla}_\perp u|^2 - \frac{g}{2}(\partial_z u)|\vec{\nabla}_\perp u|^2 + \frac{w}{8}|\vec{\nabla}_\perp u|^4 + \vec{h}(\vec{r})\cdot\vec{\nabla}u + V_p(u-\phi(\vec{r}))\right]. \tag{2.10}$$

Since $|\vec{\nabla}_\perp u|$ is proportional to the tilt angle of the smectic layers, the coefficient $D(T)$ is positive in the *A* phase (favoring alignment of the layer normal with the stretch axis) and negative in the *C* phase (favoring tilt of the layers). Hence, by continuity, at $T=T_{AC}$ $D(T)$ vanishes. In what follows, we will assume that $D(T)\propto T-T_{AC}$ near T_{AC}.

We can now treat the quenched disorder in this Hamiltonian using the replica trick [11,12]. This trick starts by assuming that the actual free energy and correlation functions measured in an experiment on a single sample will be close to the average values of these quantities when averaged over many realizations of the disorder, with a weight for this average given by the distributions described earlier. To compute, e.g., the average Free energy $\bar{F}=-T\overline{\ln Z}$, where Z is the partition function, we use on the identity $\overline{\ln Z}=\lim_{n\to 0}\frac{\overline{Z^n}-1}{n}$. $\overline{Z^n}$ can now be computed by doing a repeated functional integral over n "replicas" of the field u:

$$\begin{aligned}\overline{Z^n} &= \overline{\left(\int Du e^{-\beta H(u,\vec{h},\phi)}\right)^n} \\ &= \overline{\left(\int Du_1 e^{-\beta H(u_1,\vec{h},\phi)}\right)\left(\int Du_2 e^{-\beta H(u_2,\vec{h},\phi)}\right)} \\ &\quad \cdots \overline{\left(\int Du_n e^{-\beta H(u_n,\vec{h},\phi)}\right)} \\ &= \overline{\int \coprod_{\alpha=1}^{n} Du_\alpha \exp\left(-\beta\sum_\alpha H(u_\alpha,\vec{h},\phi)\right)}.\end{aligned} \tag{2.11}$$

The advantage gained via the replica trick is that the average over the random fields $\vec{h}$ and ϕ (which, we note, are the same for all n replicas) can now be done first, leading to an effective "replicated" Hamiltonian for the set of nu_α's alone. The average over the random fields $\vec{h}$ and ϕ couples the previously uncoupled replicas.

Details of how this averaging process is performed can be obtained in Ref. [12]. The calculations here are virtually identical, the only differences being the slightly different form of the starting Hamiltonian (2.5) and (2.6). After replicating and integrating over the disorder $\vec{h}(\vec{r})$ utilizing Eq. (2.7), we obtain

$$\begin{aligned}H[u_\alpha] = \frac{1}{2}\int d^d r\Bigg(\sum_{\alpha=1}^{n}\Bigg[&K(\nabla_\perp^2 u_\alpha)^2 + B(\partial_z u_\alpha)^2 \\ &- g(\partial_z u_\alpha)(\nabla_\perp u_\alpha)^2 + \frac{w}{4}|\vec{\nabla}_\perp u_\alpha|^4 + D(T)|\nabla_\perp u_\alpha|^2\Bigg] \\ &- \sum_{\alpha,\beta=1}^{n}\Bigg[\frac{\Delta_t}{2T}\nabla_\perp u_\alpha\cdot\nabla_\perp u_\beta + \frac{\Delta_c}{2T}\partial_z u_\alpha\cdot\partial_z u_\beta \\ &+ \frac{1}{T}\Delta_p(u_\alpha-u_\beta)\Bigg]\Bigg),\end{aligned} \tag{2.12}$$

where $\Delta_p(u_\alpha-u_\beta)$ is a periodic function with period a, the smectic-layer spacing.

III. RENORMALIZATION GROUP

In this section we derive the renormalization-group (RG) flow equations for studying the phase transition. The basic idea of the RG is to eliminate the short-length degrees of freedom of u and see how this affects the long-length physics. At length scales shorter than the correlation length, since the tilt term in Hamiltonian (2.12) is negligible compared to the bend term, our model is effectively similar to that for smectic *A* in *isotropic* aerogel, in which the tilt term is absent due to the symmetry. In the latter, Ref. [11] showed that the random field disorder $\Delta_p(u_\alpha-u_\beta)$ is irrelevant compared to the random tilt disorder in $d<5$. Repeating the (virtually identical) calculation for this problem, we also find that $\Delta_p(u_\alpha-u_\beta)$ is irrelevant in our problem at length scales

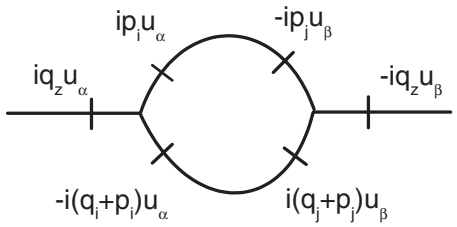

FIG. 7. The graphical correction to B coming from the combination of the two cubic vertices.

shorter than the correlation length. However, it becomes relevant at longer length scales in the A phase, which will be discussed in Sec. VI. In addition, the random compression term Δ_c can also be shown to be irrelevant in the RG sense. However, while it does *not* affect the RG recursion relations to lowest order in ϵ, it *does* prove to be important for the correlation functions. We will therefore treat it in detail later in Sec. VII.

With these simplifications, we can study the AC phase transition using the following truncated Hamiltonian:

$$H[u_\alpha] = \frac{1}{2}\int d^d r \sum_{\alpha=1}^{n}\left[K(\nabla_\perp^2 u_\alpha)^2 + B(\partial_z u_\alpha)^2 - g(\partial_z u_\alpha)(\nabla_\perp u_\alpha)^2 + \frac{w}{4}|\vec{\nabla}_\perp u_\alpha|^4 + D(T)|\nabla_\perp u_\alpha|^2\right] - \frac{\Delta_t}{2T}\int d^d r \sum_{\alpha,\beta=1}^{n} \nabla_\perp u_\alpha \cdot \nabla_\perp u_\beta. \tag{3.1}$$

This Hamiltonian's noninteracting propagator $G_{\alpha\beta}(\vec{q}) \equiv \langle u_\alpha(\vec{q}) u_\beta(-\vec{q})\rangle_0$ is found to be

$$G_{\alpha\beta}(\vec{q}) = TG(\vec{q})\delta_{\alpha\beta} + \Delta_t q_\perp^2 G(\vec{q})^2, \tag{3.2}$$

with

$$G(\vec{q}) = \frac{1}{Bq_z^2 + Kq_\perp^4}. \tag{3.3}$$

To qualitatively estimate the effect of the anharmonic terms in Hamiltonian (3.1), we use ordinary perturbation theory. We find that perturbation theory breaks down in $d < 5$. This can be seen by calculating the one-loop graphical correction to B, which is represented by the Feynman diagram in Fig. 7. An analysis of the Feynman diagram gives

$$-\frac{g^2}{4T}\sum_{\alpha=1}^{n}\sum_{\beta=1}^{n}\sum_{q} q_z^2 u_\alpha(\vec{q}) u_\beta(-\vec{q})\int_p p_\perp^4 G_{\alpha\beta}(\vec{p})^2, \tag{3.4}$$

in which

$$G_{\alpha\beta}(\vec{p})^2 = [T^2 G(\vec{p})^2 + 2T\Delta_t p_\perp^2 G(\vec{p})^3]\delta_{\alpha\beta} + \Delta_t^2 p_\perp^4 G(\vec{p})^4, \tag{3.5}$$

where $\delta_{\alpha\beta}$ is a Kronecker delta function. This diagram leads to two contributions. One of them is

$$-\frac{g^2\Delta_t^2}{4T}\sum_{\alpha=1}^{n}\sum_{\beta=1}^{n}\sum_{q} q_z^2 u_\alpha(\vec{q}) u_\beta(-\vec{q})\int_p p_\perp^8 G(\vec{p})^4, \tag{3.6}$$

which is actually a contribution to the random compression. We will not discuss this contribution here since the random compression is irrelevant. Later we will come back to it when we calculate the wave-vector dependence of Δ_c. The other contribution is

$$-\frac{g^2}{4}\sum_{\alpha=1}^{n}\sum_{q} q_z^2 u_\alpha(\vec{q}) u_\alpha(-\vec{q}) \times \int_p p_\perp^4 [TG(\vec{p})^2 + 2\Delta_t p_\perp^2 G(\vec{p})^3], \tag{3.7}$$

from which we obtain the correction to the compression modulus B:

$$\begin{aligned}\delta B &= -\frac{g^2}{2}\int_p p_\perp^4 [TG(\vec{p})^2 + 2\Delta_t p_\perp^2 G(\vec{p})^3] \\ &\approx -g^2\Delta_t \int_p \frac{p_\perp^6}{(Bp_z^2 + Kp_\perp^4)^3} \\ &\approx -g^2\Delta_t \int_{-\infty}^{\infty}\frac{dp_z}{2\pi}\int_{\frac{1}{L}}^{\Lambda}\frac{d^{d-1}p_\perp}{(2\pi)^{d-1}}\frac{p_\perp^6}{(Bp_z^2 + Kp_\perp^4)^3} \\ &\approx -\frac{3}{16}\frac{S_{d-1}B\Delta_t}{(2\pi)^{d-1}(5-d)}\left(\frac{g}{B}\right)^2\left(\frac{B}{K^5}\right)^{1/2} L^{5-d},\end{aligned} \tag{3.8}$$

where, in the second equality, we throw out the thermal fluctuation piece because it is less divergent and S_{d-1} is the surface area of a $(d-1)$-dimensional sphere with unit radius. This result diverges as a power law of the system size L right at the critical point in $d<5$, which implies that the upper critical dimension d_{uc} for this phase transition is 5, below which Gaussian theory breaks down. Since the physical dimension $d=3$ is less than d_{uc}, the standard momentum-shell RG transformation has to be employed to study the phase transition.

Because a few features of our treatment are nonstandard, we will describe our approach in some detail.

The first unusual feature is that we use an infinite hypercylindrical Brillouin zone $|\vec{q}|<\Lambda$, $-\infty<q_z<\infty$, where $\Lambda \sim 1/a$ is an ultraviolet (UV) cutoff. We separate the displacement field into high- and low-wave-vector components. $u_\alpha(\vec{r}) = u_\alpha^<(\vec{r}) + u_\alpha^>(\vec{r})$, where $u_\alpha^>(\vec{r})$ has support in the hypercylindrical shell $\Lambda e^{-\ell} < q_\perp < \Lambda$, $-\infty < q_z < \infty$, and $u_\alpha^<(\vec{r})$ has support in the remainder of the hypercylinder (i.e., $q_\perp < \Lambda e^{-\ell}$, $-\infty < q_z < \infty$). We then integrate the high-wave-vector part $u_\alpha^>(\vec{r})$ and rescale the length and long-wavelength part of the fields with $\vec{r}_\perp = \vec{r}'_\perp e^\ell$, $z = z' e^{\omega\ell}$, and $u_\alpha^>(\vec{r}) = e^{\chi\ell} u'_\alpha(\vec{r}')$ so as to restore the UV cutoff back to Λ. This rescaling leads to the zeroth-order RG flows of the effective couplings

$$K(\ell) = Ke^{(d+\omega+2\chi-5)\ell},$$

$$B(\ell) = Be^{(d-\omega+2\chi-1)\ell},$$

$$\frac{\Delta_t}{T}(\ell) = \left(\frac{\Delta_t}{T}\right) e^{(d+\omega+2\chi-3)\ell}.$$

From these dimensional couplings one can construct four dimensionless couplings

$$g_1 \equiv C_{d-1}(B/K^3)^{1/2}\Lambda^{d-3}, \tag{3.9}$$

$$g_2 \equiv C_{d-1}(B/K^5)^{1/2}\Delta_t\Lambda^{d-5}, \tag{3.10}$$

$$g_3 \equiv C_{d-1}(g/B)^2(B/K^5)^{1/2}\Delta_t\Lambda^{d-5}, \tag{3.11}$$

$$g_4 \equiv C_{d-1}(w/B)(B/K^5)^{1/2}\Delta_t\Lambda^{d-5}, \tag{3.12}$$

where $C_{d-1} \equiv S_{d-1}/(2\pi)^{d-1}$. The RG flows of the dimensionless couplings are independent of the arbitrary rescaling exponents and given, ignoring graphical corrections, by

$$g_1(\ell) = g_1 e^{(3-d)\ell}, \tag{3.13}$$

$$g_2(\ell) = g_2 e^{(5-d)\ell}, \tag{3.14}$$

$$g_3(\ell) = g_3 e^{(5-d)\ell}, \tag{3.15}$$

$$g_4(\ell) = g_4 e^{(5-d)\ell}. \tag{3.16}$$

g_1 is just the dimensionless coupling found by Grinstein and Pelcovits [16] in the pure smectic problem. It becomes marginal and leads to very weak anomalous elasticity in $d=3$. g_2 is actually the dimensionless coupling found by Radsihovsky and Toner [12] in the isotropic disordered smectic problem, where it becomes relevant in $d<5$ and leads to much stronger anomalous elasticity in $d=3$. g_3 and g_4, the truly nontrivial dimensionless couplings in our problem, also become relevant in $d<5$. As we will see below, they control the structure of the RG flows and hence the critical behavior.

Since the integration over the high-wave-vector components of u_α is always performed in the momentum shell $(-\infty<q_z<\infty,\ \Lambda e^{-d\ell}<q_\perp<\Lambda)$, it can be accomplished perturbatively in nonlinearities of $H[u]$. The change of the effective Hamiltonian of the long length modes due to the integration is

$$\delta H[u_\alpha^<] = \langle H_a[u_\alpha^< + u_\alpha^>]\rangle_> - \frac{1}{2T}\langle H_a^2[u_\alpha^< + u_\alpha^>]\rangle_> + \frac{1}{6T^2}\langle H_a^3[u_\alpha^< + u_\alpha^>]\rangle_> - \frac{1}{24T^3}\langle H_a^4[u_\alpha^< + u_\alpha^>]\rangle_> + \cdots, \tag{3.17}$$

where H_a represents the anharmonic terms which include the cubic and quartic terms, and the average over the short-length modes is done by only using the harmonic part of the Hamiltonian.

Now we will discuss $\delta H[u^<]$ to lowest order (one-loop graphical correction) in detail.

Since as shown in (3.17) the calculation of $\delta H[u_\alpha^<]$ is just a modified perturbation theory, the evaluation of the one-loop graphical correction to B for long-wavelength modes can be accomplished by modifying (3.8), restricting the integral range within the momentum shell $(-\infty<q_z<\infty,\ \Lambda e^{-d\ell}<q_\perp<\Lambda)$. Doing so, we obtain

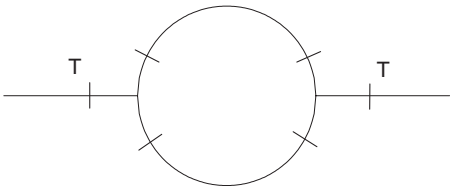

FIG. 8. Graphical corrections to the bend, tilt, and random tilt terms.

$$\begin{aligned}\delta B &= -\frac{g^2}{2}\int_p^> p_\perp^4[TG(\vec{p})^2 + 2\Delta_t p_\perp^2 G(\vec{p})^3] \\ &\approx -g^2\Delta_t\int_p^> \frac{p_\perp^6}{(Bp_z^2 + Kp_\perp^4)^3} \\ &\approx -g^2\Delta_t\int_{-\infty}^{\infty}\frac{dp_z}{2\pi}\int_{\Lambda e^{-d\ell}}^{\Lambda}\frac{d^{d-1}p_\perp}{(2\pi)^{d-1}}\frac{p_\perp^6}{(Bp_z^2 + Kp_\perp^4)^3} \\ &\approx -\frac{3}{16}C_{d-1}B\Delta_t\left(\frac{g}{B}\right)^2\left(\frac{B}{K^5}\right)^{1/2}\Lambda^{d-5}d\ell \\ &\approx -\frac{3}{16}Bg_3 d\ell.\end{aligned} \tag{3.18}$$

Now we discuss graphical corrections to the bend term (i.e., K term), the tilt term (i.e., D term), and the random tilt term (i.e., Δ_t term). The Feynman diagrams for these corrections are presented in Figs. 8 and 9. Following Feynman rules, from the diagram in Fig. 8 we obtain

$$-\frac{g^2}{2T}\sum_{\alpha=1}^{n}\sum_{\beta=1}^{n}\sum_{\vec{q}}\sum_{ij} q_i^\perp q_j^\perp u_\alpha(\vec{q})u_\beta(-\vec{q}) \times \int_p^> p_i^\perp(p_j^\perp + q_j^\perp)p_z^2 G_{\alpha\beta}(\vec{p})G_{\alpha\beta}(\vec{p}+\vec{q}), \tag{3.19}$$

$$-\frac{g^2}{2T}\sum_{\alpha=1}^{n}\sum_{\beta=1}^{n}\sum_{\vec{q}}\sum_{ij} q_i^\perp q_j^\perp u_\alpha(\vec{q})u_\beta(-\vec{q}) \times \int_p^> p_i^\perp p_j^\perp p_z^2 G_{\alpha\beta}(\vec{p})G_{\alpha\beta}(\vec{p}+\vec{q}), \tag{3.20}$$

where $G_{\alpha\beta}$ is given in (3.5). Note that we have kept the $\vec{q}$ dependence of the internal legs [i.e., the $\vec{q}$ dependence of the

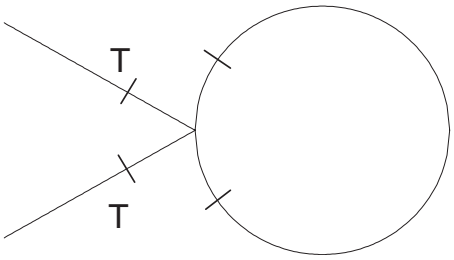

FIG. 9. A graphical correction to the tilt term.

integrands in (3.19) and (3.20)] since it is necessary for obtaining the contributions to the bend term. Taylor expanding the two integrands around $\vec{q}=0$, we find that $O(1)$ terms lead to corrections to Δ_t and D; $O(q_\perp)$ terms vanish after the integration; $O(q_\perp^2)$ terms lead to corrections to K.

Let us first calculate the corrections to Δ_t and D. Setting $\vec{q}$ inside the two integrands to $\vec{0}$, expressions (3.19) and (3.20) become identical and can be added together to get

$$-g^2\sum_{\alpha=1}^{n}\sum_{\beta=1}^{n}\sum_{\vec{q}}\sum_{ij}q_i^\perp q_j^\perp u_\alpha(\vec{q})u_\beta(-\vec{q}) \times\int_p^> p_i^\perp p_j^\perp p_z^2 G_{\alpha\beta}(\vec{p})G_{\alpha\beta}(\vec{p}), \tag{3.21}$$

from which we obtain two distinct contributions. One of them is the contribution to the random-tilt term with the corresponding correction to the random-tilt variable Δ_t:

$$\begin{aligned}\delta\Delta_t &\approx \frac{g^2}{2}\int_p^> p_z^2 p_\perp^6 \Delta_t^2 G(\vec{p})^4 \approx \frac{g^2}{2}\Delta_t^2\int_p^>\frac{p_\perp^6 p_z^2}{(Bp_z^2+Kp_\perp^4)^4}\\ &\approx \frac{g^2}{2}\Delta_t^2\int_{-\infty}^{\infty}\frac{dp_z}{2\pi}\int_{\Lambda e^{d\ell}}^{\Lambda}\frac{d^{d-1}p_\perp}{(2\pi)^{d-1}}\frac{p_\perp^6 p_z^2}{(Bp_z^2+Kp_\perp^4)^3}\\ &\approx \frac{1}{64}C_{d-1}\Delta_t^2\left(\frac{g}{B}\right)^2\left(\frac{B}{K^5}\right)^{1/2}\Lambda^{d-5}d\ell \approx \frac{1}{64}\Delta_t g_3 d\ell.\end{aligned} \tag{3.22}$$

The other one is the correction to the ordinary tilt term with the corresponding correction to the tilt modulus D:

$$\begin{aligned}(\delta D)_1 &\approx -\frac{4}{3}g^2\Delta_t\int_p^> p_z^2 p_\perp^4 G(\vec{p})^3\\ &\approx -\frac{4}{3}g^2\Delta_t\int_p^>\frac{p_\perp^4 p_z^2}{(Bp_z^2+Kp_\perp^4+Dp_\perp^2)^3}\\ &\approx \left(-\frac{1}{16}K\Lambda^2+\frac{3}{32}D\right)g_3 d\ell,\end{aligned} \tag{3.23}$$

where we have used $(\delta D)_1$ instead of (δD) since there are more corrections to D from other Feynman diagraphs, which will be calculated later in this section.

Now let us calculate the corrections to the bend term from (3.19) and (3.20). As mentioned earlier, we have to Taylor expand both of the integrands and use the $O(q_\perp^2)$ term. Fortunately, since (3.20) is part of (3.19), we only need to do the calculation once for (3.19), which, however, is still very involved. In the following we will describe the calculation in detail.

Only keeping the most divergent pieces which carry the factor $\delta_{\alpha\beta}$, the integrand in (3.19) is simplified as

$$p_i^\perp(p_j^\perp+q_j^\perp)p_z^2\left[\frac{\Delta_t p_\perp^2\delta_{\alpha\beta}}{(Kp_\perp^4+Bp_z^2)^2(K|\vec{p}+\vec{q}|^4+Bp_z^2)} + \frac{\Delta_t|\vec{p}+\vec{q}|^2\delta_{\alpha\beta}}{(Kp_\perp^4+Bp_z^2)(K|\vec{p}+\vec{q}|^4+Bp_z^2)^2}\right]. \tag{3.24}$$

For convenience, we rewrite $K|\vec{p}+\vec{q}|^4$ as

$$K|\vec{p}+\vec{q}|^4 = K(p_\perp^4+f(\vec{q}_\perp)), \tag{3.25}$$

with $f(\vec{q}_\perp)$ defined as

$$f(\vec{q}_\perp)\equiv 2p_\perp^2(2\vec{p}_\perp\cdot\vec{q}_\perp+q_\perp^2)+(2\vec{p}_\perp\cdot\vec{q}_\perp+q_\perp^2)^2. \tag{3.26}$$

Now let us do the following two Taylor expansions:

$$\frac{1}{(K|\vec{p}_\perp+\vec{q}_\perp|^4+Bp_z^2)} = \frac{1}{Bp_z^2+Kp_\perp^4}\left[1-\frac{Kf(\vec{p}_\perp)}{Bp_z^2+Kp_\perp^4}+\frac{K^2f^2(\vec{p}_\perp)}{(Bp_z^2+Kp_\perp^4)^2}\right],$$

$$\frac{1}{(K|\vec{p}_\perp+\vec{q}_\perp|^4+Bp_z^2)^2} = \frac{1}{(Bp_z^2+Kp_\perp^4)^2}\left[1-\frac{2Kf(\vec{p}_\perp)}{Bp_z^2+Kp_\perp^4}+\frac{3K^2f^2(\vec{p}_\perp)}{(Bp_z^2+Kp_\perp^4)^2}\right].$$

Plugging these two expressions into (3.24) makes it extremely long and complicated. For better management, we divided it into four pieces

$$\frac{p_i^\perp p_j^\perp p_z^2\Delta_t p_\perp^2\delta_{\alpha\beta}}{(Kp_\perp^4+Bp_z^2)^3}\left[1-\frac{Kf(\vec{q}_\perp)}{Bp_z^2+Kp_\perp^4}+\frac{K^2f^2(\vec{q}_\perp)}{(Bp_z^2+Kp_\perp^4)^2}\right], \tag{3.27}$$

$$\frac{p_i^\perp q_j^\perp p_z^2\Delta_t p_\perp^2\delta_{\alpha\beta}}{(Kp_\perp^4+Bp_z^2)^3}\left[1-\frac{Kf(\vec{q}_\perp)}{Bp_z^2+Kp_\perp^4}+\frac{K^2f^2(\vec{q}_\perp)}{(Bp_z^2+Kp_\perp^4)^2}\right], \tag{3.28}$$

$$\frac{p_i^\perp p_j^\perp p_z^2\Delta_t|\vec{p}+\vec{q}|^2\delta_{\alpha\beta}}{(Kp_\perp^4+Bp_z^2)^3}\left[1-\frac{2Kf(\vec{q}_\perp)}{Bp_z^2+Kp_\perp^4}+\frac{3K^2f^2(\vec{q}_\perp)}{(Bp_z^2+Kp_\perp^4)^2}\right], \tag{3.29}$$

$$\frac{p_i^\perp q_j^\perp p_z^2\Delta_t|\vec{p}+\vec{q}|^2\delta_{\alpha\beta}}{(Kp_\perp^4+Bp_z^2)^3}\left[1-\frac{2Kf(\vec{q}_\perp)}{Bp_z^2+Kp_\perp^4}+\frac{3K^2f^2(\vec{q}_\perp)}{(Bp_z^2+Kp_\perp^4)^2}\right]. \tag{3.30}$$

Inserting Eq. (3.26) into the above four pieces, we obtain $O(q_\perp^2)$ terms

$$\begin{aligned}I_1(\vec{q}_\perp)\equiv &-2K\Delta_t q_\perp^2\delta_{\alpha\beta}\frac{p_z^2p_\perp^4p_i^\perp p_j^\perp}{(BP_z^2+Kp_\perp^4)^4}\\ &-4K\Delta_t\delta_{\alpha\beta}\sum_k\sum_\ell q_k^\perp q_\ell^\perp\frac{p_z^2p_\perp^2p_i^\perp p_j^\perp p_k^\perp p_\ell^\perp}{(BP_z^2+Kp_\perp^4)^4}\\ &+16K^2\Delta_t\delta_{\alpha\beta}\sum_k\sum_\ell q_k^\perp q_\ell^\perp\frac{p_z^2p_\perp^6p_i^\perp p_j^\perp p_k^\perp p_\ell^\perp}{(BP_z^2+Kp_\perp^4)^5}\end{aligned} \tag{3.31}$$

from (3.27),

$$I_2(\vec{q}_\perp) = -4K\Delta_t q_j^\perp \delta_{\alpha\beta} \sum_k q_k^\perp \frac{p_z^2 p_\perp^4 p_i^\perp p_k^\perp}{(BP_z^2 + Kp_\perp^4)^4} \quad (3.32)$$

from (3.28),

$$\begin{aligned} I_3(\vec{q}_\perp) \equiv{}& \Delta_t q_\perp^2 \delta_{\alpha\beta} \frac{p_z^2 p_i^\perp p_j^\perp}{(BP_z^2 + Kp_\perp^4)^3} \\ &- 16K\Delta_t \delta_{\alpha\beta} \sum_k \sum_\ell q_k^\perp q_\ell^\perp \frac{p_z^2 p_\perp^2 p_i^\perp p_j^\perp p_k^\perp p_\ell^\perp}{(BP_z^2 + Kp_\perp^4)^4} \\ &- 4K\Delta_t q_\perp^2 \delta_{\alpha\beta} \frac{p_z^2 p_\perp^4 p_i^\perp p_j^\perp}{(BP_z^2 + Kp_\perp^4)^4} \\ &- 8K\Delta_t \delta_{\alpha\beta} \sum_k \sum_\ell q_k^\perp q_\ell^\perp \frac{p_z^2 p_\perp^2 p_i^\perp p_j^\perp p_k^\perp p_\ell^\perp}{(BP_z^2 + Kp_\perp^4)^4} \\ &+ 48K^2\Delta_t \delta_{\alpha\beta} \sum_k \sum_\ell q_k^\perp q_\ell^\perp \frac{p_z^2 p_\perp^6 p_i^\perp p_j^\perp p_k^\perp p_\ell^\perp}{(BP_z^2 + Kp_\perp^4)^5} \end{aligned} \quad (3.33)$$

from (3.29), and

$$\begin{aligned} I_4(\vec{q}_\perp) = {}& 2\Delta_t q_j^\perp \delta_{\alpha\beta} \sum_k q_k^\perp \frac{p_z^2 p_i^\perp p_k^\perp}{(BP_z^2 + Kp_\perp^4)^3} \\ &- 8K\Delta_t q_j^\perp \delta_{\alpha\beta} \sum_k q_k^\perp \frac{p_z^2 p_\perp^4 p_i^\perp p_k^\perp}{(BP_z^2 + Kp_\perp^4)^4} \end{aligned} \quad (3.34)$$

from (3.30). Finally the total correction to the bend term can be written as

$$-\frac{g^2}{2T} \sum_{\alpha=1}^{n} \sum_{\beta=1}^{n} \sum_{\vec{q}} \sum_{ijk} q_i^\perp q_j^\perp u_\alpha(\vec{q}) u_\beta(-\vec{q}) \int_p^> I_k(\vec{q}_\perp), \quad (3.35)$$

where the subscript $k=1,2,3,4$.

The main trick involving doing the integrals in (3.35) can be summarized by the following two integrals:

$$\int_{p'} p_i' p_j' \Gamma(\vec{p}') = \frac{1}{d'} \delta_{ij} \int_p' (p')^2 \Gamma(\vec{p}'), \quad (3.36)$$

$$\begin{aligned} \int_{p'} p_i' p_j' p_k' p_\ell' \Gamma(\vec{p}') = {}& \frac{1}{d'(d'+1)} (\delta_{ij}\delta_{k\ell} + \delta_{ik}\delta_{j\ell} + \delta_{i\ell}\delta_{jk}) \\ &\times \int_p' (p')^4 \Gamma(\vec{p}'), \end{aligned} \quad (3.37)$$

where both function $\Gamma(\vec{p})$ and the integral region are spherical symmetric and d' is the dimension of the space in which $\vec{p}$ lies in.

Now we plug in the expression of I_k into (3.35) and do the integrations. Let us start with I_1, which has three terms. Integrating the first term gives

$$\begin{aligned} &-2K\Delta_t q_\perp^2 \delta_{\alpha\beta} \int_p \frac{p_z^2 p_\perp^4 p_i^\perp p_j^\perp}{(BP_z^2 + Kp_\perp^4)^4} \\ &= -\frac{2K\Delta_t}{d-1} q_\perp^2 \delta_{\alpha\beta}\delta_{ij} \int_p^< \frac{p_z^2 p_\perp^6}{(BP_z^2 + Kp_\perp^4)^4} \\ &= -\frac{2K\Delta_t}{d-1} q_\perp^2 \delta_{\alpha\beta}\delta_{ij} \int_{-\infty}^{\infty} dp_z \int_{\Lambda e^{-d\ell}}^{\Lambda} dp_\perp \frac{p_z^2 p_\perp^6}{(BP_z^2 + Kp_\perp^4)^4} \\ &= -\frac{1}{64} \Delta_t \left(\frac{1}{BK}\right)^{3/2} q_\perp^2 \delta_{\alpha\beta}\delta_{ij} C_{d-1} \Lambda^{5-d} d\ell, \end{aligned} \quad (3.38)$$

integrating the second term gives

$$\begin{aligned} &-4K\Delta_t \delta_{\alpha\beta} \sum_k \sum_\ell q_k^\perp q_\ell^\perp \int_p \frac{p_z^2 p_\perp^2 p_i^\perp p_j^\perp p_k^\perp p_\ell^\perp}{(BP_z^2 + Kp_\perp^4)^4} \\ &= -\frac{4K\Delta_t}{d^2-1} \delta_{\alpha\beta} \sum_k \sum_\ell (\delta_{ij}\delta_{k\ell} + \delta_{ik}\delta_{j\ell} + \delta_{i\ell}\delta_{jk}) q_k^\perp q_\ell^\perp \\ &\quad \times \int_p^< \frac{p_z^2 p_\perp^6}{(BP_z^2 + Kp_\perp^4)^4} = -\frac{1}{192} \Delta_t \left(\frac{1}{BK}\right)^{3/2} \delta_{\alpha\beta} \\ &\quad \times \sum_k \sum_\ell (\delta_{ij}\delta_{k\ell} + \delta_{ik}\delta_{j\ell} + \delta_{i\ell}\delta_{jk}) q_k^\perp q_\ell^\perp C_{d-1} \Lambda^{5-d} d\ell \\ &= -\frac{1}{192} \Delta_t \left(\frac{1}{BK}\right)^{3/2} \delta_{\alpha\beta} (\delta_{ij} q_\perp^2 + 2q_i^\perp q_j^\perp) C_{d-1} \Lambda^{5-d} d\ell, \end{aligned}$$

and integrating the third term gives

$$\begin{aligned} &16K^2\Delta_t \delta_{\alpha\beta} \sum_k \sum_\ell q_k^\perp q_\ell^\perp \int_p \frac{p_z^2 p_\perp^6 p_i^\perp p_j^\perp p_k^\perp p_\ell^\perp}{(BP_z^2 + Kp_\perp^4)^5} \\ &= \frac{16K^2\Delta_t}{d^2-1} \delta_{\alpha\beta} \sum_k \sum_\ell (\delta_{ij}\delta_{k\ell} + \delta_{ik}\delta_{j\ell} + \delta_{i\ell}\delta_{jk}) q_k^\perp q_\ell^\perp \\ &\quad \times \int_p^< \frac{p_z^2 p_\perp^1 0}{(BP_z^2 + Kp_\perp^4)^4} = \frac{5}{384} \Delta_t \left(\frac{1}{BK}\right)^{3/2} \delta_{\alpha\beta} \\ &\quad \times \sum_k \sum_\ell (\delta_{ij}\delta_{k\ell} + \delta_{ik}\delta_{j\ell} + \delta_{i\ell}\delta_{jk}) q_k^\perp q_\ell^\perp C_{d-1} \Lambda^{5-d} d\ell \\ &= \frac{5}{384} \Delta_t \left(\frac{1}{BK}\right)^{3/2} \delta_{\alpha\beta} (\delta_{ij} q_\perp^2 + 2q_i^\perp q_j^\perp) C_{d-1} \Lambda^{5-d} d\ell. \end{aligned}$$

Adding the three results together we get

$$\begin{aligned} \int_p^< I_1(\vec{q}_\perp) = {}& \delta_{\alpha\beta} \Delta_t \left(\frac{1}{BK}\right)^{3/2} C_{d-1} \Lambda^{5-d} d\ell \\ &\times \left[-\frac{1}{64} \delta_{ij} q_\perp^2 - \frac{1}{192} (\delta_{ij} q_\perp^2 + 2q_i^\perp q_j^\perp) \right. \\ &\left. + \frac{5}{384} (\delta_{ij} q_\perp^2 + 2q_i^\perp q_j^\perp) \right]. \end{aligned} \quad (3.39)$$

Plugging this result into (3.35), we find corrections to the bend term:

$$-\frac{g^2}{2}\sum_{\alpha=1}^{n}\sum_{\beta=1}^{n}\sum_{\vec{q}}\sum_{ij} q_i^{\perp} q_j^{\perp} u_\alpha(\vec{q}) u_\beta(-\vec{q}) \delta_{\alpha\beta}\Delta_t \times \left(\frac{1}{BK}\right)^{3/2} C_{d-1}\Lambda^{5-d} d\ell \left[-\frac{1}{64}\delta_{ij} q_\perp^2 - \frac{1}{192}(\delta_{ij} q_\perp^2 + 2q_i^{\perp} q_j^{\perp}) + \frac{5}{384}(\delta_{ij} q_\perp^2 + 2q_i^{\perp} q_j^{\perp})\right]$$
$$= -\frac{g^2}{256}\Delta_t \left(\frac{1}{BK}\right)^{3/2} C_{d-1}\Lambda^{5-d} d\ell \times \sum_{\alpha}\sum_{\vec{q}} q_\perp^4 u_\alpha(\vec{q}) u_\alpha(-\vec{q}), \tag{3.40}$$

from which the corresponding correction to the bend modulus K is

$$(\delta K)_1 = -\frac{g^2}{128}\Delta_t \left(\frac{1}{BK}\right)^{3/2} C_{d-1}\Lambda^{5-d} d\ell = -\frac{1}{128} K g_3 d\ell. \tag{3.41}$$

Similarly, inserting $I_2(\vec{q}_\perp)$, $I_3(\vec{q}_\perp)$, and $I_4(\vec{q}_\perp)$ into (3.35), we obtain three more corrections to K:

$$(\delta K)_2 = -\frac{1}{32} K g_3 d\ell,$$
$$(\delta K)_3 = \frac{1}{128} K g_3 d\ell,$$
$$(\delta K)_4 = -\frac{1}{32} K g_3 d\ell. \tag{3.42}$$

Now we have found all the correction to the bend modulus K from (3.19).

As for (3.20), since it is part of (3.19), its correction to K can be easily shown to be $(\delta K)_1 + (\delta K)_3$. Thus the total correction to the bend modulus K is given by

$$\delta K = 2(\delta K)_1 + (\delta K)_2 + 2(\delta K)_3 + (\delta K)_4 = -\frac{1}{32} K \left(\frac{B}{g}\right)^2 \Delta_t \left(\frac{B}{K^5}\right)^5 C_{d-1}\Lambda^{5-d} d\ell = -\frac{1}{32} K g_3 d\ell. \tag{3.43}$$

Now let us turn to the calculation of the graphical corrections to D. The two Feynman diagrams which give the corrections to D are illustrated in Figs. 8 and 9, respectively. The former has been discussed previously and leads to $(\delta D)_1$ given in (3.23). A simple analysis of the latter gives

$$(\delta D)_2 \approx -\frac{3}{4}\omega\Delta_t \int_p^{>} p_\perp^4 G(\vec{p})^2 \approx -\frac{3}{4}\omega\Delta_t \int_p^{>} \frac{p_\perp^4}{(Bp_z^2 + Kp_\perp^4 + Dp_\perp^2)^2} \approx \left(\frac{3}{16}K\Lambda^2 - \frac{9}{32}D\right) g_4 d\ell. \tag{3.44}$$

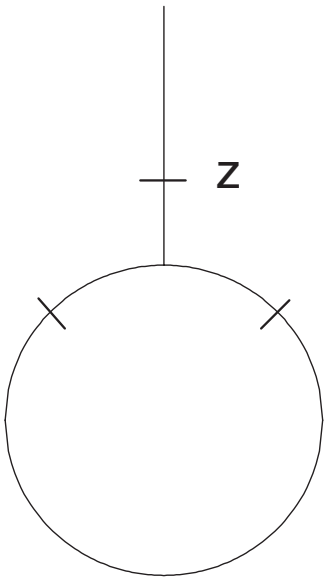

FIG. 10. The graphical correction to the linear term $\Sigma_{n=1}^{\infty}\partial_z u$.

Naively one would treat the sum of $(\delta D)_1$ and $(\delta D)_2$ as the total correction to D; however, a more careful analysis shows that this treatment is *incorrect*. One has to take into account that the disorder-averaged ground state of the rescaled system has been renormalized under the RG. The Feynman diagram in Fig. 10 shows a contribution

$$\delta L \sum_{\alpha=1}^{n} \partial_z u_\alpha, \tag{3.45}$$

which is linear and does not exist in the original Hamiltonian. This implies that the disorder-averaged minimum of the Hamiltonian has shifted from $\partial_z u_\alpha = 0$ to $\partial_z u_\alpha = -\delta L/B$. Therefore, after each cycle of the RG, the Hamiltonian needs to be reexpanded around the new minimum, which is accomplished by changing variable, defining $u'_\alpha \equiv u_\alpha + (\delta L/B)z$. This treatment then makes the cubic term $-g(\partial_z u)(\nabla_\perp u)^2/2$ to create another contribution to the tilt term $(\delta D)_3 |\nabla_\perp u'|^2/2$, where $(\delta D)_3 = g\delta L/B$. δL can be easily calculated from the Feynman diagram in Fig. 10:

$$\delta L \approx -\frac{1}{2} g\Delta_t \int_p^{>} p_\perp^4 G(\vec{p})^2 \approx -\frac{1}{2} g\Delta_t \int_p^{>} \frac{p_\perp^4}{(Bp_z^2 + Kp_\perp^4 + Dp_\perp^2)^2} \approx \left(-\frac{1}{8}K\Lambda^2 + \frac{3}{16}D\right)\left(\frac{B}{g}\right) g_3 d\ell. \tag{3.46}$$

Taking $(\delta D)_3$ into account, the total correction to D should really be

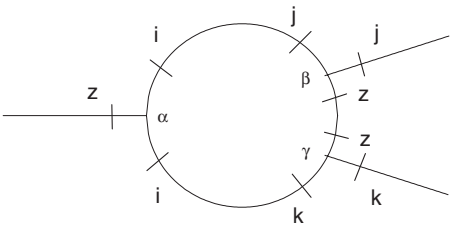

FIG. 11. A graphical correction to the cubic term.

$$\delta D = (\delta D)_1 + (\delta D)_2 + (\delta D)_3 = \frac{9}{32}(g_3 - g_4) + \frac{3}{16}K(g_4 - g_3). \tag{3.47}$$

In the isotropic-disordered smectic-*A* problem [11], the rotation invariance prohibits the tilt term and this symmetry should be preserved under the RG, which provides an extra check of our calculation. Imposing $g_3 = g_4$ (restoring the rotation invariance) in (3.47), we find indeed that δD vanishes.

Now we calculate graphical corrections to anharmonic terms in the Hamiltonian (3.1). This calculation has been avoided in the isotropic-disordered smectic-*A* problem [11] by using the symmetry argument that the global rotation invariance requires

$$\delta B = \delta g = \delta w. \tag{3.48}$$

This argument does not apply in our problem due to the symmetry breaking; however, it can be used to check our calculation. By imposing $B = g = w$, our results should also satisfy (3.48).

All the one-loop Feynman diagrams which give the corrections to the cubic and quartic terms are shown in Figs. 11–19. The corresponding graphical corrections to g and ω are in order referred as $(\delta g)_1$, $(\delta g)_2$, $(\delta g)_3$, $(\delta\omega)_1$, $(\delta\omega)_2$, $(\delta\omega)_3$, $(\delta\omega)_4$, $(\delta\omega)_5$, and $(\delta\omega)_6$, respectively. Since the evaluations of these diagrams are all similar, we choose to only show in detail the evaluation of the Feynman diagram in Fig. 19, which is the most complicated, and for the rest we only give results. An analysis of the Feynman diagram in Fig. 19 gives

$$-\frac{2g^4}{T^3}\frac{1}{V}\sum_{\alpha=1}^{\infty}\sum_{\beta=1}^{\infty}\sum_{\gamma=1}^{\infty}\sum_{\eta=1}^{\infty}\sum_{\vec{q}_1,\vec{q}_2,\vec{q}_3,\vec{q}_4}\sum_{i,j,k,l}\delta(\vec{q}_1+\vec{q}_2+\vec{q}_3+\vec{q}_3)$$
$$\times(iq_{1i}^{\perp})(iq_{2j}^{\perp})(iq_{3k}^{\perp})(iq_{4l}^{\perp})u_\alpha(\vec{q}_1)u_\beta(\vec{q}_2)u_\gamma(\vec{q}_3)u_\eta(\vec{q}_4)$$
$$\times\int_p^{>} p_i^{\perp}p_j^{\perp}p_k^{\perp}p_l^{\perp}p_z^4 G_{\alpha\beta}G_{\beta\gamma}G_{\gamma\eta}G_{\alpha\eta}, \tag{3.49}$$

in which

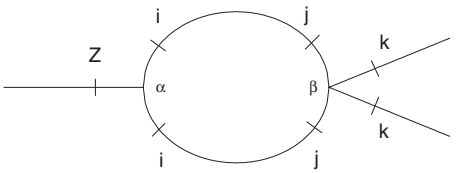

FIG. 12. Another graphical correction to the cubic term.

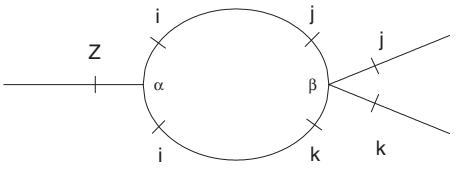

FIG. 13. One more graphical correction to the cubic term.

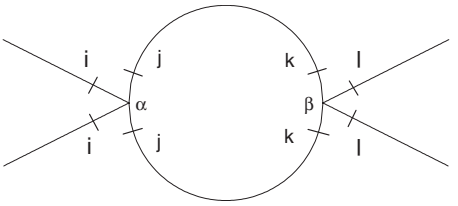

FIG. 14. A graphical correction to the quartic term.

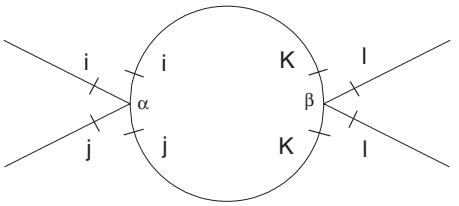

FIG. 15. Another graphical correction to the quartic term.

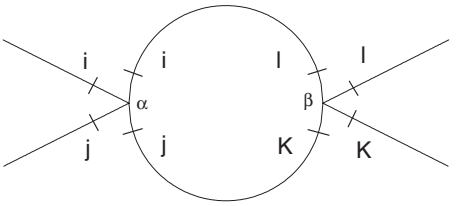

FIG. 16. Another graphical correction to the quartic term.

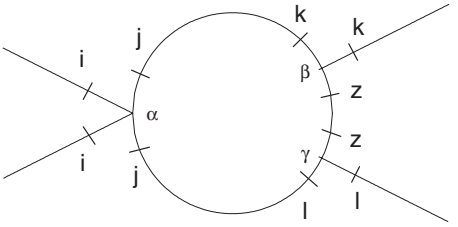

FIG. 17. Yet another graphical correction to the quartic term.

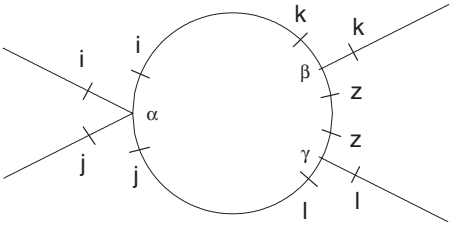

FIG. 18. One more graphical correction to the quartic term.

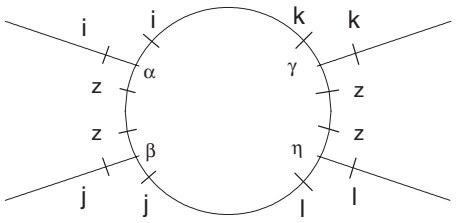

FIG. 19. The final graphical correction to the quartic term.

$$G_{\alpha\beta}G_{\beta\gamma}G_{\gamma\eta}G_{\alpha\eta} = [TG(\vec{q})\delta_{\alpha\beta} + \Delta_t q_\perp^2 G(\vec{q})^2][TG(\vec{q})\delta_{\beta\gamma} + \Delta_t q_\perp^2 G(\vec{q})^2][TG(\vec{q})\delta_{\gamma\eta} + \Delta_t q_\perp^2 G(\vec{q})^2] \times [TG(\vec{q})\delta_{\alpha\eta} + \Delta_t q_\perp^2 G(\vec{q})^2]. \quad (3.50)$$

Note that the quartic term in the Hamiltonian (3.1) only involves one sum over the replica index, while (3.49) has four. Thus only those terms in $G_{\alpha\beta}G_{\beta\gamma}G_{\gamma\eta}G_{\alpha\eta}$ that carry at least three Kronecker delta functions can lead to the contributions to the quartic term. Plugging (3.50) into (3.49) and keeping the most relevant pieces, we obtain

$$(\delta\omega)_6 = -8g^4\Delta_t \int_p^> p_\perp^6 p_z^4 G(\vec{q})^5 = -\frac{3}{32}\frac{g_3^2}{g_4}\omega\, d\ell. \quad (3.51)$$

The corrections to g and w from other Feynman diagrams can be calculated in a similar way and are

$$(\delta g)_1 = \frac{3}{32}g_3 g\, d\ell, \quad (\delta g)_2 = -\frac{3}{16}g_4 g\, d\ell,$$

$$(\delta g)_3 = -\frac{3}{32}g_4 g\, d\ell, \quad (\delta\omega)_1 = -\frac{3}{16}g_4\omega\, d\ell,$$

$$(\delta\omega)_2 = -\frac{3}{16}g_4\omega\, d\ell, \quad (\delta\omega)_3 = -\frac{3}{32}g_4\omega\, d\ell,$$

$$(\delta\omega)_4 = \frac{3}{16}g_3\omega\, d\ell, \quad (\delta\omega)_5 = \frac{3}{16}g_3\omega\, d\ell.$$

Adding them together we get

$$\delta g = \left(\frac{3}{32}g_3 - \frac{9}{32}g_4\right)d\ell, \quad (3.52)$$

$$\delta\omega = -\frac{3}{32}\frac{g_3^2}{g_4}\omega - \frac{15}{32}g_4\omega + \frac{3}{8}g_3\omega. \quad (3.53)$$

Performing the rescalings described earlier and using the graphical corrections we have calculated, we obtain the following RG flow equations:

$$\frac{dB(\ell)}{d\ell} = \left(d - 1 - \omega + 2\chi - \frac{3}{16}g_3\right)B, \quad (3.54)$$

$$\frac{dK(\ell)}{d\ell} = \left(d - 5 + \omega + 2\chi + \frac{1}{32}g_3\right)K, \quad (3.55)$$

$$\frac{d(\Delta_t/T)(\ell)}{d\ell} = \left(d - 3 + \omega + 2\chi + \frac{1}{64}g_3\right), \quad (3.56)$$

$$\frac{dg(\ell)}{d\ell} = \left(d - 3 + 3\chi + \frac{3}{32}g_3 - \frac{9}{32}g_4\right)g, \quad (3.57)$$

$$\frac{dD(\ell)}{d\ell} = \left(d - 3 + \omega + 2\chi + \frac{9}{32}g_3 - \frac{9}{32}g_4\right)D + \frac{3}{16}K(g_4 - g_3), \quad (3.58)$$

$$\frac{dw(\ell)}{d\ell} = \left(d - 5 + \omega + 4\chi - \frac{3}{32}\frac{g_3^2}{g_4}\right)w + \left(\frac{3}{8}g_3 - \frac{15}{32}g_4\right)w. \quad (3.59)$$

These equations are not very transparent telling the physics since they depend on the rescaling factor ω and χ, which are artificial. Instead, we should focus on the flow of the dimensionless couplings. Combining the above flow equations with the definition of g_3 and g_4, we find

$$\frac{dg_3}{d\ell} = \left(\epsilon - \frac{9}{16}g_4 + \frac{13}{32}g_3\right)g_3, \quad (3.60)$$

$$\frac{dg_4}{d\ell} = \left(\epsilon - \frac{15}{32}g_4 + \frac{13}{32}g_3 - \frac{3}{32}\frac{g_3^2}{g_4}\right)g_4, \quad (3.61)$$

where $\epsilon = 5 - d$.

Obviously the Gaussian fixed point ($g_3^* = 0$, $g_4^* = 0$) is one of the fixed points of Eqs. (3.60) and (3.61). To check its stability, we linearize the two equations around it by writing $g_3 = 0 + \delta g_3$ and $g_4 = 0 + \delta g_4$ and get, to linear order in $\delta g_{3,4}$,

$$\frac{d\delta g_3}{d\ell} = \epsilon\delta g_3, \quad (3.62)$$

$$\frac{d\delta g_4}{d\ell} = \epsilon\delta g_4. \quad (3.63)$$

These two linearized differential equations tell us that for $\epsilon > 0$ ($d < 5$), given a small departure from the Gaussian fixed point, both g_3 and g_4 will leave it exponentially, which implies that the Gaussian fixed point is unstable in the physical dimension $d = 3$.

In addition to the Gaussian fixed point, these RG flow equations (3.60) and (3.61) have other two fixed points. One of them is exactly the one found in the isotropic-disordered smectic-A problem [11], for which the Hamiltonian is rotation invariant. This is not a coincidence, because the Hamiltonian we start with is more general in the sense that it has no symmetry bound $(g/B)^2 = w/B$, so our solutions must include this specific fixed point as a special case. To find this particular fixed point, we can enforce this symmetry condition on the RG flow equations (3.60) and (3.61) by setting $g_3 = g_4$. After this enforcement both of those two equations reduce to the recursion relation found by Radzihovsky and Toner [11] for the isotropic problem:

$$\frac{dg_3}{d\ell} = \left(\epsilon - \frac{5}{32}g_3\right)g_3,$$

which leads to $g_3^* = 32\epsilon/5$. However, this fixed point is not stable in our more general problem. We can examine this instability by using a similar linearization analysis as for the Gaussian fixed point. Writing $g_3 = 32\epsilon/5 + \delta g_3$ and $g_4 = 32\epsilon/5 + \delta g_4$ and plugging them into Eqs. (3.60) and (3.61), we obtain

$$\frac{d\delta g_3}{d\ell} = \frac{13\epsilon}{5}\delta g_3 - \frac{18\epsilon}{5}\delta g_4, \tag{3.64}$$

$$\frac{d\delta g_4}{d\ell} = \frac{7\epsilon}{5}\delta g_3 - \frac{12\epsilon}{5}\delta g_4, \tag{3.65}$$

which has the solution near the vicinity of the fixed point:

$$\delta g_3 = C_1 e^{-\epsilon\ell} + 18C_2 e^{6\epsilon\ell/5},$$

$$\delta g_4 = C_1 e^{-\epsilon\ell} + 7C_2 e^{6\epsilon\ell/5}.$$

The C_1 and C_2 in the solution are constants determined by the initial condition $(\delta g_3)_0$ and $(\delta g_4)_0$. This solution shows that, in general, this fixed point is also unstable, although it is stable given that $(\delta g_3)_0 = (\delta g_4)_0$, which is just a verification of its stability in the isotropic-disordered smectic-*A* problem [11].

The third fixed point can be obtained by assuming that g_3 flows to zero. Under this assumption Eq. (3.61) reduces to

$$\frac{dg_4}{d\ell} = \left(\epsilon - \frac{15}{32}g_4\right)g_4, \tag{3.66}$$

which has a non-Gaussian fixed point $g_4^* = 32\epsilon/15$. The linearized differential equations around this fixed point are

$$\frac{d\delta g_3}{d\ell} = -\frac{1}{5}\epsilon\delta g_3, \tag{3.67}$$

$$\frac{d\delta g_4}{d\ell} = \frac{13}{15}\epsilon\delta g_3 - \epsilon\delta g_4, \tag{3.68}$$

which have the solution

$$\delta g_3 = c_1 e^{-\epsilon\ell/5}, \tag{3.69}$$

$$\delta g_4 = \frac{13}{12}c_1 e^{-\epsilon*\ell/5} + c_2 e^{-\epsilon\ell}. \tag{3.70}$$

Note that both eigenvalues are negative for $d < 5$, which implies that this fixed point is stable and hence controls the second-order phase transition. The RG flows of g_3 and g_4 around these three fixed points are illustrated in Fig. 20.

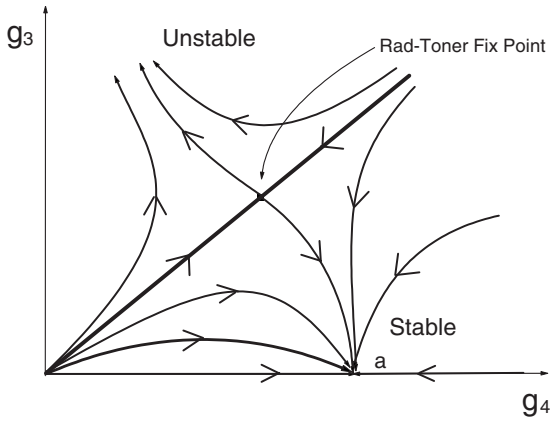

FIG. 20. Graphical RG flow of the dimensionless coupling g_3 and g_4. Point a is the stable fixed point $(0, 32\epsilon/15)$.

IV. CRITICAL EXPONENTS

The RG we derived in the previous section is only valid in the critical region and hence named "critical RG." If the system is right at the critical point, the critical RG holds for arbitrary ℓ; otherwise, it breaks down at ℓ^*, which is determined by $D(\ell^*) = K(\ell^*)\Lambda^2$. In this section we first identify the critical point, then study how fast the critical RG breaks down if the system is slightly off the critical point, so as to calculate the critical exponents. For convenience, we choose a special rescaling

$$\omega + 2\chi = 5 - d - \frac{1}{32}g_3, \tag{4.1}$$

which fixes K at its initial value K_0. The flow Eq. (3.58) then becomes

$$\frac{dD(\ell)}{d\ell} = \left(2 + \frac{1}{4}g_3 - \frac{9}{32}g_4\right)D + \frac{3}{16}K_0(g_4 - g_3). \tag{4.2}$$

Right at the critical point $D(\ell)$ also flows to a fixed value D^*, which can be calculated by plugging $g_3^* = 0$ and $g_4^* = 32\epsilon/15$ into Eq. (4.2) and requiring $dD/d\ell = 0$. Thus the fixed point controlling the phase transition is identified in $D - g_3 - g_4$ space as

$$g_3^* = 0, \quad g_4 = 32\epsilon/15, \tag{4.3}$$

$$D^* = -\epsilon/5. \tag{4.4}$$

Linearizing the flow, Eqs. (3.60), (3.61), and (4.2) around this fixed point, we obtain (3.67) and (3.68), and

$$\frac{d\delta D(\ell)}{d\ell} = \lambda_D\delta D + \left(\frac{1}{4}D^* - \frac{3}{16}K_0\right)\delta g_3 + \left(\frac{3}{16}K_0 - \frac{9}{32}D^*\right)\delta g_4, \tag{4.5}$$

where

$$\lambda_D = 2 - \frac{3\epsilon}{5} + O(\epsilon^2). \tag{4.6}$$

The solutions of these flow equations are given by (3.69) and (3.70), and

$$\delta D(\ell) = c_3 e^{\lambda_D \ell} - \frac{K_0 c_1}{128} e^{-\epsilon \ell/5} - \frac{3K_0 c_2}{32} e^{-\epsilon \ell}, \tag{4.7}$$

where $c_{1,2,3}$ are variables determined by the initial condition via

$$c_1 = g_3^0 - g_3^*, \tag{4.8}$$

$$c_2 = g_4^0 - g_4^* - \frac{13}{12}(g_3^0 - g_3^*), \tag{4.9}$$

$$c_3 = D_0 - D^* + \frac{K_0 c_1}{128} + \frac{3K_0 c_2}{32}, \tag{4.10}$$

where D_0, g_3^0, and g_4^0 are the completely bare values of D, g_3, and g_4, respectively. According to the solution given by (4.7), the fixed point is unstable with respect to D unless $c_3=0$, which defines exactly the critical point. After some algebra, the critical point is identified as

$$D_0(T_{AC}) = \frac{3K_0}{32} g_3^0 - \frac{3K_0}{32} g_4^0, \tag{4.11}$$

which actually describes a plane in $D-g_3-g_4$ space. This shows that the true critical point has dependence on g_3^0 and g_4^0, and is *not* exactly at $D_0(T)=0$, which is predicted by the mean-field theory. c_3 measures the deviation from the critical point and is often assumed to be

$$c_3 \propto T - T_{AC}. \tag{4.12}$$

For initial values D_0, g_3^0, and g_4^0 off from the critical plane, $D(\ell)$ departures exponentially under the RG and, for large ℓ, behaves as

$$D(\ell) \propto c_3 e^{\lambda_D \ell} \propto (T - T_{AC}) e^{\lambda_D \ell}. \tag{4.13}$$

The system is in the A phase for $T > T_{AC}$ (i.e., $c_3 > 0$) and in the C phase for $T < T_{AC}$ (i.e., $c_3 < 0$). The universality classes of both phases will be discussed in Sec. VI.

Now we calculate the critical exponents $\nu_\perp$ and ν_z. These two exponents are defined via the two correlation lengths $\xi_\perp$ and ξ_z by the equations

$$\xi_\perp \propto |T - T_{AC}|^{-\nu_\perp}, \tag{4.14}$$

$$\xi_z \propto |T - T_{AC}|^{-\nu_z}. \tag{4.15}$$

These two correlation lengths are the characteristic lengths beyond which the critical behavior crosses over to either the high-temperature (smectic-A) or low-temperature (smectic-C) behavior. More specifically, the correlation length $\xi_\perp$ satisfies $K(\xi_\perp)^{-2} = D$, which, under the RG, is mapped to

$$K(\ell^*)\Lambda^2 = D(\ell^*), \tag{4.16}$$

with

$$\xi_\perp = e^{\ell^*} \Lambda^{-1}, \tag{4.17}$$

where due to the special rescaling (4.1), $K(\ell^*)$ is fixed at K_0 and $D(\ell)$ is given by (4.13). Thus we obtain

$$\ell^* \propto -\frac{1}{\lambda_D} \ln|T - T_{AC}|, \tag{4.18}$$

which, combined with Eq. (4.17), gives

$$\xi_\perp \propto |T - T_{AC}|^{1/\lambda_D}. \tag{4.19}$$

Therefore, the RG predicts

$$\nu_\perp = \frac{1}{\lambda} = \frac{1}{2} + \frac{3\epsilon}{20} + O(\epsilon^2). \tag{4.20}$$

The other correlation length ξ_z can be obtained using the scaling law $\xi_z \propto \xi_\perp^\zeta$; this leads to

$$\nu_z = \zeta \nu_\perp = 1 + \frac{3\epsilon}{10} + O(\epsilon^2). \tag{4.21}$$

In order to calculate the specific heat exponent α, we need to find the temperature dependence of the free energy. Since the free energy F is invariant under the RG, we can write it as

$$\begin{aligned} F &= V_r f_r(K(\ell^*), B(\ell^*), D(\ell^*), \Delta(\ell^*), g(\ell^*), \omega(\ell^*)) \\ &= V_0 e^{-(d-1)\ell^* - w\ell^*} f_r, \end{aligned}$$

where V_r and f_r are the renormalized volume and free energy density and V_0 is the physical volume before renormalization. To factor out the temperature dependence of f_r as much as possible, we make a special choice of ℓ^*, ω, and χ:

$$\ell^* = \ln(\xi_\perp \Lambda), \tag{4.22}$$

$$\omega = 2 - \frac{\eta_B + \eta_K}{2}, \tag{4.23}$$

$$\chi = \frac{1}{4}(6 - 2d + \eta_B - \eta_K). \tag{4.24}$$

This choice fixes K and B so that they are ℓ independent and hence temperature independent. The choice of ℓ^* makes $D(\ell^*) = K_0 \Lambda^2$ and hence also temperature independent, and for such large $D(\ell^*)$ fluctuations are small, and f_r can be evaluated by ignoring the anharmonic terms. In spite of all the advantages just described, f_r is a function of $\Delta(\ell^*)$, which still has temperature dependence. Fortunately, by taking $\partial f_r / \partial \Delta(\ell^*)$, which can be easily calculated, we find that f_r is a linear function of $\Delta(\ell^*)$. Finally the free energy can be nicely written as

$$\begin{aligned} F &= V_0 e^{-(d-1)\ell^* - w\ell^*} [\Delta(\ell^*) + \text{const}] \\ &\propto |T - T_c|^{\nu_\perp [d+1-(\eta_K+\eta_B)/2]} \\ &\quad \times (|T - T_c|^{\nu_\perp (-2+\eta_K-\eta_t)} + \text{const}). \end{aligned} \tag{4.25}$$

Now taking $\partial^2 F / \partial T^2$ and keeping the most divergent part, we get the specific heat exponent

$$\alpha = 2 - \nu_\perp \left(d - 1 + \frac{\eta_K - \eta_B}{2} - \eta_t \right). \tag{4.26}$$

V. ANOMALOUS ELASTICITY RIGHT AT THE CRITICAL POINT

In this section we show that the existence of the stable fixed point leads to anomalous elasticity by using trajectory integral matching. For the sake of simplicity we assume that the system is right at the critical point, so that we do not need to worry about the crossover from the critical region to the *A* or *C* phase, which will be taken care of when we discuss correlations functions in Sec. VIII. Let us calculate the disorder-averaged correlation function $G(\vec{q}) \equiv \overline{\langle |u(\vec{q})|^2 \rangle - \langle u(-\vec{q}) \rangle \langle u(\vec{q}) \rangle}$. The RG establishes a connection between a correlation function at a small wave vector (which is impossible to calculate in perturbation theory due to the infrared divergence) and the same correlation function at a large wave vector, which can be easily calculated in a controlled perturbation theory. This connection for $G(\vec{q})$ is

$$G(\vec{q},B,K,\Delta_t,g,w) = e^{(d-1+\omega+2\chi)\ell} G(q_\perp e^{\ell}, q_z e^{\omega\ell}, B(\ell), K(\ell), \Delta_t(\ell), g(\ell), w(\ell)), \tag{5.1}$$

where the prefactor on the right-hand side comes from the dimensional and field rescaling. First let us consider the special case $q_z=0$. The rescaling variable ℓ^* is chosen as

$$q_\perp e^{\ell^*} = \Lambda. \tag{5.2}$$

We also choose $q_\perp$ sufficiently small such that $g_3(\ell^*)$ and $g_4(\ell^*)$ has reached the stable fixed point $g_3^*=0$, $g_4^*=32\epsilon/15$. Eliminating ℓ^* in favor of $q_\perp$, we get

$$G(q_\perp, q_z=0, B, K, \Delta_t, g, w) = \left(\frac{\Lambda}{q_\perp}\right)^{d-1+\omega+2\chi} \times G(\Lambda, 0, B(\ell^*), K(\ell^*), \Delta_t(\ell^*), g(\ell^*), w(\ell^*)).$$

Evaluating the right-hand side using a perturbation theory, we obtain

$$G(q_\perp, q_z=0, B, K, \Delta_t, g, w) = \frac{1}{\Lambda^4 K(\ell^*)} \left(\frac{\Lambda}{q_\perp}\right)^{d-1+\omega+2\chi} \equiv \frac{1}{K(q_\perp, q_z=0) q_\perp^4}, \tag{5.3}$$

where

$$K(\ell^*) = K_0 (\xi_{NL}^\perp \Lambda)^{d-5+\omega+2\chi} (\xi_{NL}^\perp q_\perp)^{-(d-5+\omega+2\chi-g_3^*/32)},$$

which is obtained by integrating the flow Eq. (3.55), and the anomalous bend modulus which diverges at long length scales is defined as

$$K(q_\perp, q_z=0) = K_0 (q_\perp \xi_{NL}^\perp)^{-\eta_K}, \tag{5.4}$$

with an anomalous exponent

$$\eta_K = \frac{1}{32} g_3^*. \tag{5.5}$$

$\xi_{NL}^\perp$ is the nonlinear crossover length along $\perp$ directions, beyond which the perturbation theory breaks down.

The above calculations can be generalized for arbitrary direction of $\vec{q}$ by using a more sophisticated choice of ℓ^*, which satisfies

$$K(\ell^*)\Lambda^2 = K(\ell^*)(q_\perp e^{\ell^*})^4 + B(\ell^*)(q_z e^{\omega\ell^*})^2. \tag{5.6}$$

This choice ensures that the right-hand side of (5.1) can be evaluated in a controlled perturbation theory and is consistent with (5.2) in the special case $q_z=0$. Solving (5.6), we obtain

$$e^{\ell^*} = \left(\frac{\Lambda}{q_\perp}\right) f_\ell \left[\frac{(q_\perp \xi_{NL})^\zeta}{q_z \xi_{NL}^z}\right], \tag{5.7}$$

where the anisotropy exponent ζ is given by

$$\zeta = 2 - \frac{\eta_K + \eta_B}{2}, \tag{5.8}$$

η_B is defined as the anomalous exponent of the compression modulus B,

$$B(q_\perp, q_z=0) = B_0 (q_\perp \xi_{NL}^\perp)^{\eta_B}, \tag{5.9}$$

and given by

$$\eta_B = \frac{3}{16} g_3^*, \tag{5.10}$$

and $f_\ell(x)$ is a scaling function:

$$f_\ell(x) = \begin{cases} 1, & x \ll 1, \\ x^{1/\zeta}, & x \gg 1. \end{cases} \tag{5.11}$$

Plugging (5.7) into (5.1) leads to the general $\vec{q}$ dependence of both K and B, which is summarized in (1.27) and (1.33).

The $\vec{q}$ dependence of Δ_t cannot be calculated by using the correlation function $G(\vec{q}) \equiv \overline{\langle |u(\vec{q})|^2 \rangle - \langle u(-\vec{q}) \rangle \langle u(\vec{q}) \rangle}$ since it is independent of Δ_t. Instead we perform trajectory integral matching on the correlation function $\overline{\langle u(\vec{q}) \rangle \langle u(-\vec{q}) \rangle} = \Delta_t q_\perp^2 G(\vec{q})^2$. After a similar calculation for the special case $q_z=0$, we find that Δ_t also diverges at small $q_\perp$ as

$$\Delta_t(q_\perp, q_z=0) = \Delta_t^0 (q_\perp \xi_{NL}^\perp)^{-\eta_t}, \tag{5.12}$$

where the anomalous exponent η_t is given by

$$\eta_t = \tfrac{1}{64} g_3^*. \tag{5.13}$$

Generalizing the calculation for arbitrary $\vec{q}$, we get the result summarized in (1.32).

Since g_3^* is zero, $\eta_{K,t}$ are zero to $O(\epsilon)$ and η_B is zero *exactly*. To calculate $\eta_{K,t}$ to $O(\epsilon^2)$, we performed a two-loop RG calculation showing that

$$\eta_K = C_K \epsilon^2 + O(\epsilon^3), \qquad \eta_t = C_\Delta \epsilon^2 + O(\epsilon^3), \tag{5.14}$$

where $C_K = [32 \ln(4/3) - 10]/225$ and $C_\Delta = [12 \ln(4/3) - 1/3]/225$.

VI. *A* AND *C* PHASES

In this section we will identify the universality classes of both the high-temperature (*A*) and low-temperature (*C*)

phases. For now let us assume that the system is far away from the critical point so that we do not need to worry about the crossovers between the critical region and the two phases, which will be discussed in Sec. VIII. First we discuss the A phase. The model we start with is the Hamiltonian (2.10). Since at long wavelengths the tilt term $D_0|\vec{\nabla}_\perp u|^2/2$ dominates the bend term $K(\nabla_\perp^2 u)^2/2$, the latter can be neglected. The model reduces to

$$H = \int d^d r \left[\frac{B}{2}(\partial_z u)^2 + \frac{D}{2}|\vec{\nabla}_\perp u|^2 - \frac{g}{2}(\partial_z u)|\vec{\nabla}_\perp u|^2 + \frac{w}{8}|\vec{\nabla}_\perp u|^4 + \vec{h}(\vec{r})\cdot\vec{\nabla} u + V_p(u-\phi(\vec{r}))\right]. \tag{6.1}$$

For this model a simple power counting shows that both the anharmonic terms and the random tilt disorder are irrelevant in $d>2$. Thus in $d=3$ the effective model for the A phase is simply

$$H = \int d^d r \left[\frac{B}{2}(\partial_z u)^2 + \frac{D}{2}|\vec{\nabla}_\perp u|^2 + V_p(u-\phi(\vec{r}))\right], \tag{6.2}$$

which is just the random-field XY model with anisotropic stiffness. This model has been studied extensively, and the correlation $\langle[u(\vec{r})-u(\vec{0})]^2\rangle$ has a logarithmic divergence as $r\to\infty$. As a result, the density correlation function for the A phase decays as a power law, which implies that the A phase only has quasi-long-range translational order. However, unlike the conventional smectic A phase, in which the power-law exponent depends on the temperature, here the exponent is *universal*. These correlation functions will be calculated in detail in Sec. VIII.

Deep in the C phase, $D|\vec{\nabla}_\perp u|^2/2$ is negative. Let us first use a mean-field theory to find the new *disorder-averaged* ground state of the *disordered* Hamiltonian (2.10). Since the two disordered interactions in the Hamiltonian are totally random and isotropic, they should not affect the mean-field theory. Therefore we ignore them for the moment and work on the *clean* Hamiltonian

$$H = \int d^d r \left[\frac{B}{2}(\partial_z u)^2 + \frac{D_0}{2}|\vec{\nabla}_\perp u|^2 + \frac{K}{2}(\nabla^2 u)^2 - \frac{g}{2}(\partial_z u)|\vec{\nabla}_\perp u|^2 + \frac{w}{8}|\vec{\nabla}_\perp u|^4\right], \tag{6.3}$$

which can be rewritten as

$$H = \int d^d r \left[\frac{B}{2}\left(\partial_z u - \frac{g}{2B}|\vec{\nabla}_\perp u|^2\right)^2 + \frac{K}{2}(\nabla^2 u)^2 + \frac{w'}{8}\left(|\vec{\nabla}_\perp u|^2 + \frac{2D}{w'}\right)^2 - \frac{D^2}{2w'}\right], \tag{6.4}$$

where

$$w' \equiv w - (g^2/B). \tag{6.5}$$

$w'=0$ is the tricritical point separating the first-order ($w'<0$) and second-order ($w'>0$) phase transitions. Assuming $w'>0$, since we are interested in the second-order phase transition, the ground state of the Hamiltonian (6.4) is given by

$$|\vec{\nabla}_\perp u| = \sqrt{-\frac{2D}{w'}}, \tag{6.6}$$

$$\partial_z u = \frac{gD}{Bw'}. \tag{6.7}$$

Now we go back to the disordered Hamiltonian (2.10) and expand it around its *disorder-averaged* minimum by making the substitution

$$u = \sqrt{-\frac{2D}{w'}}x + \frac{gD}{Bw'}z + u', \tag{6.8}$$

where we have assumed that in the C phase the system spontaneously breaks azimuthal rotation symmetry and the layer normal tilts along $\hat{x}$, which is an arbitrary direction within $\perp$ plane. Also for simplicity we throw away the random-field term by using *a posterior* reasoning; that is, if the C phase is $m=1$ Bragg glass, then the random-field disorder is irrelevant [6]. For brevity, we define $\theta_0 \equiv \sqrt{-2D/w'}$. After the substitution and simplification, the Hamiltonian (2.10) becomes

$$H[u'] = \frac{1}{2}\int d^d r \left[K(\nabla_s^2 u')^2 + B(\partial_z u')^2 + w\theta_0^2(\partial_x u')^2 - 2g\theta_0(\partial_x u')(\partial_z u') - g(\partial_z u')|\vec{\nabla}_s u'|^2 + w\theta_0(\partial_x u')|\vec{\nabla}_s u'|^2 + \frac{w}{4}|\vec{\nabla}_s u'|^4 + \vec{h}(\vec{r})\cdot\vec{\nabla} u'\right], \tag{6.9}$$

where $\hat{s}$ denotes the direction which is perpendicular to both $\hat{x}$ and $\hat{z}$. Treating the tilt disorder by using the replica trick, we get

$$H[u'_\alpha] = \frac{1}{2}\int d^d r \sum_{\alpha=1}^{n} \left[K(\nabla_s^2 u'_\alpha)^2 + B(\partial_z u'_\alpha)^2 + w\theta_0^2(\partial_x u'_\alpha)^2 - 2g\theta_0(\partial_x u'_\alpha)(\partial_z u'_\alpha) - g(\partial_z u'_\alpha)|\vec{\nabla}_s u'_\alpha|^2 + w\theta_0(\partial_x u'_\alpha)|\vec{\nabla}_s u'_\alpha|^2 + \frac{w}{4}|\vec{\nabla}_s u'_\alpha|^4\right] - \frac{\Delta_t}{2T}\int d^d r \sum_{\alpha,\beta=1}^{n} \nabla_\perp u'_\alpha \cdot \nabla_\perp u'_\beta - \frac{\Delta_c}{2T}\int d^d r \sum_{\alpha,\beta=1}^{n} \partial_z u'_\alpha \cdot \partial_z u'_\beta, \tag{6.10}$$

whose universality class is still not clear. Then we make the following coordinate transformation:

$$r_{z'} = (g/w\theta_0)r_x + r_z,$$

$$r_{x'} = r_x,$$

$$r_{s'} = r_s, \tag{6.11}$$

which, in momentum space, corresponds to the transformation

$$q_{z'} = q_z,$$

$$q_{x'} = q_x - \Gamma q_z,$$

$$q_{s'} = q_s, \tag{6.12}$$

with

$$\Gamma = g/w\theta_0 = \frac{g}{w}\sqrt{\frac{w'}{-2D}}. \tag{6.13}$$

After this coordinate transformation the Hamiltonian (6.10) becomes

$$\begin{aligned} H[u'_\alpha] = \frac{1}{2}\int d^d r' \sum_{\alpha=1}^{n} \Big[& \tilde{K}(\nabla_{s'}^2 u'_\alpha)^2 + \tilde{B}(\partial_{z'} u'_\alpha)^2 + \gamma(\partial_{x'} u'_\alpha)^2 \\ & + \tilde{g}(\partial_{x'} u'_\alpha)|\vec{\nabla}_{s'} u'_\alpha|^2 + \frac{w}{4}|\vec{\nabla}_{s'} u'_\alpha|^4 \Big] \\ & - \frac{1}{2T}\int d^d r' \sum_{\alpha,\beta=1}^{n} [\Delta_{s'}(\vec{\nabla}_{s'} u'_\alpha \cdot \vec{\nabla}_{s'} u'_\beta) \\ & + \Delta_{x'}(\partial_{x'} u'_\alpha)(\partial_{x'} u'_\beta) + \Delta_{z'}(\partial_{z'} u'_\alpha)(\partial_{z'} u'_\beta)] \\ & + \frac{1}{2T}\int d^d r' \sum_{\alpha,\beta=1}^{n} \Delta_{x'z'}(\vec{\nabla}_{x'} u'_\alpha \cdot \vec{\nabla}_{z'} u'_\beta), \end{aligned} \tag{6.14}$$

with

$$\tilde{B} = B - \frac{g^2}{w}, \tag{6.15}$$

$$\tilde{K} = K, \tag{6.16}$$

$$\gamma = w\theta_0^2, \tag{6.17}$$

$$\tilde{g} = w\theta_0, \tag{6.18}$$

$$\Delta_{s'} = \Delta_t, \tag{6.19}$$

$$\Delta_{x'} = \Delta_t, \tag{6.20}$$

$$\Delta_{x'z'} = \frac{2g\Delta_t}{w\theta_0}, \tag{6.21}$$

$$\Delta_{z'} = \Delta_t\left(\frac{g}{w\theta_0}\right)^2 + \Delta_c. \tag{6.22}$$

It is easy to check that γ, $\tilde{g}$, and w satisfy the magic relation $\tilde{g} = \sqrt{w\gamma}$. This is not a coincidence, but due to the symmetry; that is, the Hamiltonian must be invariant under the rotation about the $\hat{z}$ axis since the environment (i.e., the aerogel stretched along $\hat{z}$) is azimuthally symmetric. Because of this symmetry, the model (6.14) belongs to the universality class of $m=1$ smectic Bragg glass.

VII. WAVE-VECTOR DEPENDENCES OF IRRELEVANT DISORDER VARIANCES

In our RG calculations in Sec. III we have not included in the Hamiltonian (3.1) the random compression disorder

$$-\frac{\Delta_c}{2T}\int d^d r \sum_{\alpha,\beta=1}^{n} \partial_z u_\alpha \cdot \partial_z u_\beta. \tag{7.1}$$

A simple power counting shows that this term is irrelevant and thus has no effect on the critical behavior and anomalous elasticity. However, while it does not affect the anomalous elasticity, the disorder invariance Δ_c itself develops strong power-law dependence on the wave vector at long wavelength. Now we calculate the power-law exponent, which we denote as η_c, to $O(\epsilon)$. This is necessary since the random compression disorder has a nontrivial contribution to the correlation function $\langle|u(\vec{q})|^2\rangle$ and therefore affects the light-scattering predictions.

The most important one-loop graphical correction to Δ_c comes from the Feynman diagram in Fig. 7, from which we obtain

$$\begin{aligned} \delta\Delta_c &= \frac{g^2}{2}\int_q^> \Delta_t^2 q_\perp^8 G(\vec{q})^4 \\ &= \frac{g^2\Delta_t^2}{2}\int_{-\infty}^{\infty}\frac{dq_z}{2\pi}\int^> \frac{d^{d-1}q_\perp}{(2\pi)^{d-1}}\frac{q_\perp^8}{(Kq_\perp^4 + Bq_z^2)^4} \\ &= \frac{5}{64}C_{d-1}\Delta_t^2\left(\frac{g^4}{K^7 B}\right)^{1/2}\Lambda^{d-7}. \end{aligned} \tag{7.2}$$

Thus using the dimension and field rescaling we used in Sec. III, the RG flow equation of Δ_c to one-loop order is given by

$$\frac{d\Delta_c(\ell)}{d\ell} = \left(d + 1 - \omega + 2\chi + \frac{5}{64}g_5\right)\Delta_c, \tag{7.3}$$

where the dimensionless coupling g_5 is defined as

$$g_5 \equiv B\Delta_t g_3/K\Delta_c. \tag{7.4}$$

Combining this RG flow equation with the flow, Eqs. (3.54)–(3.56), (3.60), and (3.61), we get

$$\frac{dg_5}{d\ell} = \left(2 - \frac{1}{5}\epsilon - \frac{5}{64}g_5\right)g_5, \tag{7.5}$$

which flows to a stable nontrivial fixed point $g_5^* = 64(10-\epsilon)/25$. Then the wave-vector dependence of Δ_c can be calculated by performing trajectory integral matching on the correlation function $\overline{\langle u(-\vec{q})\rangle\langle u(\vec{q})\rangle} = (\Delta_t q_\perp^2 + \Delta_c q_z^2)G(\vec{q})^2$. The calculations are essentially the same as those in Sec. V and will not be repeated here again. The result is given in (1.32) with the anomalous exponent

$$\eta_c = \tfrac{5}{64}g_5^* = 2 - \tfrac{1}{5}\epsilon + O(\epsilon^2). \tag{7.6}$$

Note that η_c is nonzero even to the *zeroth* order of ϵ, which is quite common for irrelevant variables.

It is also interesting to point out that η_c is not fully independent, but are related to other anomalous exponents by an *exact* scaling relation, which is implied by the fact that g_5 flows to a nonzero stable fixed point. For large enough ℓ, g_5 reaches the fixed point and thus

$$\frac{d\ln g_5}{d\ell} = 0. \tag{7.7}$$

This equation, after decomposing g_5 into small pieces by its definition (7.4), leads to

$$\frac{d\ln B}{d\ell} + \frac{d\ln \Delta_t}{d\ell} + \frac{d\ln g_3}{d\ell} - \frac{d\ln K}{d\ell} - \frac{d\ln \Delta_c}{d\ell} = 0. \tag{7.8}$$

After plugging the flow, Eqs. (3.54)–(3.56), (B3), and (7.3) into the above equation, the rescaling factors χ and ω vanish and we are left with

$$\eta_c = 2 + \eta_t - \eta_B - \eta_K - \eta_3. \tag{7.9}$$

Since we already know the value of η_t, η_B, η_K, and η_3 to $O(\epsilon)$, using (7.9) also leads to (7.6).

Likewise, in the model of the C phase, which is given by (6.14), there are also disordered terms which are irrelevant in the RG calculation, but important for making light-scattering predictions. These terms are

$$-\frac{\Delta_{x'}}{2T}\int d^d r \sum_{\alpha,\beta=1}^{n} \partial_{x'}u'_\alpha \cdot \partial_{x'}u'_\beta,$$

$$\frac{\Delta_{x'z'}}{2T}\int d^d r \sum_{\alpha,\beta=1}^{n} \partial_{z'}u'_\alpha \cdot \partial_{x'}u'_\beta,$$

$$-\frac{\Delta_{z'}}{2T}\int d^d r \sum_{\alpha,\beta=1}^{n} \partial_{z'}u'_\alpha \cdot \partial_{z'}u'_\beta.$$

$\Delta z'$ and $\Delta_{x'z'}$ have no wave-vector dependences since there are no graphical corrections to them.

As for $\Delta_{x'}$, we will use a different RG—namely, the RG calculation for $m=1$ Brag glass—to show the power-law wave-vector dependence of $\Delta_{x'}$ and calculate the power-law exponent, which we denote as $\tilde{\eta}_{x'}$. For convenience, we transform the Hamiltonian (6.14) into the exact form studied in [6]. This transformation is accomplished by doing the field rescaling

$$u' = \theta_0 u''. \tag{7.10}$$

In terms of u'' the Hamiltonian (6.14) can be written as

$$H[u''_\alpha] = \frac{1}{2}\int d^d r' \sum_{\alpha=1}^{n}\left[\tilde{K}'(\nabla^2_{s'}u''_\alpha)^2 + \tilde{B}'(\partial_{z'}u''_\alpha)^2 + \gamma'(\partial_{x'}u''_\alpha)^2 + \gamma'(\partial_{x'}u''_\alpha)|\vec{\nabla}_{s'}u''_\alpha|^2 + \frac{\gamma'}{4}|\vec{\nabla}_{s'}u''_\alpha|^4\right]$$
$$-\frac{1}{2T}\int d^d r' \sum_{\alpha,\beta=1}^{n}[\Delta'_{s'}(\vec{\nabla}_{s'}u''_\alpha \cdot \vec{\nabla}_{s'}u''_\beta) + \Delta'_{x'}(\partial_{x'}u''_\alpha)(\partial_{x'}u''_\beta)], \tag{7.11}$$

where the coefficients of the quadratic terms are related to the original ones by

$$\tilde{K}', \tilde{B}', \gamma', \Delta'_{s',x'} = \theta_0^2(\tilde{K}, \tilde{B}, \gamma, \Delta_{s',x'}). \tag{7.12}$$

For this model, the detailed RG calculation can be found in [6]. Here we describe the calculation very briefly. A hypercylindrical Brillouin zone is used: $-\Lambda < q_{s'} < \Lambda$, $-\infty < q_{x'} < \infty$, $0 < |\vec{q}_{z'}| < \infty$, where Λ is an ultraviolet cutoff. Note that based on the arguments in the previous section, Λ has to be replaced by $\xi_\perp^{-1}$ when the system is within the critical region. The displacement field is separated into high- and low-wave-vector components, $u''_\alpha(\vec{r}) = u''^{<}_\alpha(\vec{r}) + u''^{<}_\alpha(\vec{r})$, where $u''^{>}_\alpha(\vec{r})$ has support in the hypercylindrical shell $\Lambda e^{-\ell} < |q_{s'}| < \Lambda$, $-\infty < q_{x'} < \infty$, $0 < |\vec{q}_{z'}| < \infty$, and $u''^{<}_\alpha(\vec{r})$ has support in the remainder of the hypercylinder (i.e., $0 < |q_{s'}| < \Lambda e^{-\ell}$, $-\infty < q_{x'} < \infty$, $0 < |\vec{q}_{z'}| < \infty$). Then integrate out the high-wave-vector part $u''^{>}_\alpha(\vec{r})$ and rescale the length and long-wavelength part of the fields with $r_{s'} = r'_{s'}e^{\ell}$, $r_{x'} = r'_{x'}e^{\omega_{x'}\ell}$, $r_{z'} = r'_{z'}e^{\omega_{z'}\ell}$, $u''_\alpha(\vec{r}) = e^{\chi'\ell}u'''_\alpha(\vec{r}')$ so as to restore the UV cutoff back to Λ.

The underlying symmetry of the model (7.11) guarantees that the unit $[\partial_{x'}u''_\alpha - (\nabla_{s'}u''_\alpha)^2/2]$ is graphically renormalized as a whole. Therefore it is convenient to choose the rescaling which also preserve the unit; the appropriate choice is $\chi' = 2 - \omega_{x'}$.

Using the hard continuation (namely, keeping the number of the *soft* directions fixed at 1 for all spatial dimension d), the RG to one-loop order gives the following flow equations:

$$\frac{d\gamma'(\ell)}{d\ell} = \left[5 + (d-2)\omega_{z'} - 3\omega_{x'} - \frac{3g_6}{32\sqrt{2}}\right]\gamma', \tag{7.13}$$

$$\frac{d\tilde{K}'(\ell)}{d\ell} = \left[1 + (d-2)\omega_{z'} - \omega_{x'} + \frac{g_6}{8\sqrt{2}}\right]K', \tag{7.14}$$

$$\frac{d(\Delta'_{s'}/T)(\ell)}{d\ell} = \left[3 + (d-2)\omega_{z'} - \omega_{x'} + \frac{g_6}{32\sqrt{2}}\right](\Delta'_{s'}/T), \tag{7.15}$$

where $g_6 \equiv \Delta'_{s'}[\gamma'/(K'^{7-d}B'^{d-2})]^{1/2}C_{d-1}\Lambda^{2d-7}$ is a dimensionless measure of disorder, whose flow equation is

$$\frac{dg_6(\ell)}{d\ell} = 2\tilde{\epsilon}g_6 - \frac{15}{64\sqrt{2}}g_6^2, \tag{7.16}$$

where $\tilde{\epsilon} = 7/2 - d$. This equation has a stable fixed point

$$g_6 = \frac{128\sqrt{2}}{15}\tilde{\epsilon}. \tag{7.17}$$

Using trajectory integral matching we can calculate the wave-vector dependences of γ', $\tilde{K}'$, and $\Delta'_{s'}$, which, combined with (7.12), leads to the wave-vector dependences of K, $\Delta_{s'}$, and γ summarized by (1.5), (1.7), and (1.6), with the exponents

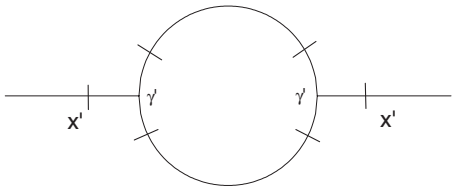

FIG. 21. The graphical correction to $\Delta'_{x'}$.

$$\tilde{\zeta}_{x'} = 2 - \frac{\tilde{\eta}_\gamma + \tilde{\eta}_K}{2}, \tag{7.18}$$

$$\tilde{\zeta}_{z'} = 2 - \frac{\tilde{\eta}_K}{2}, \tag{7.19}$$

$$\tilde{\eta}_K = \frac{g_6^*}{8\sqrt{2}} = \frac{16}{15}\tilde{\epsilon} + O(\tilde{\epsilon}^2), \tag{7.20}$$

$$\tilde{\eta}_{s'} = \frac{g_6^*}{32\sqrt{2}} = \frac{4}{15}\tilde{\epsilon} + O(\tilde{\epsilon}^2), \tag{7.21}$$

$$\tilde{\eta}_\gamma = \frac{3}{32\sqrt{2}} g_6^* = \frac{4}{5}\tilde{\epsilon} + O(\tilde{\epsilon}^2). \tag{7.22}$$

So far, we have briefly reviewed the RG calculation for $m=1$ Brag glass; now, we use it to calculate the wave-vector dependence of the irrelevant disorder invariance $\Delta'_{x'}$. The Feynman diagram for the one-loop graphical correction to $\Delta'_{x'}$ is presented in Fig. 21. An analysis of the diagram gives

$$\delta\Delta'_{x'} = \frac{\gamma'^2 \Delta'^2_{s'}}{2} \int_{-\infty}^{\infty} \frac{dq_{z'}}{2\pi} \int_{-\infty}^{\infty} \frac{d^{d-2}q_{x'}}{(2\pi)^{d-2}} \times \int^{>} \frac{dq_{s'}}{(2\pi)} \frac{q_{s'}^8}{(K' q_{s'}^4 + \tilde{B}' q_{z'}^2 + \gamma' q_{x'}^2)^4} = \frac{21}{128\sqrt{2}} g_7, \tag{7.23}$$

where g_7 is another dimensionless coupling defined as $g_7 \equiv g_6 \gamma' \Delta'_{s'} \Lambda^{-2} / (K' \Delta'_{x'})$. Thus the RG flow of $\Delta'_{x'}$ to one-loop order is given by

$$\frac{d\Delta'_{x'}(\ell)}{d\ell} = \left[5 + (d-2)\omega_{z'} - 3\omega_{x'} + \frac{21}{128\sqrt{2}} g_7 \right] \Delta'_{x'}. \tag{7.24}$$

Combining this flow equation with (7.13)–(7.15), we obtain the flow equation of the dimensionless coupling g_7:

$$\frac{dg_7}{d\ell} = \left(2 - \frac{8}{5}\tilde{\epsilon}\right) g_7 - \frac{21}{128\sqrt{2}} g_7^2, \tag{7.25}$$

which flows to the fixed point $g_7^* = 256\sqrt{2}(5-4\tilde{\epsilon})/105$. At this point, our experience from the previous calculations immediately gives us the wave-vector dependence of $\Delta'_{x'}$, which, combined with (7.12), leads to the wave-vector dependence of $\Delta_{x'}$ summarized by (1.6). The power-law exponent $\tilde{\eta}_{x'}$ is given by

$$\tilde{\eta}_{x'} = \frac{21}{128\sqrt{2}} g_7^* = 2 - \frac{8}{5}\tilde{\epsilon} + O(\tilde{\epsilon}^2). \tag{7.26}$$

That both g_6 and g_7 flow to nonzero fixed points implies the *exact* scaling relations (1.18) and (1.19). For the derivation, please refer to how we derive (7.9).

In addition, using soft continuation (i.e., keeping the number of *hard* directions fixed at 2) one obtains

$$\tilde{\eta}_{x'} = 2 + \tilde{\tilde{\epsilon}} + O(\tilde{\tilde{\epsilon}}^2) \tag{7.27}$$

and the same *exact* scaling relation given by (1.19), where $\tilde{\tilde{\epsilon}} = 4 - d$. The numerical estimate and error bar for $\eta_{x'}$ can be obtained using the approach described in Appendix A.

VIII. CORRELATION FUNCTIONS

In this section we discuss correlation functions and make x-ray- and light-scattering predictions. We start with the calculation of the disorder-averaged fluctuations in momentum space, $\overline{\langle |u(\vec{q})|^2 \rangle}$. In our problem this quantity has three main distinct types of behavior. They are characterized by fluctuations in the *A* phase, fluctuations in the *C* phase, and fluctuations right at the critical point, respectively. The first two types have been well studied and known, and the third type is unique to this problem. Our main interest is the rich crossovers between these distinct behaviors near the critical point, which leads to amazing experimental consequences. We warn the reader of heavy algebra in this section.

As we pointed out earlier, in some cases, while a certain type of disorder is irrelevant in the RG sense, it can have important contributions to correlation functions. Thus we prefer to use the complete model given by (2.12) to calculate $\overline{\langle |u(\vec{q})|^2 \rangle}$.

For large $\vec{q}$'s (i.e., $q_\perp \ll \xi_\perp^{-1}$ or $q_z \ll \xi_z^{-1}$), the model can be treated by the critical RG, and we get

$$\overline{\langle |u(\vec{q})|^2 \rangle} = \overline{\langle |u(\vec{q})|^2 \rangle_{AC}} \equiv \frac{\Delta_t(\vec{q}) q_\perp^2}{[B q_z^2 + D(T,\vec{q}) q_\perp^2 + K(\vec{q}) q_\perp^4]^2} + \frac{\Delta_c(\vec{q}) q_z^2}{[B q_z^2 + D(T,\vec{q}) q_\perp^2 + K(\vec{q}) q_\perp^4]^2}, \tag{8.1}$$

where K and $\Delta_{t,c}$ are all $\vec{q}$ dependent and given by (1.27) and (1.32), B is $\vec{q}$ independent, and D has dependences on both $\vec{q}$ and the temperature:

$$D(\vec{q}, T = T_{AC}) \approx \begin{cases} (T - T_{AC})(\xi_{NL}^\perp q_\perp)^{\eta_D}, & \xi_{NL}^z q_z \ll (\xi_{NL}^\perp q_\perp)^\zeta, \\ (T - T_{AC})(\xi_{NL}^z q_z)^{\eta_D/\zeta}, & \xi_{NL}^z q_z \gg (\xi_{NL}^\perp q_\perp)^\zeta, \end{cases} \tag{8.2}$$

where $\eta_D = 2 - \eta_K - 1/\nu_\perp$. The first and second terms in the Eq. (8.1) come from the random-tilt and random-compression disorders, respectively. In this case the random-field disorder is not only irrelevant in the RG calculation, but

also has negligible contributions to $\overline{\langle|u(\vec{q})|^2\rangle}$ in any region in $\vec{q}$ space and is thus neglected.

For small $\vec{q}$s (i.e., $q_\perp \ll \xi_\perp^{-1}$ or $q_z \ll \xi_z^{-1}$), the tilt term in the model dominates the bend term and the critical RG is no longer valid. A different RG needs to be used to treat the model. First let us derive the effective model for small $\vec{q}$'s. The derivation has two steps. The first step is to run the critical RG to the crossover point $\ell^* = \ln(\Lambda \xi_\perp)$ to obtain a model for the rescaled system. The second step is to undo the dimension and field rescaling we performed during the RG. Implementing this procedure, we obtain

$$H[u_\alpha] = \frac{1}{2}\int d^d r \Bigg(\sum_{\alpha=1}^{n} \Bigg[K(T)(\nabla_\perp^2 u_\alpha)^2 + B(\partial_z u_\alpha)^2 - g(T)(\partial_z u_\alpha) \times (\nabla_\perp u_\alpha)^2 + \frac{w(T)}{4}|\vec{\nabla}_\perp u_\alpha|^4 + D(T)|\nabla_\perp u_\alpha|^2 \Bigg] - \sum_{\alpha,\beta=1}^{n} \Bigg[\frac{\Delta_t(T)}{2T}\nabla_\perp u_\alpha \cdot \nabla_\perp u_\beta + \frac{\Delta_c(T)}{2T}\partial_z u_\alpha \cdot \partial_z u_\beta + \frac{1}{T}\Delta_p(u_\alpha - u_\beta) \Bigg] \Bigg), \tag{8.3}$$

where the coefficients are renormalized by the critical fluctuations and hence temperature dependent.

In the A-side critical region, based on the argument we give in Sec. VI, the model (8.3) belongs to the universality class of the random-field XY model. We treat it using the functional RG [7] and obtain

$$\overline{\langle|u(\vec{q})|^2\rangle} = \overline{\langle|u(\vec{q})|^2\rangle_A} \equiv \frac{\Delta_t(\vec{q},T)q_\perp^2}{(Bq_z^2 + D(T)q_\perp^2 + K(T)q_\perp^4)^2} + \frac{\Delta_c(\vec{q},T)q_z^2}{(Bq_z^2 + D(T)q_\perp^2 + K(T)q_\perp^4)^2} + \frac{CB^{1/2}D}{(Bq_z^2 + D(T)q_\perp^2 + K(T)q_\perp^4)^{3/2}q_0^2}, \tag{8.4}$$

where the third piece comes from the random-field disorder. The random-tilt and -compression disorder are irrelevant in the RG calculation; however, their contributions to $\overline{\langle|u(\vec{q})|^2\rangle}$ are important in some region in $\vec{q}$ space and hence kept. The constants K, D, and $\Delta_{t,c}$ in (8.4) are *not* wave vector dependent and given by

$$B = B_0(\xi_{NL}^\perp/\xi_\perp)^{\eta_B} = B_0,$$

$$K = K_0(\xi_{NL}^\perp/\xi_\perp)^{-\eta_K} \propto (T - T_{AC})^{-\eta_K \nu_\perp},$$

$$D = D_0(\xi_{NL}^\perp/\xi_\perp)^{\eta_D} \propto (T - T_{AC})^{(2-\eta_K)\nu_\perp},$$

$$\Delta_{t,c} = \Delta_{t,c}^0(\xi_{NL}^\perp/\xi_\perp)^{-\eta_{t,c}} \propto (T - T_{AC})^{-\eta_{t,c}\nu_\perp}.$$

In the C-side critical region, we have to expand the Hamiltonian (8.3) around the disorder-averaged minimum. Following the procedure in Sec. VI leads to the model (6.14), where for convenience a special coordinate system other than the laboratory one has been used. The relations between these two coordinate systems are controlled by the parameter Γ and, in Fourier space, given in Eqs. (1.8)–(1.10). Γ is now renormalized by critical fluctuations and hence temperature dependent, given by

$$\Gamma \sim (\xi_\perp \Lambda)^{1-(\eta_K+\eta_3)/2}. \tag{8.5}$$

The exponent is equal to 4/5 in $d=3$ to $O(\epsilon)$; therefore, Γ is expected to be very large as $T \to T_{AC}$. The derivation of this result is given in Appendix B. The temperature dependences of the coefficients in the model (6.14) can be derived in a similar way and are given by

$$\tilde{K}_c = K_0(\xi_{NL}^\perp/\xi_\perp)^{-\eta_K} \propto (T_{AC} - T)^{-\eta_K \nu_\perp}, \tag{8.6}$$

$$\gamma_c = D_0(\xi_{NL}^\perp/\xi_\perp)^{\eta_D} \propto (T_{AC} - T)^{(2-\eta_K)\nu_\perp}, \tag{8.7}$$

$$\Delta_{s',x'}^c = \Delta_t^0(\xi_{NL}^\perp/\xi_\perp)^{-\eta_t} \propto (T_{AC} - T)^{-\eta_t \nu_\perp}, \tag{8.8}$$

$$\Delta_{z'}^c = \left[\left(\frac{\xi_{NL}^\perp}{\lambda} \right)^2 \Delta_t^0 + \Delta_c^0 \right] \left(\frac{\xi_\perp}{\xi_{NL}^\perp} \right)^{\eta_c} \propto (T - T_{AC})^{-\eta_c \nu_\perp}. \tag{8.9}$$

These coefficients have been named "half-dressed" values (i.e., unrenormalized by the C fluctuations) in Eqs. (1.5)–(1.7). Treating the model (6.14) using the RG for $m=1$ smectic Bragg glass [6], we obtain

$$\overline{\langle|u(\vec{q})|^2\rangle} = \overline{\langle|u(\vec{q})|^2\rangle_C} \equiv \frac{\Delta_{s'}(\vec{q}',T)q_{s'}^2}{[\gamma(\vec{q}',T)q_{x'}^2 + \tilde{B}q_{z'}^2 + \tilde{K}(\vec{q}',T)q_{s'}^4]^2} + \frac{\Delta_{x'}(\vec{q}',T)q_{x'}^2}{[\gamma(\vec{q}',T)q_{x'}^2 + \tilde{B}q_{z'}^2 + \tilde{K}(\vec{q}',T)q_{s'}^4]^2} + \frac{\Delta_{z'}(T)q_{z'}^2}{[\gamma(\vec{q}',T)q_{x'}^2 + Bq_{z'}^2 + \tilde{K}(\vec{q}',T)q_{s'}^4]^2}, \tag{8.10}$$

where the $\vec{q}$ dependence's of $\tilde{K}$, γ, and $\Delta_{s',x'}$ are given in Eqs. (1.5), (1.7), and (1.6), and $\tilde{B}$ and $\Delta_{z'}$ are $\vec{q}$ independent. The first and second terms correspond to the contributions from the random-tilt disorder along the soft and hard directions in the original $m=1$ smectic problem, respectively, and the third term corresponds to the contribution from the random-compression disorder in the same problem. The random-field disorder is neglected since its contribution to $\overline{\langle|u(\vec{q})|^2\rangle}$ is always subdominant to the others.

Thus, near the critical point the behavior of $\overline{\langle|u(\vec{q})|^2\rangle}$ can be summarized in the following compact way:

$$\overline{\langle|u(\vec{q})|^2\rangle} = \begin{cases} \overline{\langle|u(\vec{q})|^2\rangle_A}, & q_\perp \ll \xi_\perp^{-1}, \quad q_z \ll \xi_z^{-1}, \quad \text{for } T > T_{AC}, \\ \overline{\langle|u(\vec{q})|^2\rangle_{AC}}, & q_\perp \gg \xi_\perp^{-1} \quad \text{or } q_z \gg \xi_z^{-1}, \\ \overline{\langle|u(\vec{q})|^2\rangle_C}, & q_\perp \ll \xi_\perp^{-1}, \quad q_z \ll \xi_z^{-1}, \quad \text{for } T < T_{AC}. \end{cases} \tag{8.11}$$

The x-ray-scattering pattern for both A and C phases has been studied before. It is quasisharp, isotropic for the A

phase, broad, anisotropic for the *C* phase. In the following we will discuss the crossover between the two distinct patterns in the critical region. The x-ray-scattering intensity is given by the Fourier transform of the thermal- and disorder-averaged $\rho-\rho$ correlation function

$$I(\vec{q}) \propto \int d^d r' d^d r'' \overline{\langle \rho(\vec{r}')\rho(\vec{r}'')\rangle} e^{-i\vec{q}\cdot(\vec{r}'-\vec{r}'')}, \tag{8.12}$$

where $\rho(\vec{r})$ is the molecule density. $\rho(\vec{r})$ can be expanded in a Fourier series with period a, the distance between nearest layers, via

$$\rho(\vec{r}) = \sum_{n=-\infty}^{\infty} \rho_n e^{inq_0[Z+u(\vec{r})]}, \tag{8.13}$$

where ρ_n is the (complex) amplitude of the nth harmonic of the smectic density wave and $u(\vec{r})$ is layer displacement at the point $\vec{r}$. Inserting the decomposition (8.13) into (8.12) gives

$$I(\vec{q}) \propto \sum_{n,n'} \rho_n \rho_{n'} \int d^d r' d^d r'' e^{-i\vec{q}\cdot(\vec{r}'-\vec{r}'')} e^{iq_0(nZ'+n'Z'')} \times \overline{\langle e^{iq_0[nu(\vec{r}')+n'u(\vec{r}'')]}\rangle}. \tag{8.14}$$

Changing variables of integration from $\vec{r}'$ to the different variable $\vec{r} \equiv \vec{r}' - \vec{r}''$ and using the fact that, in a homogeneous system

$$\overline{\langle e^{iq_0[nu(\vec{r}+\vec{r}'')+n'u(\vec{r}'')]}\rangle} = \overline{\langle e^{iq_0[nu(\vec{r})+n'u(\vec{0})]}\rangle}, \tag{8.15}$$

the integral over $\vec{r}''$ now just gives $V\delta_{n+n'}$, where V is the volume of the system and $\delta_{n+n'}$ is a Kronecker delta which can be used to collapse the sum on n' to the single term $n'=-n$. Doing so, we obtain

$$I(\vec{q}) \propto V \sum_n |\rho_n|^2 \int d^d r\, e^{i(nq_0\hat{Z}-\vec{q})\cdot\vec{r}} F_n(\vec{r}'), \tag{8.16}$$

where

$$F_n(\vec{r}) \equiv \overline{\langle e^{iq_0[nu(\vec{r})+n'u(\vec{0})]}\rangle}. \tag{8.17}$$

Now approximating the u fluctuation as a Gaussian, we can write

$$F_n(\vec{r}) = \exp\left(-\frac{n^2 q_0^2}{2} C(\vec{r})\right), \tag{8.18}$$

with

$$C(\vec{r}) \equiv \overline{\langle [u(\vec{r})-u(0)]^2\rangle} = \int \frac{d^d k}{(2\pi)^d} 2[1-\cos(\vec{r}\cdot\vec{q})]\overline{\langle u(\vec{q})u(-\vec{q})\rangle}. \tag{8.19}$$

Putting (8.18) into (8.16), we get

$$I(\vec{q}) \propto \sum_{n=1}^{\infty} \int d^d r\, e^{i(nq_0\hat{Z}-\vec{q})\cdot\vec{r}} \exp\left(-\frac{n^2 q_0^2}{2} C(\vec{r})\right). \tag{8.20}$$

For $\vec{q}$ near the Bragg peaks at the $mq_0\hat{Z}$, the sum is readily seen to be dominated by the $n=m$ term; thus, the scattering near the Bragg peaks is essentially the Fourier transform of $\exp[-n^2 q_0 C(\vec{r})/2]$.

Right at the critical point ($T=T_{AC}$), in spite of the symmetry broken we mentioned earlier, the fluctuations of the system is still qualitatively like those of "glassy smectic *A*;" hence, the x-ray-scattering pattern is also broad and anisotropic.

For $T \to T_{AC}^{+}$, plugging Eq. (8.11) into Eq. (8.19) and performing an asymptotic analysis, we obtain, in three dimensions (3D),

$$C(\vec{r}) = \begin{cases} \lambda^2 (r_\perp/\xi_{NL}^\perp)^\Gamma f_\Gamma((r_z/\xi_N^z)/(r_\perp/\xi_N^\perp)^\zeta), & r_\perp \ll \xi_\perp, \quad r_z \ll \xi_z, \\ \lambda^2 (\xi_\perp/\xi_{NL}^\perp)^\Gamma + \dfrac{\lambda^5 (\xi_\perp/\xi_{NL}^\perp)^{\eta_t}}{\varrho^3 (\xi_{NL}^\perp)^2}\left(\dfrac{1}{\xi_\perp} - \dfrac{1}{\sqrt{r_\perp^2 + (\varrho r_z)^2}}\right) + \dfrac{\varsigma}{q_0^2} \ln\left(\dfrac{\sqrt{r_\perp^2 + (\varrho r_z)^2}}{\xi_\perp}\right), & r_\perp \gg \xi_\perp \quad \text{or} \quad r_z \gg \xi_z, \end{cases}$$

where $\Gamma \equiv 2+\eta_t-(3\eta_K/2)$, f_Γ is another universal scaling function, $\varsigma \approx 1.10$, and $\varrho = (\lambda/\xi_\perp)(\xi_\perp/\xi_{NL}^\perp)^{\eta_K/2}$. For small r—i.e., $r_\perp \ll \xi_\perp$, $r_z \ll \xi_z$—$C(\vec{r})$ increases as a power law, while for large r—i.e., $r_\perp \gg \xi_\perp$ or $r_z \gg \xi_z$—$C(\vec{r})$ increases logarithmically. This indicates that $F_n(\vec{r})$ varies faster (exponentially) for small r ($r_\perp \ll \xi_\perp, r_z \ll \xi_z$) and slower (as a power law) for large r ($r_\perp \gg \xi_\perp$ or $r_z \gg \xi_z$). So the x-ray-scattering intensity $I(\delta\vec{q})$ for large $|\delta\vec{q}| = |\vec{G}-\vec{q}|$, which is dominated by $I^f(\delta\vec{q})$, defined as the contribution coming from the fast varying part of $F_n(\vec{r})$, should be broad and *anisotropic*, qualitatively like a Lorentzian squared. The linewidths δq_z^x and $\delta q_\perp^x$ of this Lorentzian squared are defined as $\delta q_z^x = (\xi_z^x)^{-1}$ and $\delta q_\perp^x = (\xi_\perp^x)^{-1}$ with ξ_z^x and $\xi_\perp^x$ satisfying

$$C(0,\xi_z^x) = a^2, \tag{8.21}$$

$$C(\xi_\perp^x, 0) = a^2. \tag{8.22}$$

Solving these two equations, we get

$$\xi_\perp^x = \xi_{NL}^\perp \left(\frac{a}{\lambda}\right)^{2/\Gamma}, \tag{8.23}$$

$$\xi_z^x = \xi_{NL}^z \left(\frac{a}{\lambda}\right)^{2\zeta/\Gamma}. \tag{8.24}$$

The temperature dependence of $\xi_\perp^x$ and ξ_z^x could be used to determine the exponents $2/\Gamma$, $2\zeta/\Gamma$, η_k, and η_Δ since the bulk $K(T)$ and $B(T)$ that implicitly appear in Eqs. (8.23) and (8.24) have a temperature dependence that can be extracted from measurements on bulk materials.

For small δq, $I(\delta\vec{q})$ is dominated by $I^s(\delta\vec{q})$, which is defined as the contribution coming from the slow varying part of $F_n(\vec{r})$. Thus, $I(\delta\vec{q})$ is quasisharp and *isotropic*, and diverges as a power law as δq approaches 0.

The crossover between these two distinct scattering patterns is defined as the point where the two contributions become comparable—that is, $I^s(\delta\vec{q}) = I^f(\delta\vec{q})$. Assuming that this happens at very small $|\delta\vec{q}|$, $I^f(\delta\vec{q})$ can be treated as a constant $(\xi_\perp^x)^2\xi_z^x$. We will verify this assumption as *a posterioni*. Let us first calculate the crossover in the $\perp$ directions,

$$I(\delta q_\perp = \delta q_\perp^c, \delta q_z = 0) \propto (\delta q_\perp^c)^{-3+0.55n^2} \xi_\perp^{-0.55n^2} \times e^{-n^2\lambda^2 q_0^2 (\xi_\perp/\xi_{NL}^\perp)^{\Gamma/2}} \propto (\xi_\perp^x)^2 \xi_z^x, \tag{8.25}$$

which gives

$$\delta q_\perp^c \propto |T - T_{AC}|^{0.55n^2\Omega/(3-0.55n^2)} \times \exp\left(-\frac{n^2}{3-0.55n^2}|T-T_{AC}|^{-\Omega}\right), \tag{8.26}$$

where $\Omega \equiv \Gamma\nu_\perp$. Likewise the crossover in z direction is found to be

$$\delta q_z^c \propto |T - T_{AC}|^{(2-\eta_k)\nu_\perp/2} \delta q_\perp^c. \tag{8.27}$$

Both $\delta q_\perp^c$ and δq_z^c become extremely small when $T \to T_{AC}^+$, which is consistent with our earlier assumption.

As for $T \to T_{AC}^-$, since the x-ray-scattering pattern is always broad, there is no significant crossover which can be detected by experiments.

Now we investigate light-scattering behavior near the critical region. The-light scattering intensity is proportional to a linear sum of the fluctuations of the nematic director, $\Sigma_{ij} A_{ij} \overline{\langle \delta n_i^\perp(-\vec{q}) \delta n_j^\perp(\vec{q})\rangle}$ [13], where the values of A_{ij} are determined by the electric polarization directions of the incident and transmitted light. Since in Sec. II we have shown that the fluctuations of $\hat{n}$ and the layer normal $\hat{N}$ are bound together, the light-scattering intensity is thus proportional to a linear sum of $C_{ij}(\vec{q})$, which is defined as

$$C_{ij}(\vec{q}) \equiv \overline{\langle N_i^\perp(-\vec{q}) N_j^\perp(\vec{q})\rangle} = L_{ij}^\perp(\vec{q}) q_\perp^2 \overline{\langle |u(\vec{q})|^2\rangle}. \tag{8.28}$$

We now derive the eight distinct regions with qualitatively different wave-vector dependences of $C_{ij}(\vec{q})$ in the A-side critical region, which are illustrated in Fig. 4. For large q's (i.e., $q_\perp \gg \xi_\perp^{-1}$ or $q_z \gg \xi_z^{-1}$, which corresponds to the regions outside the rectangle $OJFI$), $C_{ij}(\vec{q})$ is given by

$$C_{ij}(\vec{q}) = L_{ij}^\perp \left(\frac{\Delta_t(\vec{q}) q_\perp^2}{[Bq_z^2 + D(T)q_\perp^2 + K(\vec{q})q_\perp^4]^2} + \frac{\Delta_c(\vec{q}) q_z^2}{[Bq_z^2 + D(T)q_\perp^2 + K(\vec{q})q_\perp^4]^2} \right), \tag{8.29}$$

where in the denominator $Dq_\perp^2$ is negligible compared to $Kq_\perp^4$. The function for the crossover (i.e., locus EG) between the random compression and tilt can be obtained by doing

$$\frac{\Delta_t(\vec{q}) q_\perp^4}{[D(T)q_\perp^2 + Bq_z^2 + K(\vec{q},T)q_\perp^4]^2} = \frac{\Delta_c(\vec{q}) q_z^2 q_\perp^2}{[D(T)q_\perp^2 + Bq_z^2 + K(\vec{q},T)q_\perp^4]^2}, \tag{8.30}$$

which leads to

$$\Delta_t^0 (q_z \xi_{NL}^z)^{-\eta_t/\zeta} q_\perp^2 = \Delta_c^0 (q_z \xi_{NL}^z)^{-\eta_c/\zeta} q_z^2. \tag{8.31}$$

Using the scaling relation (7.9), this equation can be further transformed into

$$q_z \xi_{NL}^z = (q_\perp \xi_{NL}^z \sqrt{\Delta_t^0/\Delta_c^0})^A, \tag{8.32}$$

where $A \equiv \zeta/(1+\eta_3/2)$. Above EG (i.e., in region 8), $C_{ij}(\vec{q})$ is dominated by the random compression fluctuations and given by

$$C_{ij}(\vec{q}) \approx L_{ij}^\perp(\vec{q}) \left(\frac{\Delta_c q_z^2 q_\perp^2}{B^2 q_z^4}\right) \approx L_{ij}^\perp(\vec{q}) \left[\left(\frac{\Delta_c^0}{B_0^2}\right)\left(\frac{q_\perp}{q_z}\right)^2 (q_z \xi_{NL}^z)^{-\eta_c/\zeta}\right] \sim L_{ij}^\perp(\vec{q}) \left[\frac{\lambda^5 \Delta_c^0}{\Delta_t^0 (\xi_{NL}^\perp)^2}\left(\frac{q_\perp}{q_z}\right)^2 (q_z \xi_{NL}^z)^{-\eta_c/\zeta}\right], \tag{8.33}$$

where we remind the reader that λ is the smectic penetration length defined by $\lambda = \sqrt{K_0/B_0}$ and $\xi_{NL}^{\perp,z}$ are the nonlinear crossover lengths defined in Eqs. (1.30) and (1.31). Below EG, $C_{ij}(\vec{q})$ is dominated by the random tilt fluctuations, but still has two different wave-vector dependences due to the crossover (locus FH) between $Kq_\perp^4$ and Bq_z^2 in the common denominator, which satisfies

$$q_z \xi_{NL}^z = (q_\perp \xi_{NL}^\perp)^\zeta \tag{8.34}$$

and is below locus EG since $\zeta > A$. $C_{ij}(\vec{q})$ is given by

$$C_{ij}(\vec{q}) \approx L_{ij}^\perp(\vec{q}) \left(\frac{\Delta_t q_\perp^4}{B^2 q_z^4}\right) \approx L_{ij}^\perp(\vec{q}) \left[\left(\frac{\Delta_t^0}{B_0^2}\right)\left(\frac{q_\perp}{q_z}\right)^4 (q_z \xi_{NL}^z)^{-\eta_t/\zeta}\right] \sim L_{ij}^\perp(\vec{q}) \left[\frac{\lambda^5 \Delta_c^0}{(\xi_{NL}^\perp)^2}\left(\frac{q_\perp}{q_z}\right)^4 (q_z \xi_{NL}^z)^{-\eta_t/\zeta}\right] \tag{8.35}$$

above locus FH (i.e., in region 7) and

$$C_{ij}(\vec{q}) \approx L_{ij}^{\perp}(\vec{q})\left(\frac{\Delta_t q_\perp^4}{K^2 q_\perp^8}\right) \approx L_{ij}^{\perp}(\vec{q})\left[\left(\frac{\Delta_t^0}{K_0^2}\right)\left(\frac{1}{q_\perp}\right)^4 (q_\perp \xi_{NL}^{\perp})^{2\eta_K-\eta_t}\right] \sim L_{ij}^{\perp}(\vec{q})\left[\frac{\lambda}{(\xi_{NL}^{\perp})^2}\left(\frac{1}{q_\perp}\right)^4 (q_\perp \xi_{NL}^{\perp})^{2\eta_K-\eta_t}\right] \quad (8.36)$$

below locus *FH* (i.e., in region 6).

For small q's (i.e., $q_\perp \ll \xi_\perp^{-1}$, $q_z \ll \xi_z^{-1}$, which corresponds to the regions within the rectangle *OJFI* in Fig. 4), $\langle |u(\vec{q})|^2 \rangle$ is given by (8.4) and $C_{ij}(\vec{q})$ is thus

$$C_{ij}(\vec{q}) = L_{ij}^{\perp}(\vec{q})\left(\frac{\Delta_t(\vec{q},T)q_\perp^4}{[Bq_z^2 + D(T)q_\perp^2 + K(\vec{q},T)q_\perp^4]^2} + \frac{\Delta_c(\vec{q},T)q_z^2 q_\perp^2}{[Bq_z^2 + D(T)q_\perp^2 + K(\vec{q},T)q_\perp^4]^2} + \frac{CB^{1/2}Dq_\perp^2}{[Bq_z^2 + D(T)q_\perp^2 + K(\vec{q},T)q_\perp^4]^{3/2} q_0^2}\right), \quad (8.37)$$

where in the denominator $Kq_\perp^4$ is negligible compared to $Dq_\perp^2$. Now since $C_{ij}(\vec{q})$ has three pieces, the crossovers are quite complicated. For simplicity, let us divide the rectangle *OJEI* into two subregions separated by locus *OF*, which satisfies $Bq_z^2 = Dq_\perp^2$ and hence

$$q_z = \frac{\lambda}{\xi_{NL}^{\perp}}(\xi_{NL}^{\perp}/\xi_\perp)^{1-\eta_K/2} q_\perp. \quad (8.38)$$

First we consider the subregion above locus *OF* (i.e., triangle *IOF*), in which Bq_z^2 dominates $Dq_\perp^2$ in the common denominator in Eq. (8.37). In this region, the three pieces in Eq. (8.37), which correspond to the contributions from the the random tilt, the random compression, and the random field, respectively, are given, respectively, by

$$L_{ij}^{\perp}(\vec{q})\left(\frac{\Delta_t q_\perp^4}{B^2 q_z^4}\right) = L_{ij}^{\perp}(\vec{q})\left[\left(\frac{\Delta_t^0}{B_0^2}\right)\left(\frac{q_\perp}{q_z}\right)^4 (\xi_{NL}^{\perp}/\xi_\perp)^{-\eta_t}\right] \sim L_{ij}^{\perp}(\vec{q})\left[\frac{\lambda^5}{(\xi_{NL}^{\perp})^2}\left(\frac{q_\perp}{q_z}\right)^4 (\xi_{NL}^{\perp}/\xi_\perp)^{-\eta_t}\right], \quad (8.39)$$

$$L_{ij}^{\perp}(\vec{q})\left(\frac{\Delta_c q_z^2 q_\perp^2}{B^2 q_z^4}\right) = L_{ij}^{\perp}(\vec{q})\left[\left(\frac{\Delta_c^0}{B_0^2}\right)\left(\frac{q_\perp}{q_z}\right)^2 (\xi_{NL}^{\perp}/\xi_\perp)^{-\eta_c}\right] \sim L_{ij}^{\perp}(\vec{q})\left[\frac{\lambda^5 \Delta_c^0}{\Delta_t^0 (\xi_{NL}^{\perp})^2}\left(\frac{q_\perp}{q_z}\right)^2 (\xi_{NL}^{\perp}/\xi_\perp)^{-\eta_c}\right], \quad (8.40)$$

$$L_{ij}^{\perp}(\vec{q})\left(\frac{CD}{Bq_0^2}\frac{q_\perp^2}{q_z^3}\right) = L_{ij}^{\perp}(\vec{q})\left(\frac{CK_0}{B_0 q_0^2}\frac{q_\perp^2}{q_z^3}(\xi_{NL}^{\perp}/\xi_\perp)^{-\eta_K}\xi_\perp^{-2}\right) \sim L_{ij}^{\perp}(\vec{q})\left(\frac{\lambda^2}{(\xi_{NL}^{\perp})^2 q_0^2}\frac{q_\perp^2}{q_z^3}(\xi_{NL}^{\perp}/\xi_\perp)^{2-\eta_K}\right). \quad (8.41)$$

The crossovers between them are obtained by equating them to each other. The function for the crossover (i.e., locus *DC*) between the random compression and random field is given by

$$q_z = \frac{\Delta_t^0}{\lambda^3 q_0^2 \Delta_c^0}(\xi_{NL}^{\perp}/\xi_\perp)^{2-\eta_K+\eta_c} = \frac{\Delta_t^0}{\lambda^3 q_0^2 \Delta_c^0}(\xi_{NL}^{\perp}/\xi_\perp)^{4+\eta_t-2\eta_K-\eta_3}, \quad (8.42)$$

where we have used the *exact* scaling relation given in the Eq. (7.9); the function for the crossover (i.e., locus *CE*) between the random compression and random tilt is given by

$$q_z = \sqrt{\Delta_c^0/\Delta_t^0}(\xi_{NL}^{\perp}/\xi_\perp)^{(\eta_c-\eta_t)/2} q_\perp = \sqrt{\Delta_c^0/\Delta_t^0}(\xi_{NL}^{\perp}/\xi_\perp)^{1-(\eta_K+\eta_3)/2} q_\perp, \quad (8.43)$$

where again we have used the same *exact* scaling relation given in Eq. (7.9); the function for the crossover (i.e., locus *BC*) between the random tilt and random field is given by

$$q_z = \lambda^3 q_0^2 (\xi_{NL}^{\perp}/\xi_\perp)^{\eta_K-2-\eta_t} q_\perp^2. \quad (8.44)$$

These three loci intersect at point *C*, at which

$$q_\perp \propto \xi_\perp^{\eta_3/2+(3/2)\eta_K-\eta_t-3}, \qquad q_z \propto \xi_\perp^{\eta_3+2\eta_K-\eta_t-4}. \quad (8.45)$$

It is easy to show that this point is within the triangle *IOF*, as illustrated in Fig. 4. Thus, these three loci divide the triangle *IOF* into three distinct regions with different wave-vector-dependence of $C_{ij}(\vec{q})$ for each region. Specifically, $C_{ij}(\vec{q})$ is dominated by the random compression and given by Eq. (8.40) in region 5, dominated by the random tilt and given by Eq. (8.39) in region 4, and dominated by the random field and given by the Eq. (8.41) in region 2.

Now we consider the subregion (i.e., triangle *OJF*) below the locus *OF*, in which Bq_z^2 is dominated by $Dq_\perp^2$ in the common denominator in Eq. (8.37). It is easy to show that the contribution to $C_{ij}(\vec{q})$ from the random compression never dominates in this region. The contributions from the random-tilt and random-field disorder are given by

$$L_{ij}^{\perp}(\vec{q})\left(\frac{\Delta_t q_\perp^4}{D^2 q_\perp^4}\right) = L_{ij}^{\perp}(\vec{q})\left[\frac{\Delta_t^0}{K_0^2}\left(\frac{1}{q_\perp}\right)^4 (\xi_{NL}^{\perp}/\xi_\perp)^{2\eta_K-\eta_t}\right] \sim L_{ij}^{\perp}(\vec{q})\left[\frac{\lambda}{(\xi_{NL}^{\perp})^2}\left(\frac{1}{q_\perp}\right)^4 (\xi_{NL}^{\perp}/\xi_\perp)^{2\eta_K-\eta_t}\right] \quad (8.46)$$

and

$$L_{ij}^{\perp}(\vec{q})\left(\frac{CB^{1/2}}{D^{1/2}}\frac{1}{q_\perp}\right)=L_{ij}^{\perp}(\vec{q})\left(\frac{CB_0^{1/2}}{K_0^{1/2}\xi_\perp^{-1}}\frac{1}{q_\perp}(\xi_{NL}^{\perp}/\xi_\perp)^{\eta_K/2}\right)$$
$$\sim L_{ij}^{\perp}(\vec{q})\left(\frac{\xi_{NL}^{\perp}}{\lambda q_0^2}\frac{1}{q_\perp}(\xi_{NL}^{\perp}/\xi_\perp)^{\eta_K/2-1}\right), \tag{8.47}$$

respectively. The crossover (i.e., locus AB) between them is

$$q_\perp = q_\perp^R \propto \xi_\perp^{(3/2)\eta_K-\eta_t-3}. \tag{8.48}$$

$C_{ij}(\vec{q})$ is dominated by the random field and given by Eq. (8.47) in region 1 and dominated by the random tilt and given by the Eq. (8.46) in region 2.

Now we discuss the wave-vector dependence of $C_{ij}(\vec{q})$ in the C-side critical region. For large q's (i.e., $q_\perp \gg \xi_\perp^{-1}$ or $q_z \gg \xi_z^{-1}$), the wave-vector dependence of $C_{ij}(\vec{q})$ is the same as that in the A-side critical region. For small q's (i.e., $q_\perp \ll \xi_\perp^{-1}$, $q_z \ll \xi_z^{-1}$), $C_{ij}(\vec{q})$ is given by

$$C_{ij}(\vec{q})=L_{ij}^{\perp}(\hat{q})\left(\frac{\Delta_{s'}(\vec{q}',T)q_{s'}^2q_\perp^2}{[\gamma(\vec{q}',T)q_{x'}^2+\tilde{B}q_{z'}^2+\tilde{K}(\vec{q}',T)q_{s'}^4]^2}\right.$$
$$+\frac{\Delta_{z'}(T)q_{z'}^2q_\perp^2}{[\gamma(\vec{q}',T)q_{x'}^2+\tilde{B}q_{z'}^2+\tilde{K}(\vec{q}',T)q_{s'}^4]^2}$$
$$\left.+\frac{\Delta_{x'}(\vec{q}',T)q_{x'}^2q_\perp^2}{[\gamma(\vec{q}',T)q_{x'}^2+\tilde{B}q_{z'}^2+\tilde{K}(\vec{q}',T)q_{s'}^4]^2}\right), \tag{8.49}$$

where we have neglected the contribution from the $\Delta_{x'z'}$ disorder [see Hamiltonian (6.14)] since it is not important compared to the contributions from the other disorders. For convenience, we name the three pieces in the above equation as "$\Delta_{s'}$ piece," "$\Delta_{z'}$ piece," and "$\Delta_{x'}$ piece," respectively. We find that there are five distinct regions in the wave-vector space with qualitatively different wave-vector dependences of $C_{ij}(\vec{q})$. Since the azimuthal symmetry about the $\hat{z}$ axis is now broken due to the tilting of the layers, the five regions have to be illustrated in a three-dimensional picture, which is shown in Fig. 5. In the following we will show how we derive the five regions and the wave-vector dependence of $C_{ij}(\vec{q})$ for each region.

First we calculate the various crossovers within the three planes (i.e., $q_{z'}-q_{x'}$, $q_{z'}-q_{s'}$, $q_{s'}-q_{x'}$). Let us start with $q_{z'}-q_{x'}$ plane, in which case $\Delta_{s'}$ piece vanishes. One crossover in this plane is the scaling locus OG, which divides the rectangle $OHGI$ into two distinct regions with different wave-vector dependences of $\Delta_{s',x'}$, K, and γ. The function for OG is given by

$$q_{z'}\xi_z=(q_{x'}\xi_\perp)^{\tilde{\zeta}_{z'}/\tilde{\zeta}_{x'}}. \tag{8.50}$$

The other one is the crossover (i.e., locus OB) between $\Delta_{z'}$ piece and $\Delta_{x'}$ piece, which satisfies

$$\Delta_{z'}q_{z'}^2=\Delta_{x'}q_{x'}^2, \tag{8.51}$$

where $\Delta_{z'}$ is wave vector independent, but temperature dependent and given in (8.9), and $\Delta_{x'}$ has dependences on both the temperature and wave vector, which is summarized in (1.6). Assuming that OB is in one of the two regions separated by OG which is closer to the $q_{z'}$ axis (this assumption will be verified as a posterior), from (8.51) we obtain

$$\left[\left(\frac{\xi_{NL}^{\perp}}{\lambda}\right)^2\Delta_t^0+\Delta_c^0\right]\left(\frac{\xi_\perp}{\xi_{NL}^{\perp}}\right)^{\eta_c}q_{z'}^2=\Delta_t^0\left(\frac{\xi_\perp}{\xi_{NL}^{\perp}}\right)^{\eta_t}(\xi_zq_{z'})^{-\tilde{\eta}_{x'}/\tilde{\zeta}_{z'}}q_{x'}^2.$$

A further reorganization leads to

$$q_{z'}\xi_z=\left[\sqrt{\frac{\Delta_t^0}{\Delta_n^0}}\left(\frac{\xi_\perp}{\xi_{NL}^{\perp}}\right)^{\eta_3/2}\left(\frac{\xi_{NL}^{\perp}}{\lambda}\right)(q_{x'}\xi_\perp)\right]^{\tilde{\phi}_{x'z'}}, \tag{8.52}$$

where

$$\Delta_n^0\equiv\left(\frac{\xi_{NL}^{\perp}}{\lambda}\right)^2\Delta_t^0+\Delta_c^0,$$

$$\phi_{x'z'}\equiv 2\tilde{\zeta}_{z'}/(2\tilde{\zeta}_{z'}+\tilde{\eta}_{x'}).$$

It is easy to verify that the function for the locus OB given by Eq. (8.52) is indeed consistent with the assumption we just made.

The crossovers in the other two planes can be obtained through similar calculations, which will not be repeated. We only give the results. In the $q_{z'}-q_{s'}$ plane, in which case $\Delta_{x'}$ piece vanishes, the scaling locus (i.e., OF) and the crossover (i.e., locus OA) between $\Delta_{z'}$ piece and $\Delta_{s'}$ piece are given, respectively, by

$$q_{z'}\xi_z=(q_{s'}\xi_\perp)^{\tilde{\zeta}_{z'}} \tag{8.53}$$

and

$$q_{z'}\xi_z=\left[\sqrt{\frac{\Delta_t^0}{\Delta_n^0}}\left(\frac{\xi_\perp}{\xi_{NL}^{\perp}}\right)^{\eta_3/2}\left(\frac{\xi_{NL}^{\perp}}{\lambda}\right)(q_{s'}\xi_\perp)\right]^{\tilde{\phi}_{s'z'}}, \tag{8.54}$$

where

$$\tilde{\phi}_{s'z'}\equiv 2\tilde{\zeta}_{z'}/(2\tilde{\zeta}_{z'}+\tilde{\eta}_{s'}). \tag{8.55}$$

In the $q_{x'}-q_{s'}$ plane, in which case $\Delta_{z'}$ piece vanishes, coincidentally, the scaling locus and the crossover between $\Delta_{x'}$ piece and $\Delta_{s'}$ piece merge into one (i.e., OD), and both are given by the same function

$$q_{x'}\xi_\perp=(q_{s'}\xi_\perp)^{\tilde{\zeta}_{x'}}. \tag{8.56}$$

Having found the crossovers in the three planes, now we can use them to obtain the crossovers in 3D wave-vector space. Moving the loci OA and OB along $\hat{q}_{x'}$ and $\hat{q}_{s'}$, respectively, we obtain the two boundaries OAC and OBC as the trajectories of OA and OB, which meet at the locus OC. Thus, OAC and OBC are the crossovers between $\Delta_{z'}$ piece, $\Delta_{s'}$ piece and $\Delta_{z'}$ piece, $\Delta_{x'}$ piece, respectively, and they are also defined by the functions (8.54) and (8.52), respectively, and OC is hence defined by the the combination of (8.54) and (8.52). Likewise, OEF, OEG, and ODE are the scaling crossovers, which separate distinct regions with different wave-vector dependence of $\Delta_{x',s'}$, γ, and K and are defined by the functions (8.53), (8.50), and (8.56), respectively. It is

easy to show that these three crossovers meet at the same locus *OE*, whose function is thus the combination of any two of (8.53), (8.50), and (8.56). In addition, *ODE* also serves as the crossover between $\Delta_{x'}$ piece and $\Delta_{s'}$ piece due to the duality of the locus *OD*. *OCE* is another crossover between $\Delta_{x'}$ piece and $\Delta_{s'}$ piece; however, since *OCE* and *ODE* are in different regions with different wave-vector dependences of $\Delta_{x'}$ and $\Delta_{s'}$, *OCE* is defined by a function which is different from (8.56):

$$q_{x'} = (q_{z'}\xi_z)^{\tilde{\phi}_{s'x'}} q_{s'}, \tag{8.57}$$

with $\tilde{\phi}_{s'x'} = (2-\tilde{\eta}_K-\tilde{\eta}_\gamma)/2\tilde{\zeta}_{z'}$.

After the definitions of the crossovers separating the five regions in Fig. 5 become known, the calculation of the wave-vector dependence of $C_{ij}(\vec{q})$ in each region is straightforward. In the region *O-ABCH*, $C_{ij}(\vec{q})$ is dominated by $\Delta_{z'}$ piece and given by

$$\begin{aligned} &L_{ij}^{\perp}(\hat{q})\left(\frac{\Delta_{z'}(T)q_{z'}^2,q_\perp^2}{[\gamma(\vec{q}',T)q_{x'}^2+\tilde{B}q_{z'}^2+\tilde{K}(\vec{q}',T)q_{s'}^4]^2}\right) \\ &= L_{ij}^{\perp}(\hat{q})\left(\frac{\Delta_{z'}(T)q_\perp^2}{\tilde{B}^2 q_{z'}^2}\right) \\ &= L_{ij}^{\perp}(\hat{q})\left(\frac{\Delta_n^0}{B_0^2}\frac{q_\perp^2}{q_{z'}^2}(\xi_\perp/\xi_{NL}^\perp)^{\eta_c}\right) \\ &\sim L_{ij}^{\perp}(\hat{q})\left(\frac{\Delta_n^0}{\Delta_t^0}\frac{\lambda^5}{(\xi_{NL}^\perp)^2}\frac{q_\perp^2}{q_{z'}^2}(\xi_\perp/\xi_{NL}^\perp)^{\eta_c}\right). \end{aligned} \tag{8.58}$$

In both regions *O-AFEC* and *O-FJDE*, $C_{ij}(\vec{q})$ is dominated by $\Delta_{s'}$ piece, but with different wave-vector dependences, since these two regions are separated by the scaling crossover *OEF*. In *O-AFEC*, $C_{ij}(\vec{q})$ is given by

$$\begin{aligned} &L_{ij}^{\perp}(\hat{q})\left(\frac{\Delta_{s'}(\vec{q}',T)q_{s'}^2,q_\perp^2}{\tilde{B}^2 q_{z'}^4}\right) \\ &= L_{ij}^{\perp}(\hat{q})\left(\frac{\Delta_t^0}{B_0^2}\frac{q_{s'}^2,q_\perp^2}{q_z^4}(\xi_\perp/\xi_{NL}^\perp)^{\eta_t}(q_{z'}\xi_z)^{-\tilde{\eta}_{s'}/\tilde{\zeta}_{z'}}\right) \\ &\sim L_{ij}^{\perp}(\hat{q})\left(\frac{\lambda^5}{(\xi_{NL}^\perp)^2}\frac{q_{s'}^2,q_\perp^2}{q_z^4}(\xi_\perp/\xi_{NL}^\perp)^{\eta_t}(q_{z'}\xi_z)^{-\tilde{\eta}_{s'}/\tilde{\zeta}_{z'}}\right), \end{aligned} \tag{8.59}$$

while in *O-FJDE*, it is given by

$$\begin{aligned} &L_{ij}^{\perp}(\hat{q})\left(\frac{\Delta_{s'}(\vec{q}',T)q_\perp^2}{K^2 q_{s'}^6}\right) \\ &= L_{ij}^{\perp}(\hat{q})\left(\frac{\Delta_t^0}{K_0^2}\frac{q_\perp^2}{q_{s'}^6}(\xi_\perp/\xi_{NL}^\perp)^{\eta_t-2\eta_K}(q_{s'}\xi_\perp)^{2\eta_K-\eta_{s'}}\right) \\ &\sim L_{ij}^{\perp}(\hat{q})\left(\frac{\lambda}{(\xi_{NL}^\perp)^2}\frac{q_\perp^2}{q_{s'}^6}(\xi_\perp/\xi_{NL}^\perp)^{\eta_t-2\eta_K}(q_{s'}\xi_\perp)^{2\eta_K-\eta_{s'}}\right). \end{aligned} \tag{8.60}$$

Likewise, in both regions *O-CEBG* and *O-EDIG*, $C_{ij}(\vec{q})$ is dominated by $\Delta_{x'}$ piece, but with different wave-vector dependences. In *O-CEGB*, it is given by

$$\begin{aligned} &L_{ij}^{\perp}(\hat{q})\left(\frac{\Delta_{x'}(\vec{q}',T)q_{x'}^2,q_\perp^2}{\tilde{B}^2 q_{z'}^4}\right) \\ &= L_{ij}^{\perp}(\hat{q})\left(\frac{\Delta_t^0}{B_0^2}\frac{q_{s'}^2,q_\perp^2}{q_z^4}(\xi_\perp/\xi_{NL}^\perp)^{\eta_t}(q_{z'}\xi_z)^{-\tilde{\eta}_{x'}/\tilde{\zeta}_{z'}}\right) \\ &\sim L_{ij}^{\perp}(\hat{q})\left(\frac{\lambda^5}{(\xi_{NL}^\perp)^2}\frac{q_{s'}^2,q_\perp^2}{q_z^4}(\xi_\perp/\xi_{NL}^\perp)^{\eta_t}(q_{z'}\xi_z)^{-\tilde{\eta}_{x'}/\tilde{\zeta}_{z'}}\right), \end{aligned} \tag{8.61}$$

while in *O-EDIG*, it is

$$\begin{aligned} &L_{ij}^{\perp}(\hat{q})\left(\frac{\Delta_{x'}(\vec{q}',T)q_\perp^2}{\gamma^2 q_{x'}^2}\right) \\ &= L_{ij}^{\perp}(\hat{q})\left[\frac{\Delta_t^0(\xi_{NL}^\perp)^4}{K_0^2}\left(\frac{q_\perp}{q_{x'}}\right)^2(\xi_\perp/\xi_{NL}^\perp)^{\eta_t+4-2\eta_K}\right. \\ &\quad\left.\times(q_{x'}\xi_\perp)^{-(2\tilde{\eta}_\gamma+\tilde{\eta}_K)/\tilde{\zeta}_{x'}}\right] \\ &\sim L_{ij}^{\perp}(\hat{q})\left[\lambda(\xi_{NL}^\perp)^2\left(\frac{q_\perp}{q_{x'}}\right)^2(\xi_\perp/\xi_{NL}^\perp)^{\eta_t+4-2\eta_K}\right. \\ &\quad\left.\times(q_{x'}\xi_\perp)^{-(2\tilde{\eta}_\gamma+\tilde{\eta}_K)/\tilde{\zeta}_{x'}}\right]. \end{aligned} \tag{8.62}$$

So far, we have discussed $C_{ij}(\vec{q})$ for small q's (i.e., $q_\perp \ll \xi_\perp^{-1}$, $q_z \ll \xi_z^{-1}$) in the *C*-side critical region in the transformed reciprocal coordinate system. However, what is needed for experiments is the behavior of $C_{ij}(\vec{q})$ in the laboratory reciprocal coordinate system. Since the relation between these two coordinate systems is known, the calculation is straightforward, but somewhat tedious. Instead of listing $C_{ij}(\vec{q})$ for all $\vec{q}$'s, which is quite complicated and far more than necessary, we now discuss $C_{ij}(\vec{q})$ for special $\vec{q}$'s, which is simple and adequate for making useful experiment predictions. First we consider the case in which $\vec{q}$ is restricted in the q_z-q_x plane. In this case, $\Delta_{s'}$ piece vanishes and $C_{ij}(\vec{q})$ reduces to

$$C_{xx}(\vec{q}) = \frac{\Delta_{z'}(T)q_z^2q_x^2}{[\gamma(\vec{q}',T)q_{x'}^2+\tilde{B}q_z^2]^2} + \frac{\Delta_{x'}(\vec{q}',T)q_{x'}^2,q_x^2}{[\gamma(\vec{q}',T)q_{x'}^2+\tilde{B}q_z^2]^2}. \tag{8.63}$$

The crossover between $\Delta_{z'}$ and $\Delta_{x'}$ has been calculated previously and given by Eq. (8.52), which, in terms of $\vec{q}$, becomes

$$q_z\xi_z = \left[\sqrt{\frac{\Delta_t^0}{\Delta_n^0}}\left(\frac{\xi_\perp}{\xi_{NL}^\perp}\right)^{\eta_3/2}\left(\frac{\xi_{NL}^\perp}{\lambda}\right)(q_x-\Gamma q_z)\xi_\perp\right]^{\tilde{\phi}_{x'z'}}$$
$$= \left[\sqrt{\frac{\Delta_t^0}{\Delta_n^0}}\left(\frac{\xi_z}{\Gamma}\right)(q_x-\Gamma q_z)\right]^{\tilde{\phi}_{x'z'}}. \quad (8.64)$$

This function defines the loci OE and OE' in Fig. 6. The coordinates of E and E' are given, respectively, by

$$q_z \sim (\xi_z)^{-1},$$

$$q_\perp \sim \pm q_\perp^F \equiv \pm(\xi_z)^{-1}(\xi_\perp/\xi_{NL}^\perp)^{1-(\eta_K+\eta_3)/2},$$

and OE and OE' thus connect with EG and $E'G'$, respectively, which are the crossover between the random-tilt and random-compression fluctuations for large q's (i.e., $q_\perp \gg \xi_\perp^{-1}$ or $q_z \gg \xi_z^{-1}$). The crossover between the two terms in the common denominator has also been calculated and given by Eq. (8.50), which, in terms of $\vec{q}$, is

$$q_z\xi_z = [(q_x+\Gamma q_z)\xi_\perp]^{\tilde{\zeta}_{z'}/\tilde{\zeta}_{x'}}. \quad (8.65)$$

It is easy to check that the loci defined by this function satisfy $|q_x| \gg \Gamma q_z$. Thus this function can be further simplified as

$$q_z\xi_z = (q_x\xi_\perp)^{\tilde{\zeta}_{z'}/\tilde{\zeta}_{x'}}, \quad (8.66)$$

which defines OF and OF' in Fig. 6. These two loci also serve as the scaling crossover separating the region for small q's into three distinct ones with different wave-vector dependences of $\Delta_{x'}$. Now we calculate the $\vec{q}$ dependences of $C_{xx}(\vec{q})$ in different regions separated by these crossovers. In region 4, $C_{xx}(\vec{q})$ is dominated by $\Delta_{z'}$ piece and given by

$$\frac{\Delta_{z'}(T)q_x^2}{\tilde{B}^2q_z^2} = \frac{\Delta_n^0}{B_0^2}\left(\frac{\xi_\perp}{\xi_{NL}^\perp}\right)^{\eta_c}\left(\frac{q_x}{q_z}\right)^2 \sim \frac{\Delta_n^0}{\Delta_t^0}\frac{\lambda^5}{(\xi_{NL}^\perp)^2}\left(\frac{\xi_\perp}{\xi_{NL}^\perp}\right)^{\eta_c}\left(\frac{q_x}{q_z}\right)^2; \quad (8.67)$$

in regions 5 and 6, $C_{xx}(\vec{q})$ is dominated by $\Delta_{x'}$ piece and given by

$$\frac{\Delta_{x'}(\vec{q}',T)q_{x'}^2q_x^2}{\tilde{B}^2q_z^4} = \frac{\Delta_t^0}{B_0^2}\left(\frac{\xi_\perp}{\xi_{NL}^\perp}\right)^{\eta_t}\frac{q_{x'}^2q_x^2}{q_z^4}(q_z\xi_z)^{-\tilde{\eta}_{x'}/\tilde{\zeta}_{z'}}$$
$$\sim \frac{\lambda^5}{(\xi_{NL}^\perp)^2}\left(\frac{\xi_\perp}{\xi_{NL}^\perp}\right)^{\eta_t}\frac{q_x^4}{q_z^4}(q_z\xi_z)^{-\tilde{\eta}_{x'}/\tilde{\zeta}_{z'}}; \quad (8.68)$$

in regions 7 and 8, $C_{xx}(\vec{q})$ is also dominated by $\Delta_{x'}$ piece but given by

$$\frac{\Delta_{x'}(\vec{q}',T)q_x^2}{\gamma^2q_{x'}^2} = \frac{\Delta_t^0\xi_\perp^4}{K_0^2}\left(\frac{\xi_\perp}{\xi_{NL}^\perp}\right)^{\eta_t-2\eta_K}(q_x\xi_\perp)^{-(\tilde{\eta}_{x'}+2\tilde{\eta}_\gamma)/\tilde{\zeta}_{x'}}$$
$$\sim \frac{\lambda\xi_\perp^4}{(\xi_{NL}^\perp)^2}\left(\frac{\xi_\perp}{\xi_{NL}^\perp}\right)^{\eta_t-2\eta_K}(q_x\xi_\perp)^{-(\tilde{\eta}_{x'}+2\tilde{\eta}_\gamma)/\tilde{\zeta}_{x'}}, \quad (8.69)$$

which is different from Eq. (8.68) since regions 5 and 6 are separated from regions 7 and 8 by the scaling loci. In both of the above two equations, we approximated $q_{x'}$ as q_x, since we have $|q_x| \gg \Gamma q_z$ in regions 5, 6, 7, and 8.

The second special case we consider is when $\vec{q}$ is along the $\hat{q}_x$ axis. In this case both $\Delta_{z'}$ piece and $\Delta_{x'}$ piece vanish, and $C_{ij}(\vec{q})$ is simply given by

$$C_{ss}(\vec{q}) = \frac{\Delta_{s'}}{\tilde{K}^2q_s^4} = \frac{\Delta_t^0}{K_0^2}\left(\frac{\xi_\perp}{\xi_{NL}^\perp}\right)^{\eta_t-2\eta_K}(q_s\xi_\perp)^{2\tilde{\eta}_K-\tilde{\eta}_t}\left(\frac{1}{q_s}\right)^4$$
$$\sim \frac{\lambda}{(\xi_{NL}^\perp)^2}\left(\frac{\xi_\perp}{\xi_{NL}^\perp}\right)^{\eta_t-2\eta_K}(q_s\xi_\perp)^{2\tilde{\eta}_K-\tilde{\eta}_t}\left(\frac{1}{q_s}\right)^4. \quad (8.70)$$

IX. STABILITY OF THE TRANSITION AGAINST DEFECTS AND ORIENTATIONAL DISORDER

The stability of the A phase follows from the stability of the random-field XY model; the stability of the C phase follows from the stability of $m=1$ smectic. Both phases are stable against orientational fluctuations and the unbinding of neutral pairs of topological defects (i.e., smectic dislocation loops). This implies a existence of a phase transition between the two phases. However, in order for our theory for the critical behavior to be valid, the system also needs to be dislocation bound and orientationally ordered right at the critical point.

The orientational fluctuations are defined as the mean-square fluctuations of the layer normal $\hat{N}$. Assuming the system is orientationally ordered, the dominating orientational fluctuations can be calculated as

$$\langle|\vec{N}_\perp(x)|^2\rangle = \int \frac{d^dq}{(2\pi)^d}\frac{\Delta(\vec{q})q_\perp^4}{(K(\vec{q})q_\perp^4+Bq_z^2)^2}, \quad (9.1)$$

where $\vec{N}_\perp$ is the projection of $\hat{N}$ on the $\perp$ plane (i.e., x-y plane). We have only kept the fluctuations contributed by the random-tilt disorder, which are the most divergent right at the critical point. The $\vec{q}$ dependences of $\Delta(\vec{q})$ and $K(\vec{q})$ are given in Eqs. (1.27) and (1.32), respectively. B is $\vec{q}$ independent. Then requiring the fluctuations to be finite leads to

$$\eta_t - \frac{3\eta_K}{2} < d-3, \quad (9.2)$$

which is one of the conditions for our theory for the critical behavior to be valid.

Now we check if the topological defects are bound right at the critical point. The starting point of the theory is the tilt-only Hamiltonian

$$H = \int d^dr\left[\frac{K}{2}(\nabla_\perp^2u)^2+\frac{B}{2}(\partial_zu)^2+\vec{h}(\vec{r})\cdot\vec{\nabla}u\right], \quad (9.3)$$

where random-field disorder is not included. It can be justified that random-field disorder is also irrelevant when dislocations are included. Since the model (9.3) is virtually the same as that for dislocations in the smectic-A phase in an isotropic random environment [11], the theory is also the same. Therefore, we will describe the theory very briefly.

When the smectic has a dislocation, the displacement field u is no longer single valued. Mathematically this can be represented as

$$\vec{\nabla} \times \vec{\nabla} u = \vec{m}, \tag{9.4}$$

with

$$\vec{m}(\vec{r}) = \sum_i \int a M_i t(s_i) \delta^3(\vec{r} - \vec{r}_i(s_i)) ds_i, \tag{9.5}$$

where s_i stands for the whole configuration of the ith dislocation loop, M_i is an integer giving the charge of that loop, $t(s_i)$ is the local tangent of the loop, and $\vec{r}_i$ is a parametrization of the path of the loop. Furthermore, Eq. (9.4) implies

$$\vec{\nabla} \cdot \vec{M} = 0, \tag{9.6}$$

which means that dislocation lines cannot end in the bulk of the sample.

To obtain a dislocation Hamiltonian, we need to trace over field u which is constrained by Eq. (9.4). This can be done in the following standard way [11]. We separate the field $\vec{v} = \vec{\nabla} u$ into

$$\vec{v} = \vec{v}_d + \delta\vec{v}, \tag{9.7}$$

where $\vec{v}_p$ minimizes Hamiltonian (9.3) for a given dislocation configuration $\vec{m}(\vec{r})$ and $\delta\vec{v}$ can be viewed as the fluctuation from the ground state. Inserting (9.7) into Hamiltonian (9.3), we find that $\vec{v}_p$ and $\delta\vec{v}$ are decoupled due to the construction that $\vec{v}_d$ minimizes Hamiltonian (9.3). Thus we obtain the effective model for $\vec{m}(\vec{r})$.

Now let us go through the procedure. The Euler-Lagrange equation, obtained by minimizing Hamiltonian (9.3), is

$$(B\partial_z^2 + K\nabla_\perp^4) u + \vec{\nabla}_\perp \cdot \vec{h} = 0. \tag{9.8}$$

Rewriting this in terms of $\vec{v}_d = \vec{\nabla} u$ gives

$$\partial_z v_d^z - \lambda^2 \nabla_\perp^2 \vec{\nabla}_\perp \cdot \vec{v}_d^\perp + \frac{1}{B} \vec{\nabla}_\perp \cdot \vec{h} = 0, \tag{9.9}$$

where $\lambda^2 \equiv K/B$. In Fourier space, this equation becomes

$$q_z v_d^z + \lambda^2 q_\perp^2 \vec{q}_\perp \cdot \vec{v}_d^\perp + \frac{1}{B} \vec{q}_\perp \cdot \vec{h}(\vec{q}) = 0, \tag{9.10}$$

and the solution for the constraint (9.4) is

$$\vec{v}_d = \frac{i\vec{q} \times \vec{m}}{q^2} + \vec{q}\phi, \tag{9.11}$$

where ϕ is the smooth elastic distortion around the dislocation line. Inserting (9.11) into Eq. (9.10) gives

$$\phi = -\frac{i q_z (1 - \lambda^2 q_\perp^2) \epsilon_{zij} q_i m_j}{\Gamma_q q^2} - \frac{\vec{q}_\perp \cdot \vec{h}}{B\Gamma_q}, \tag{9.12}$$

where we have defined the inverse of the smectic propagator:

$$\Gamma_q = q_z^2 + \lambda^2 q_\perp^4. \tag{9.13}$$

Inserting (9.12) into the solution for $\vec{v}_d$ and plugging Equation (9.7) into Hamiltonian (9.3), we obtain the dislocation Hamiltonian

$$H_d = \int d^d q \left[\frac{K q_\perp^2}{2\Gamma_q} P_{ij}^\perp m_i m_j + \vec{m} \cdot \vec{a} \right], \tag{9.14}$$

where $P_{ij}^\perp = (1 - \delta_{iz})(1 - \delta_{iz})(\delta_{ij} - q_i^\perp q_j^\perp / q_\perp^2)$, $\Gamma_q = q_z^2 + \lambda^2 q_\perp^4$, and

$$\vec{a} = i \left[\frac{\vec{q} \times \vec{h}}{q^2} - \frac{(\hat{z} \times \vec{q}) \cdot \vec{h}}{\Gamma_q q^2} q_z (1 - \lambda^2 q_\perp^2) \right]. \tag{9.15}$$

By putting the model on a a simple cubic lattice, the partition function can be written as

$$Z = \sum_{\vec{m}\vec{r}} e^{-S[\vec{m}]}, \tag{9.16}$$

where

$$\vec{m}(\vec{r}) = \frac{a}{d^2} [n_x(\vec{r}), n_y(\vec{r}), n_z(\vec{r})], \tag{9.17}$$

$$S[\vec{m}] = \frac{1}{T} \left[H_d[\vec{m}] + \frac{E_c d^4}{a^2} \sum_{\vec{r}} |\vec{m}(\vec{r})|^2 \right], \tag{9.18}$$

where the n_i's are integers, d is the cubic lattice constants used in the discretization, and $\frac{E_c d^4}{a^2} \Sigma_{\vec{r}} |\vec{m}(\vec{r})|^2$ is the core energy term coming from the core of the defect line, which is not accurately treated by continuum elastic theory.

To cope with the constraint $\vec{\nabla} \cdot \vec{m} = 0$, we introduce an auxiliary field $\theta(\vec{r})$, rewriting the partition function equation (9.16) as

$$Z = \prod_{\vec{r}} \int d\theta(\vec{r}) \sum_{\vec{m}(\vec{r})} \exp\left(- S[\vec{m}] + i \sum_{\vec{r}} \theta(\vec{r}) \vec{\nabla} \cdot \vec{m}(\vec{r}) d^2 / a \right), \tag{9.19}$$

where the sum over $\vec{m}(\vec{r})$ is now unconstrained.

Then we introduce a dummy vector field $\vec{A}$ to mediate the long-range interaction between defect loops in the Hamiltonian (9.14). This is accomplished by rewriting the partition function as

$$Z = \prod_{\vec{r}} \int d\theta(\vec{r}) d\vec{A}(\vec{r}) \sum_{\vec{m}(\vec{r})} e^{-S[\vec{m}, \theta, \vec{a}]} \delta(\vec{\nabla} \cdot \vec{A}) \delta(A_z), \tag{9.20}$$

with

$$S = \frac{1}{T} \sum_{\vec{r}} \left[\vec{m} \cdot \left(- i \frac{T d^2}{a} \vec{\nabla} \theta(\vec{r}) + d^3 [i\vec{A}(\vec{r}) + \vec{a}(\vec{r})] \right) + E_c \frac{d^4}{a^2} |\vec{m}|^2 \right] + \frac{1}{2T} \sum_{\vec{q}} \frac{\Gamma_q}{K q_\perp^2} |\vec{A}|^2. \tag{9.21}$$

Now the sum over $\vec{m}(\vec{r})$ is recognized to be the "periodic Gaussian" made by Villain [18]. Then the partition function (9.20) can be rewritten as

$$Z = \prod_{\vec{r}} \int d\theta(\vec{r}) d\vec{A}(\vec{r}) \delta(\vec{\nabla}\cdot\vec{A}) \delta(A_z) \times \exp\left[-\sum_{\vec{r}i} V_p\left(\theta(\vec{r}+\hat{x}_i) - \theta(\vec{r}) - \frac{ad}{T}[A_i(\vec{r}) - ia_i(\vec{r})] \right) - \frac{1}{2T}\sum_{\vec{q}} \frac{\Gamma_q}{Kq_\perp^2} |\vec{A}|^2 \right], \quad (9.22)$$

where the 2π-period Villain potential $V_p(x)$ is defined as

$$e^{-V_p(x)} \equiv \sum_{-\infty}^{\infty} e^{-n^2 E_c/T + ixn}. \quad (9.23)$$

Since $V_p(x)$ has sharper minima for *smaller* E_c/T, which corresponds to higher temperature, raising the temperature in the original model is equivalent to lowering the temperature in the dual-model equation (9.22).

Standard universality class arguments imply that the model equation (9.22) has the same universality class as the "soft spin," or Landau-Ginsburg-Wilson, model with the *complex* "action"

$$S_r = \sum_{r,\alpha} \left[\frac{c}{2}\left(\vec{\nabla} + \frac{ad}{T}(i\vec{A}_\alpha + \vec{a}) t \right) \phi_\alpha^* \cdot \left(\vec{\nabla} - \frac{ad}{T}(i\vec{A}_\alpha + \vec{a}) \right) \times \phi_\alpha + t_d |\phi_\alpha|^2 + u_d |\phi_\alpha|^4 \right] + \sum_{q,\alpha} \frac{\Gamma_q}{2TKq_\perp^2} |\vec{A}_\alpha|^2, \quad (9.24)$$

where ϕ is a complex order parameter whose phase is $\theta(\vec{r})$. Because of the duality transformation's inversion of the temperature axis, the reduced temperature t_d is a monotonically decreasing function of the temperature T (of the original dislocation loop model), which vanishes at the mean-field transition temperature of the dislocation model (9.22). Disorder is included in the model (9.24) through $\vec{a}(\vec{r})$, which is related to the random tilt field $\vec{h}(\vec{r})$ by Eq. (9.15).

Because of the duality inversion of the temperature axis, the ordered phase of the dual model (9.24) corresponds to the disordered phase (dislocation loops unbound) of the original dislocation model.

A complete analysis of the dislocation-loop-unbinding transition described by the model (9.24) is beyond the scope of this paper. The goal here is to know if a dislocation bound state ever exists near the critical region of the smectic A-to-C transition. To answer that question, let us check the one-loop graphical correction to the dual temperature:

$$t_R = t_0 - \frac{(d-2)ca^2d^2}{T^2} \int \frac{d^dq}{(2\pi)^d} \frac{\Delta_t q_z^2 q_\perp^2}{q^2 \Gamma_q^2}. \quad (9.25)$$

It is easy to see that the integral diverges when K and Δ_t are considered as constants. This implies that t_R is always negative and the dual model is always in its ordered state, which corresponds to the dislocation unbound state. This implies that the system would have become disorder *before* reaching the critical point, which signals either a first-order transition or a reentrant nematic phase intervening between the A and C phases. However, this conclusion only holds within the *harmonic* approximation. In Sec. III we have shown that anharmonic effects are important. A crude way to include the effects is to treat $K(\vec{q})$ and $\Delta_t(\vec{q})$ as anomalous. Implementing this in the integral and requiring it to be finite, we obtain a restriction on η_K and η_t:

$$2\eta_t - \eta_K < 0, \quad (9.26)$$

which is another condition for our theory to be valid.

X. CONCLUSION

In summary, a theory of smectic the AC phase transition in anisotropic-disordered-media is developed. We show that the phase transition can be second order and calculated the critical exponents to first order in an $\epsilon = 5-d$ expansion. In addition, the elasticity and fluctuations of this system (at the phase-transition temperature) are studied. The implications of these results are expected to be observable.

The anisotropy of the disordered media we considered in this paper is realized by stretching the aerogel. We could also think about compressing the aerogel, which leads to another type of anisotropy with different symmetries. In the stretched case, the rotation symmetry of the model is completely destroyed. While in the compressed case, the model still preserves the rotation symmetry about the compressed direction. Therefore, it is expected that the smectic-A- to -C phase transition in these two cases have qualitatively different behavior. There may be more different ways to create the anisotropy, which can lead to other interesting problems. We postpone some of the studies to our future publications.

APPENDIX A

In this appendix, we review the derivation in Ref. [6] of the numerical estimates of the anomalous elastic exponents for the C phase. These are obtained from two different ϵ expansions, based on two different analytic continuations of the model to higher-dimensions. In the "hard" continuation, the higher-dimensional ($d>3$) model is chosen to still have only one "soft" direction for all spatial dimensions d, as it does in $d=3$. In this case, the exponents are given by

$$\tilde{\zeta}_{x'} = 2 - \frac{\tilde{\eta}_\gamma + \tilde{\eta}_K}{2}, \quad (A1)$$

$$\tilde{\zeta}_{z'} = 2 - \frac{\tilde{\eta}_K}{2}, \quad (A2)$$

$$\tilde{\eta}_K = \tfrac{16}{15}\tilde{\epsilon} + O(\tilde{\epsilon}^2), \quad (A3)$$

$$\tilde{\eta}_\gamma = \tfrac{4}{5}\tilde{\epsilon} + O(\tilde{\epsilon}^2), \quad (A4)$$

$$\tilde{\eta}_{s'} = \tfrac{4}{5}\tilde{\epsilon} + O(\tilde{\epsilon}^2), \quad (A5)$$

with $\tilde{\epsilon} = \frac{7}{2} - d$, and obey two exact scaling relations

$$-\frac{1}{2}\tilde{\eta}_\gamma - \frac{7-d}{2}\tilde{\eta}_K + \tilde{\eta}_{s'} = 2d - 7. \tag{A6}$$

In addition, by analytically continuing the problem to higher dimensions ($d>3$) in a different way (namely, by keeping the number of *hard* directions fixed at 2, as opposed to the $d=\frac{7}{2}-\tilde{\epsilon}$ expansion, which is based on keeping the number of the *soft* directions fixed at one), this problem was been studied in [6] using a $d=4-\tilde{\tilde{\epsilon}}$ expansion, yielding the following exponents and the exact scaling relation:

$$\tilde{\eta}_K = \tfrac{3}{8}\tilde{\tilde{\epsilon}} + O(\tilde{\tilde{\epsilon}}^2), \tag{A7}$$

$$\tilde{\eta}_\gamma = \tfrac{3}{4}\tilde{\tilde{\epsilon}} + O(\tilde{\tilde{\epsilon}}^2), \tag{A8}$$

$$\tilde{\eta}_{s'} = \tfrac{1}{8}\tilde{\tilde{\epsilon}} + O(\tilde{\tilde{\epsilon}}^2), \tag{A9}$$

$$4 - d + \tilde{\eta}_{s'} = \frac{\eta_\gamma}{2} + 2\tilde{\eta}_K. \tag{A10}$$

As argued in [6], combining the results from the $d=4-\tilde{\tilde{\epsilon}}$ and the earlier $d=\frac{7}{2}-\tilde{\epsilon}$ expansion, we see that the exponents $\tilde{\eta}_K$ and $\tilde{\eta}_{s'}$ are more consistent between the two. This suggests that the most accurate estimate of all three exponents will be obtained by taking $\tilde{\eta}_K$ and η_s from the weighted average of the $4-\tilde{\tilde{\epsilon}}$ and $\frac{7}{2}-\tilde{\epsilon}$ exponents:

$$\tilde{\eta}_K = \frac{4\tilde{\eta}_K\left(\frac{7}{2}-\tilde{\epsilon}\right) + \tilde{\eta}_K(4-\tilde{\tilde{\epsilon}})}{5}, \tag{A11}$$

$$\tilde{\eta}_{s'} = \frac{4\tilde{\eta}_{s'}\left(\frac{7}{2}-\tilde{\epsilon}\right) + \tilde{\eta}_{s'}(4-\tilde{\tilde{\epsilon}})}{5} \tag{A12}$$

[the factor of 4 appearing because, *a priori*, we expect the $\frac{7}{2}-\tilde{\epsilon}$ expansion to be 4 times as accurate as the $4-\tilde{\tilde{\epsilon}}$ expansion, since the errors in both are $O(\epsilon^2)$ and $\tilde{\tilde{\epsilon}}$ (=1) is twice as large as $\tilde{\epsilon}$ (=$\frac{1}{2}$)], and then obtaining η_γ from the *exact* scaling relation (A6) in $d=3$ [note that (A10) reduces to (A6) in $d=3$]. One can also estimate the errors in the exponents obtained in this way as the differences between the weighted averages (A11) and (A12) and the $\frac{7}{2}-\tilde{\epsilon}$ expansion results. Doing all of this, Ref. [6] obtains

$$\tilde{\eta}_K = 0.50 \pm 0.03, \tag{A13}$$

$$\tilde{\eta}_\gamma = 0.26 \pm 0.12, \tag{A14}$$

$$\tilde{\eta}_{s'} = 0.132 \pm 0.002. \tag{A15}$$

In addition, inserting $\tilde{\eta}_K$, $\tilde{\eta}_\gamma$, and $\tilde{\eta}_{s'}$ into the *exact* scaling relation (1.19) gives

$$\tilde{\eta}_{x'} = 1.37 \pm 0.15. \tag{A16}$$

APPENDIX B

During the discussion of the universality class of the *C* phase, we have shown the advantage of writing the model in a special coordinate. The relation between this coordinate and the laboratory one is fully determined by the parameter Γ, which is defined by (6.13). Now we show that near the critical point, Γ is also renormalized by the critical fluctuations and hence strongly temperature dependent. Using the critical RG, the renormalized Γ can be calculated as

$$\Gamma = e^{(\omega-1)\ell^*}\Gamma(\ell^*), \tag{B1}$$

where the RG is stopped at $\ell^*=\ln(\Lambda\xi_\perp)$ and the prefactor on the right-hand side comes from the dimensional rescaling. To calculate $\Gamma(\ell^*)$, it is convenient to reorganize (6.13) as

$$\Gamma(\ell^*) = \sqrt{-\frac{g_3(\ell^*)B(\ell^*)}{g_4(\ell^*)D(\ell^*)}}\sqrt{\frac{w(\ell^*)}{w'(\ell^*)}}, \tag{B2}$$

where g_3 and g_4 are defined by (3.11) and (3.12), respectively. Previous calculation shows that for large ℓ^* (which is true near the critical region), $g_4(\ell^*)=32\epsilon/15$ and $g_3(\ell^*) \sim e^{-\eta_3\ell^*}$, where η_3 is defined via

$$\frac{dg_3(\ell)}{d\ell} = -\eta_3 g_3(\ell). \tag{B3}$$

According to the linearized flow equation of g_3 given by (3.67), η_3 is given, to the leading order in $\epsilon=5-d$, by

$$\eta_3 = \tfrac{1}{5}\epsilon + O(\epsilon^2). \tag{B4}$$

To calculate $w'(\ell^*)$, we rewrite (6.5) as

$$w'(\ell^*) = w(\ell^*)\left[1 - \frac{g_3(\ell^*)}{g_4(\ell^*)}\right]. \tag{B5}$$

Since $g_3(\ell^*)/g_4(\ell^*)$ is much less than 1, the above equation implies $w(\ell^*)/w'(\ell^*)=1$. Based on these arguments, we obtain from (B2)

$$\Gamma(\ell^*) \sim e^{-\eta_3\ell^*/2}\sqrt{\frac{B(\ell^*)}{D(\ell^*)}} = \frac{e^{-\eta_3\ell^*/2}}{\Lambda}\sqrt{\frac{B(\ell^*)}{K(\ell^*)}}, \tag{B6}$$

where $B(\ell^*)$ and $K(\ell^*)$ can be calculated by integrating the RG flow equations (3.54) and (3.55). Plugging the above equation into (B1), we get

$$\Gamma \sim e^{[1-(\eta_K+\eta_3)/2]\ell^*} \sim (\xi_\perp\Lambda)^{1-(\eta_K+\eta_3)/2}. \tag{B7}$$

[1] D. S. Fisher, M. P. A. Fisher, and D. A. Huse, Phys. Rev. B **43**, 130 (1991); C. Ebner and D. Stroud, *ibid.* **31**, 165 (1985); D. A. Huse and H. S. Seung, *ibid.* **42**, 1059 (1990).
[2] *Charge Density Waves in Solids*, edited by L. P. Gorkov and G. Gruner (Elsevier, Amsterdam, 1989).
[3] E. Granato and J. M. Kosterlitz, Phys. Rev. B **33**, 6533 (1986); Phys. Rev. Lett. **62**, 823 (1989).
[4] M. Chan *et al.*, Phys. Today **49**(8), 30 (1996).
[5] L. Chen and J. Toner, Phys. Rev. Lett. **94**, 137803 (2005); **94**, 209902(E) (2005).
[6] B. Jacobsen, K. Saunders, L. Radzihovsky, and J. Toner, Phys. Rev. Lett. **83**, 1363 (1999).
[7] T. Giamarchi and P. Le Doussal, Phys. Rev. Lett. **72**, 1530 (1994); D. S. Fisher, *ibid.* **78**, 1964 (1997).
[8] J. L. Cardy and S. Ostlund, Phys. Rev. B **25**, 6899 (1982).
[9] J. Toner and D. P. DiVincenzo, Phys. Rev. B **41**, 632 (1990).
[10] The only exception we know of to this statement are the so-called "reentrant nematic" phases, which are translationally disordered phases that occur at *lower* temperatures than the translationally ordered smectic-*A* phases in some materials. Unlike our smectic *C* phase, however, the low-temperature reentrant nematic, despite occuring at lower temperature, is a lower-symmetry state than the higher-temperature smectic-*A* phase, so its poorer translational order is less counterintuitive.
[11] T. Bellini, L. Radzihovsky, J. Toner, and N. Clark, Science **294**, 1074 (2001); L. Radzihovsky, A. M. Ettouhami, K. Saunders, and J. Toner, Phys. Rev. Lett. **87**, 027001 (2001); K. Saunders, L. Radzihovsky, and J. Toner, *ibid.* **85**, 4309 (2000); L. Radzihovsky and J. Toner, Phys. Rev. B **60**, 206 (1999). The last of these deals with ferromagnetic superconductors, rather than liquid crystals; however, the elastic model describing such superconductors is identical to that describing a liquid crystal in aerogel.
[12] L. Radzihovsky and J. Toner, Phys. Rev. Lett. **78**, 4414 (1997).
[13] P. M. Chaikin and T. C. Lubensky, *Principles of Condensed Matter Physics* (University Press, Cambridge, 2001).
[14] The thoughtful reader will quickly see why we do *not* choose $\vec{q}_\perp = 0$.
[15] P. G. de Gennes and J. Prost, *The Physics of Liquid Crystal*, 2nd ed. (Clarendon Press, Oxford, 1993).
[16] G. Grinstein and R. A. Pelcovits, Phys. Rev. A **26**, 2196 (1982).
[17] D. Liang, M. A. Borthwick, and R. L. Leheny, J. Phys.: Condens. Matter **16**, S1989 (2004).
[18] J. Villain, J. Phys. (Paris) **36**, P581 (1975).